SUPPORTING INFORMATION

Osmium- and Iridium-Promoted C-H Bond Activation of 2,2'-Bipyridines and Related Heterocycles: Kinetic and Thermodynamic Preferences

Lara Cancela, Miguel A. Esteruelas,* Ana M. López, Montserrat Oliván, Enrique Oñate, Ainhoa San-Torcuato, and Andrea Vélez

Departamento de Química Inorgánica – Instituto de Síntesis Química y Catálisis Homogénea (ISQCH) – Centro de Innovación en Química Avanzada (ORFEO-CINQA), Universidad de Zaragoza – CSIC, 50009 Zaragoza, Spain

* e-mail: maester@unizar.es

Contents:

● Experimental Details

General Information. All reactions were carried out with exclusion of air using Schlenk-tube techniques or in a drybox. Pentane and toluene were obtained oxygen- and water-free from an MBraun solvent purification apparatus, while methanol was dried and distilled under argon prior to use. ^{1}H, $^{13}C\{^{1}H\}$, $^{31}P\{^{1}H\}$, ^{2}H, and ^{19}F NMR spectra were recorded on Bruker 300 ARX, Bruker Avance 300 MHz, or Bruker Avance 400 MHz instruments. Chemical shifts (expressed in ppm) are referenced to residual solvent peaks (^{1}H, $^{13}C\{^{1}H\}$), external 85% H_3PO_4 ($^{31}P\{^{1}H\}$), or $CFCl_3$ (^{19}F). Coupling constants J and N ($N = J_{P\text{-}H} + J_{P'\text{-}H}$ for ^{1}H and $N = J_{P\text{-}C} + J_{P'\text{-}C}$ for $^{13}C\{^{1}H\}$) are given in hertz. Attenuated total reflection infrared spectra (ATR-IR) of solid samples were run on a PerkinElmer Spectrum 100 FT-IR spectrometer. Elemental analyses were carried out in a PerkinElmer 2400 CHNS/O analyzer. High-resolution electrospray mass spectra were acquired using a MicroTOF-Q hybrid quadrupole time-of-flight spectrometer (Bruker Daltonics, Bremen, Germany). $OsH_6(P^iPr_3)_2$,[1] $OsH_2Cl_2(P^iPr_3)_2$,[1] $IrH_5(P^iPr_3)_2$,[2] $IrCl_2H(P^iPr_3)_2$,[2] 6-phenyl-2,2'-bipyridine,[3] 6-methyl-2,2'-bipyridine,[4] 3-methyl-1-(6-phenylpyridin-2-yl)-1*H*-benzymidazolium iodide,[5] and 3-methyl-1-(6-phenylpyridin-2-yl)-1*H*-imidazolium iodide[5] were prepared as reported previously.

Reaction of 3-methyl-1-(6-phenylpyridin-2-yl)-1*H*-benzymidazolium Iodide with Silver Tetrafluoroborate: Anion Exchange. A solution of 3-methyl-1-(6-phenylpyridin-2-yl)-1*H*-benzymidazolium iodide (600 mg, 145 mmol) in MeCN: MeOH (15:15 mL) was treated with $AgBF_4$ (342 mg, 170 mmol). The resulting mixture was stirred in the dark for 10 min, obtaining a colorless solution and a white-yellow solid. The solution was filter through Celite, and it was concentrated to approx. 0.5 mL Addition of acetone affords a white solid. Yield: 480 mg (89 %). ^{1}H NMR (300.13 MHz, CD_2Cl_2, 298 K): δ 10.0 (s, 1H, NCHN), 8.58 (m, 1H, CH Ar), 8.18 (t, $^{3}J_{H\text{-}H}$= 7.9, 1H, CH Ar), 8.12 (m, 2H, CH Ar), 8.02 (d, $^{3}J_{H\text{-}H}$ = 7.5, 1H, CH Ar), 7.94 (d, $^{3}J_{H\text{-}H}$ = 7.9, 1H, CH Ar), 7.84 (m, 1H, CH Ar), 7.80 (m, 2H, CH Ar), 7.54 (m, 3H, CH Ar) 4.34 (s, 3H, CH_3). $^{13}C\{^{1}H\}$ (75.48 MHz, CD_2Cl_2, 298 K): δ 158.2, 147.6 (both s, C Ar), 144.94 (s, NCHN, inferred from the HSQC spectrum), 141.9 (s, CH Ar), 137.6, 132.9 (both s, C Ar), 130,7 (s, CH Ar), 130.6 (s, C Ar), 129.5, 128.8, 128.4, 127.4, 121.9, 116.9, 115.2, 113.3 (all s, CH ar), 34.4 (s, CH_3).

Reaction of 3-Methyl-1-(6-phenylpyridin-2-yl)-1*H*-imidazolium Iodide with Silver Tetrafluoroborate: Anion Exchange. A solution of 3-methyl-1-(6-phenylpyridin-2-yl)-1*H*-imidazolium iodide (600 mg, 165 mmol) in MeCN:MeOH (15:15 mL) was treated with $AgBF_4$ (389 mg, 198 mmol). The resulting mixture was stirred in the dark for 10 min, obtaining a colorless solution and a white-yellow solid. The solution was filter through Celite, and it was concentrated to approx. 0.5 mL addition of acetone affords a white solid. Yield: 485 mg (91%). ^{1}H NMR (300.13 MHz, DMSO-d_6, 298K): δ 10.14 (s, 1H, NCHN), 8.60 (br, 1H, CH Im), 8.26 (m, 3H, CH Ar), 8.20 (m, 1H, CH Ar), 7.97 (br, 1H, CH Im), 7.93 (m, 2H, CH Ar), 7.55 (m, 3H, CH Ar), 4.01 (s, 3H, CH_3). ^{13}C{^{1}H} (75.48 MHz, DMSO-d_6, 298 K): δ 155.7, 146,1 (both s, C Ar), 141,6 (s, CH, Ar), 136.4 (s, C Ar), 135.5 (s, NCHN), 130,2, 128,9, 126.9 (all s, CH Ar), 124.8 (s, CH Im), 120.9 (s, CH Ar), 119.0 (s, CH Im), 112.2 (s, CH Ar), 36.3 (s, CH_3).

● **Structural Analysis of Complexes 2, 3, 5, 6, and 7.**

X-ray data were collected for the complexes on a Bruker Smart APEX or Bruker Smart APEX DUO CCD diffractometers equipped with a normal focus, and 2.4 kW sealed tube source (Mo radiation, λ = 0.71073 Å). Data were collected over the complete sphere covering 0.3^o in w. Data were corrected for absorption by using a multiscan method applied with the SADABS program.[6] The structures were solved by Patterson or direct methods and refined by full-matrix least squares on F^2 with SHELXL2016,[7] including isotropic and subsequently anisotropic displacement parameters. The hydrogen atoms were observed in the last Fourier Maps or calculated, and refined freely or using a restricted riding model. The hydrides were refined with a fixed distance Os-H.

For **2**, the osmium atom is located on a binary symmetry axis which divides the asymmetric C,N-bipyridine coordinated ligand into two moieties related by symmetry. Because of that, there is a positional disorder between the 2/6 and 2'/6' locations of nitrogen/carbon atoms of the C,N-coordinated bipyridine ligand refined with occupancy of 50% each with the aid of the EXYZ and EADP options of SHELXL. For **3**-**6** the disordered groups were refined with different moieties, complementary occupancy factors, restrained geometries, and isotropic displacement factors.

Crystal data for **2** (CCDC 1987592): $C_{28}H_{52}N_2OsP_2$, M_W 668.85, orange, irregular block (0.143 x 0.100 x 0.046 mm^3), orthorhombic, space group Pbcn, *a*: 8.5429(5) Å, *b*: 18.7702(12) Å, *c*: 17.9964(11) Å, *V* = 2885.8(3) $Å^3$, *Z* = 4, *Z'* = 0.5, D_{calc}: 1.540 g cm^{-3}, F(000): 1360, T = 100(2) K, μ = 4.548 mm^{-1}. 48084 measured reflections (2θ: 3-57°, ω scans 0.3°), 3642 unique (R_{int} = 0.0366); min./max. transm. factors 0.670/0.862. Final agreement factors were R^1 = 0.0189 (2955 observed reflections, I > 2σ(I)) and wR^2 = 0.0464; data/restraints/parameters 3642/2/160; GoF = 1.021. Largest peak and hole: 1.285 (close to osmium atoms) and -0.668 e/ $Å^3$.

Crystal data for **3** (CCDC 1987590): $C_{34}H_{56}N_2OsP_2$, M_W 744.94, orange, irregular block (0.142 x 0.127 x 0.055 mm^3), triclinic, space group P-1, *a*: 8.9477(5) Å, *b*: 12.8386(7) Å, *c*: 15.3127(9) Å, *α*: 83.7190(10)°, *β*: 74.8350(10)°, *γ*: 79.0300(10)°, *V* = 1663.48(16)$Å^3$, *Z* = 2, *Z'* = 1, D_{calc}: 1.487 g cm^{-3}, F(000): 760, T = 100(2) K, μ = 3.954 mm^{-1}. 15961 measured reflections (2θ: 3-51°, ω scans 0.3°), 7735 unique (R_{int} = 0.0209); min./max. transm. factors 0.640/0.862. Final agreement factors were R^1 = 0.0276 (6990 observed reflections, I > 2σ(I)) and wR^2 = 0.0659; data/restraints/parameters 7735/27/370; GoF = 1.061. Largest peak and hole 1.402 (close to osmium atoms) and -1.827 e/ $Å^3$.

Crystal data for **5** (CCDC 1987594): $C_{36}H_{58}N_2OsP_2$, 1.5(C_6H_6), M_W 888.14, orange, irregular block (0.231 x 0.210 x 0.118 mm^3), monoclinic, space group $P2_1/n$, *a*: 11.2086(10) Å, *b*: 20.6449(18) Å, *c*: 18.1317(15) Å, *β*: 99.7910(10)°, *V* = 4134.6(6) $Å^3$, *Z* = 4, *Z'* = 1, D_{calc}: 1.427 g cm^{-3}, F(000): 1828, T = 100(2) K, μ = 3.194 mm^{-1}. 76754 measured reflections (2θ: 3-57°, ω scans 0.3°), 11379 unique (R_{int} = 0.0294); min./max. transm. factors 0.762/0.862. Final agreement factors were R^1 = 0.0198 (10195 observed reflections, I > 2σ(I)) and wR^2 = 0.0485; data/restraints/parameters 11379/4/ 448; GoF = 1.024. Largest peak and hole 0.939 (close to osmium atoms) and -0.564 e/ $Å^3$.

Crystal data for **6** (CCDC 1987591): $C_{37}H_{59}N_3OsP_2$, M_W 798.01, colorless, irregular block (0.143 x 0.098 x 0.093 mm^3), triclinic, space group P-1, *a*: 12.7290(6) Å, *b*: 15.5400(8) Å, *c*: 18.4985(9) Å, *α*: 81.3860(10)°, *β*: 81.4380(10)°, *γ*: 82.3890(10)°, *V* = 3554.8(3) $Å^3$, *Z* = 4, *Z'* = 2, D_{calc}: 1.491 g cm^{-3}, F(000): 1632, T = 100(2) K, μ = 3.707 mm^{-1}. 56695 measured reflections (2θ: 3-57°, ω scans 0.3°), 17036 unique (R_{int} =

0.0456); min./max. transm. factors 0.735/0.862. Final agreement factors were R^1 = 0.0307 (13143 observed reflections, I > 2σ(I)) and wR^2 = 0.0738; data/restraints/parameters 17036/16/ 818; GoF = 0.951. Largest peak and hole 1.560 (close to osmium atoms) and -1.025e/ Å^3.

Crystal data for **7** (CCDC 1987593): $C_{33}H_{56}BF_4N_3OsP_2$, M_W 833.75, yellow, irregular block (0.178 x 0.152 x 0.104 mm^3), monoclinic, space group $P2_1/n$, *a*: 11.1123(10) Å, *b*: 14.7336(14) Å, *c*: 22.192(2) Å, *β*: 102.3770(10)°, *V* = 3548.9(6) Å^3, *Z* = 4, *Z'* = 1, D_{calc}: 1.560 g cm^{-3}, F(000): 1688, T = 100(2) K, μ = 3.731 mm^{-1}. 47193 measured reflections (2θ: 3-57°, ω scans 0.3°), 9635 unique (R_{int} = 0.0372); min./max. transm. factors 0.712/0.862. Final agreement factors were R^1 = 0.0228 (8135 observed reflections, I > 2σ(I)) and wR^2 = 0.0493; data/restraints/parameters 9635/2/ 422; GoF = 1.028. Largest peak and hole 1.028 (close to osmium atoms) and -0.416 e/ Å^3.

● **NMR spectra**

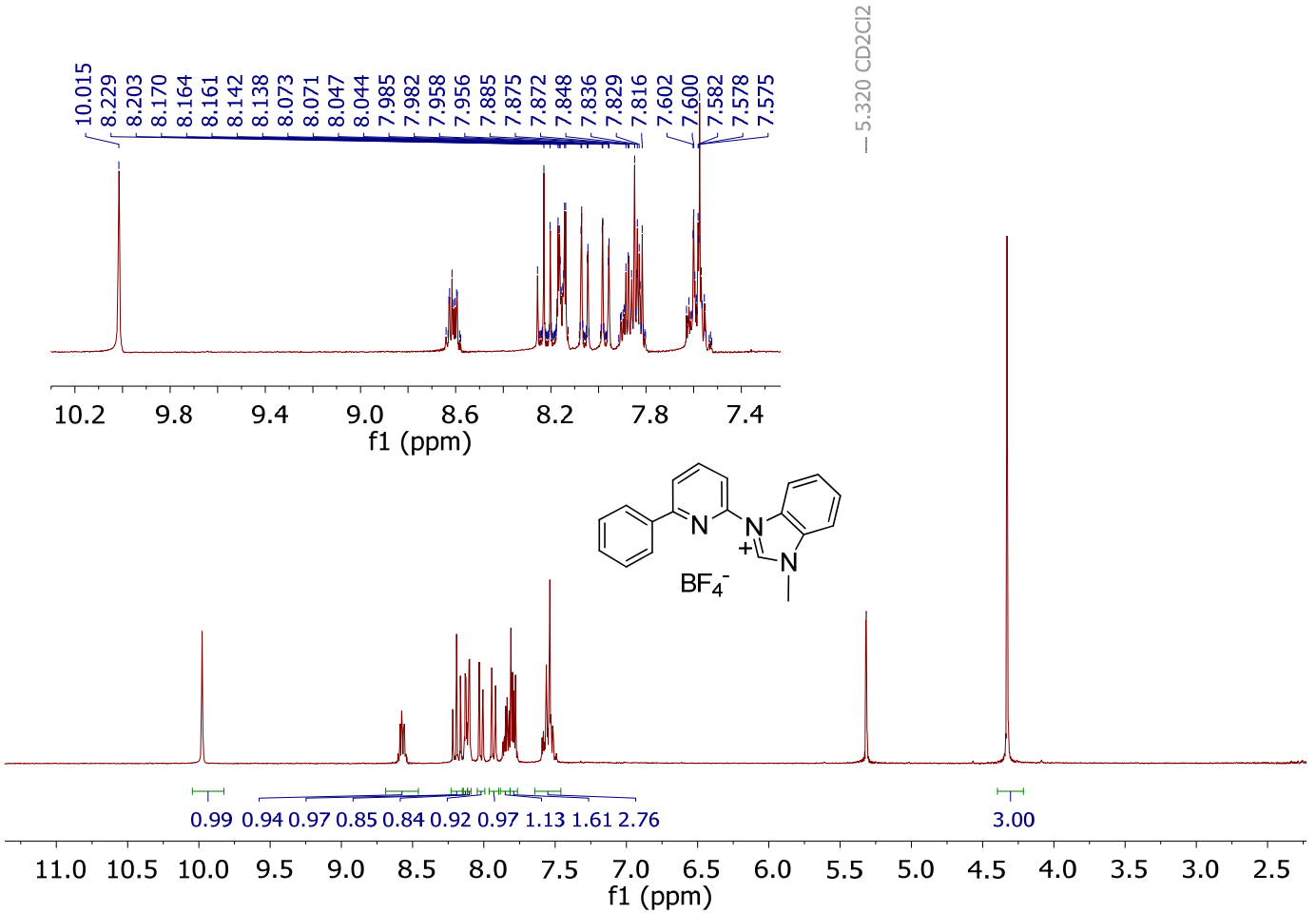

Figure S1. ^{1}H NMR spectrum (300.13 MHz CD_2Cl_2, 298 K) of 3-methyl-1-(6-phenylpyridin-2-yl)-1*H*-benzymidazolium tetrafluoroborate.

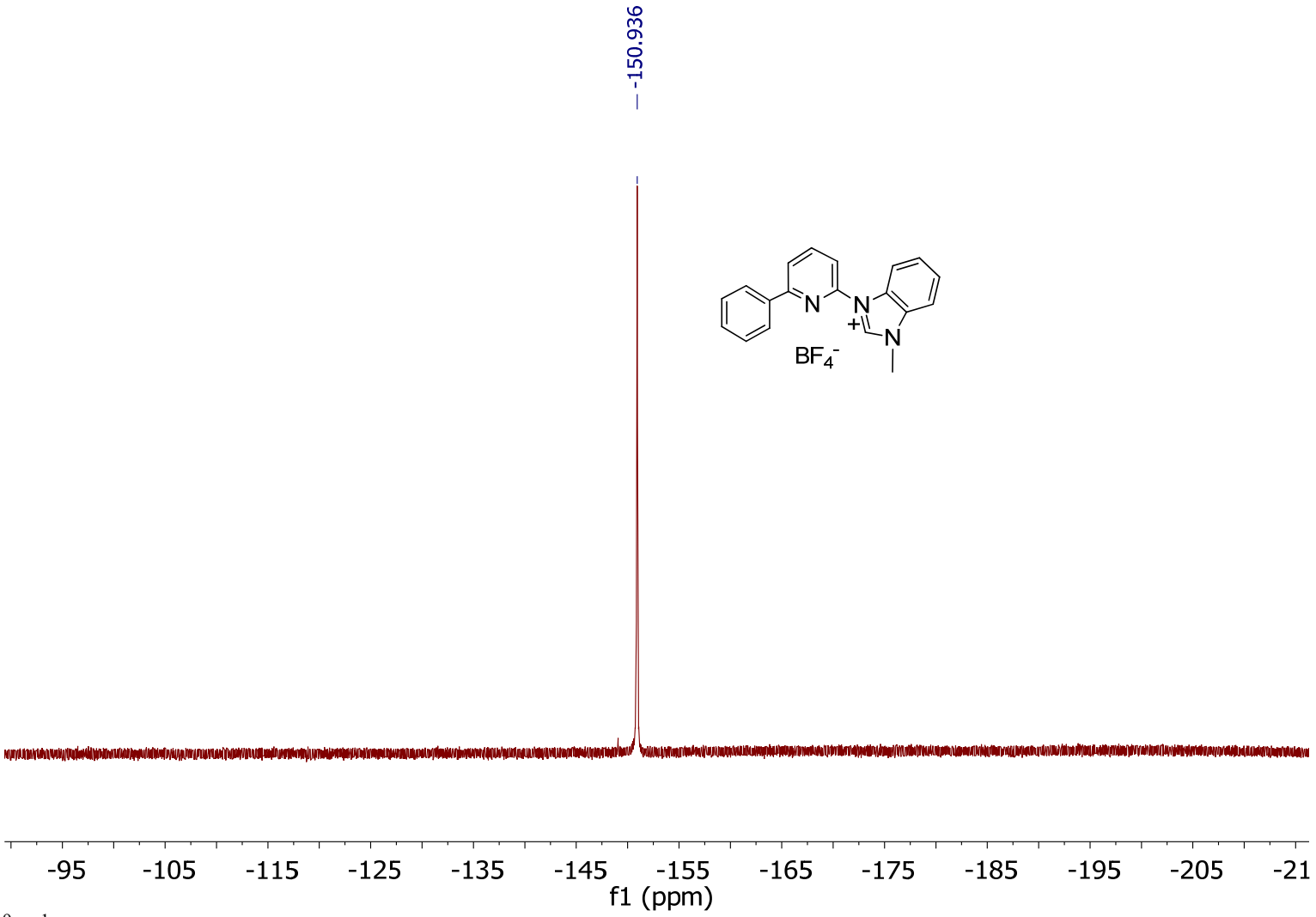

Figure S2. $^{19}F\{^{1}H\}$-NMR spectrum (376.49 MHz CD_2Cl_2, 298 K) of 3-methyl-1-(6-phenylpyridin-2-yl)-1*H*-benzymidazolium tetrafluoroborate.

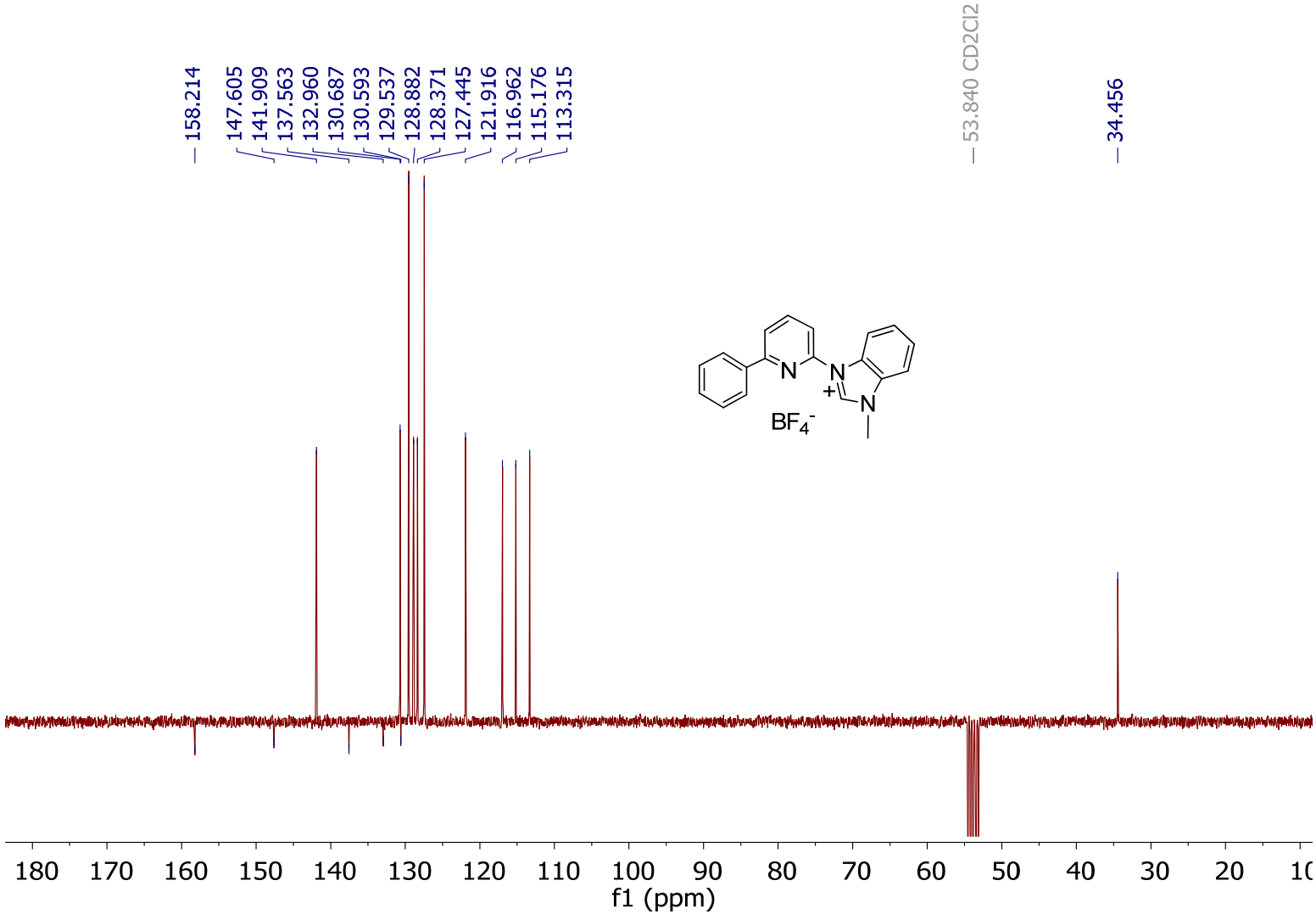

Figure S3. $^{13}C\{^{1}H\}$-apt NMR spectrum (75.48 MHz CD_2Cl_2, 298 K) of 3-methyl-1-(6-phenylpyridin-2-yl)-1*H*-benzymidazolium tetrafluoroborate.

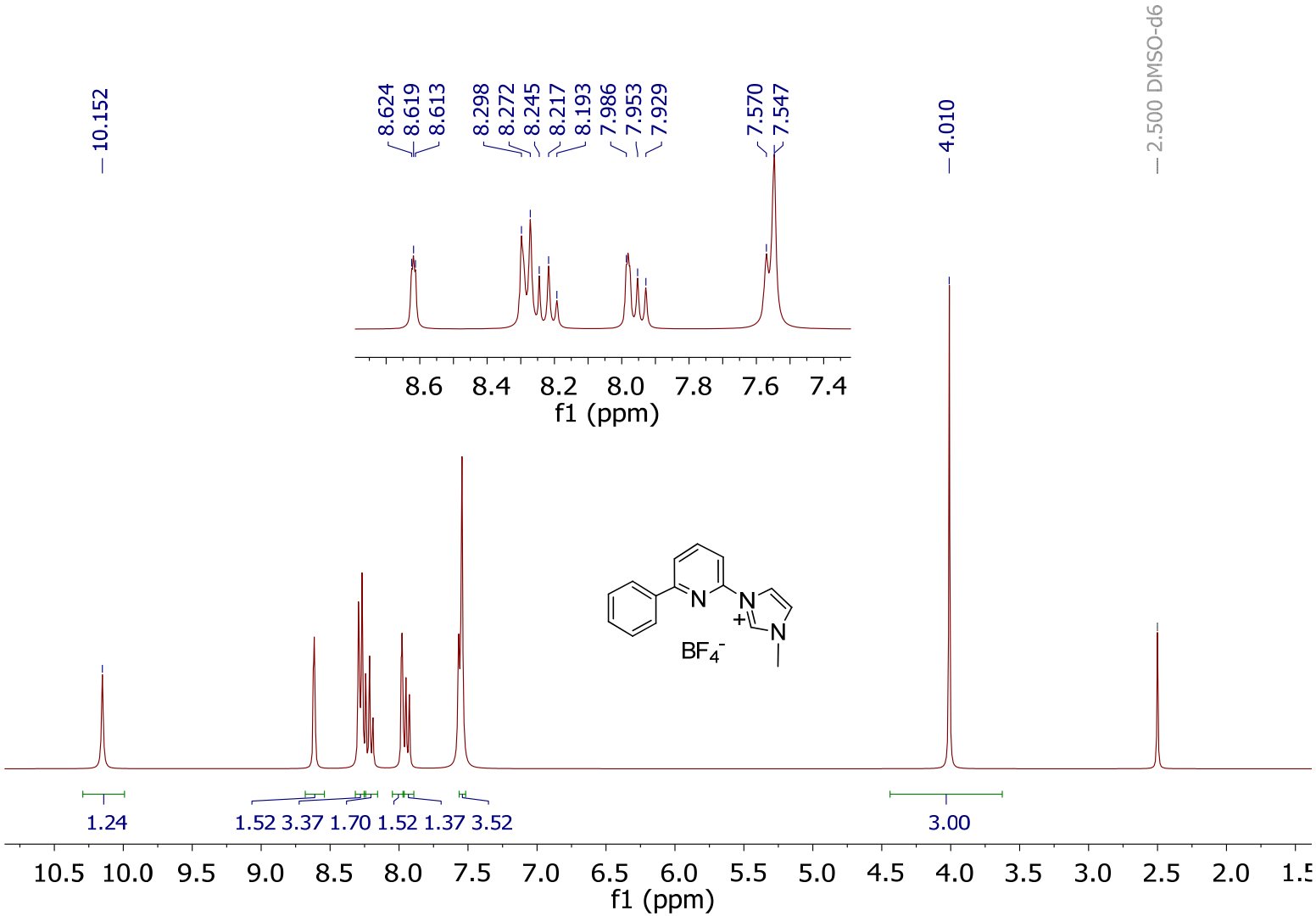

Figure S4. [1]H NMR spectrum (300.13 MHz, DMSO-d_6, 298 K) of 3-methyl-1-(6-phenylpyridin-2-yl)-1*H*-Imidazolium tetrafluoroborate.

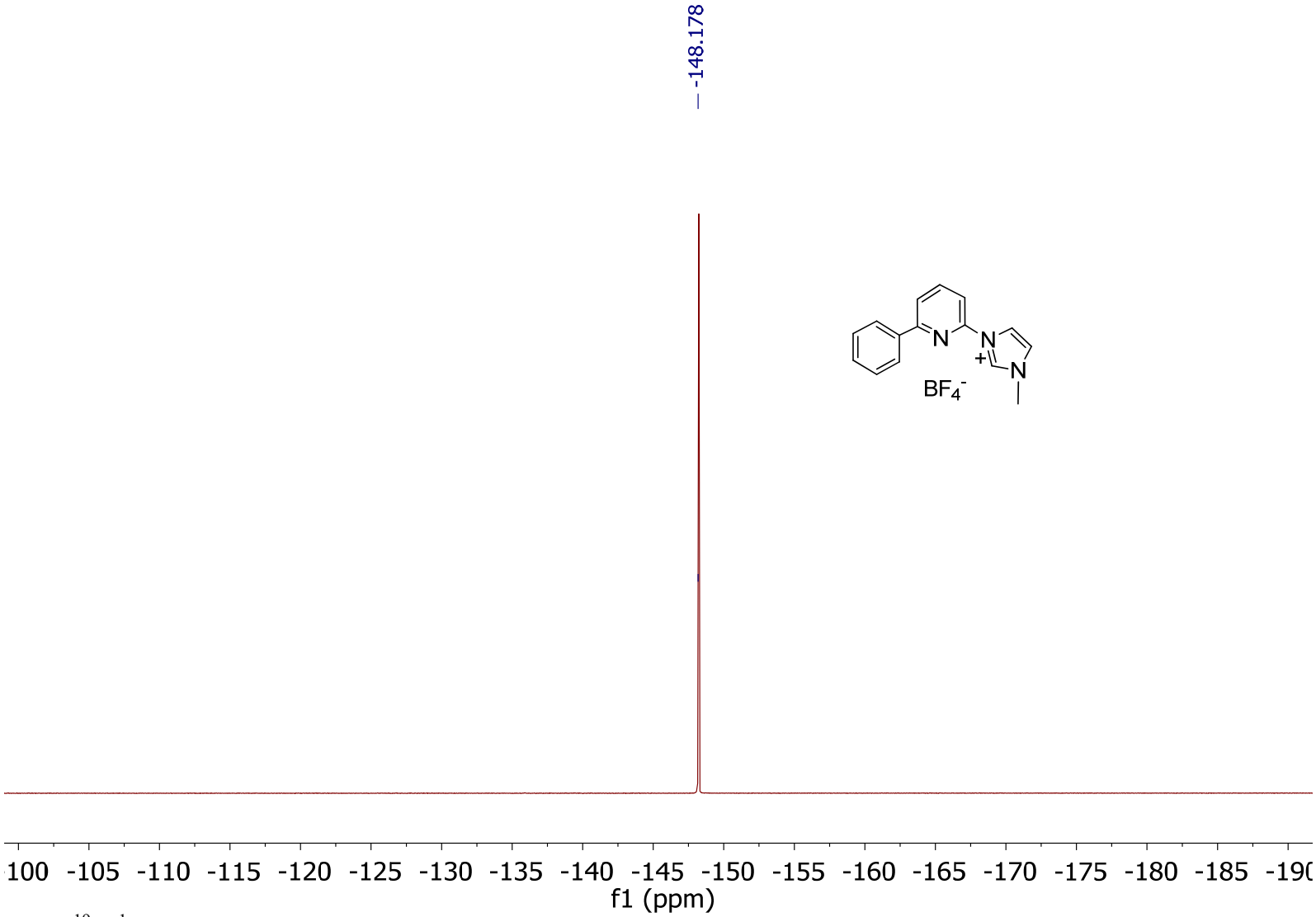

Figure S5. $^{19}F\{^{1}H\}$ NMR spectrum (376.49 MHz DMSO-d_6, 298 K) of 3-methyl-1-(6-phenylpyridin-2-yl)-1*H*-Imidazolium tetrafluoroborate.

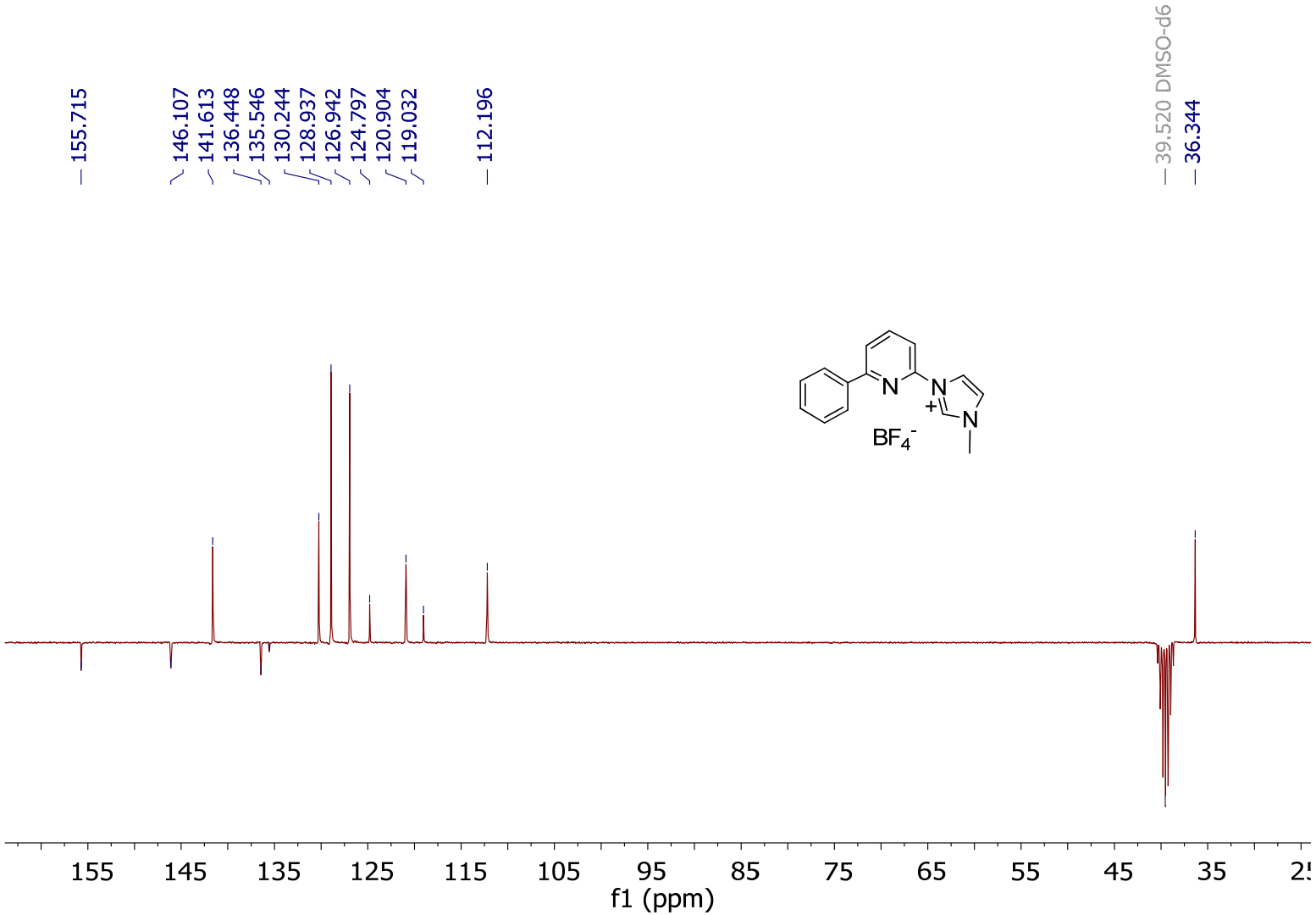

Figure S6. $^{13}C\{^{1}H\}$-apt NMR spectrum (75.48 MHz, DMSO-d_6, 298 K) of 3-methyl-1-(6-phenylpyridin-2-yl)-1*H*-Imidazolium tetrafluoroborate

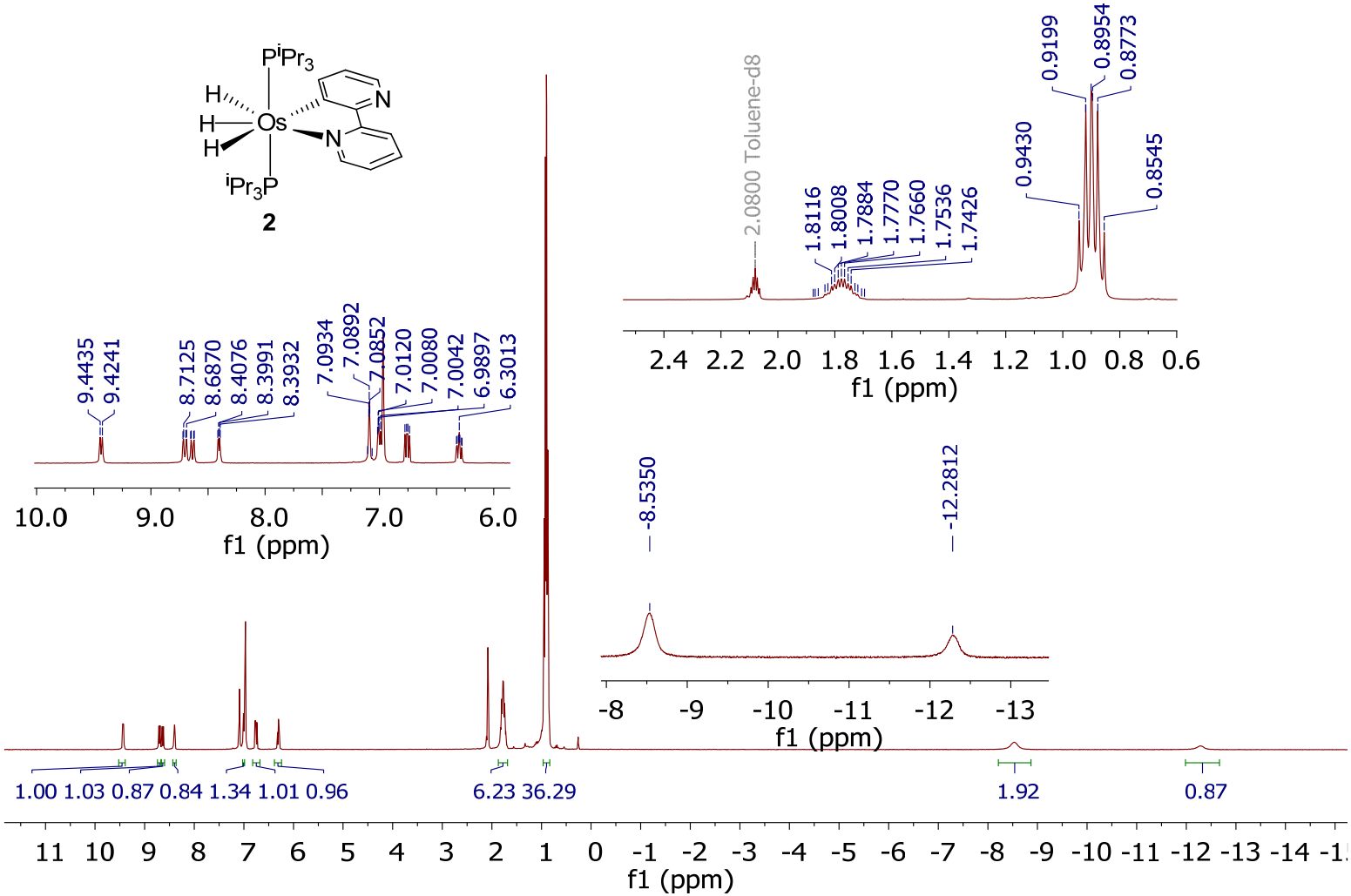

Figure S7. ^{1}H NMR spectrum (300.13 MHz, toluene-d_8, 298 K) of compound **2**.

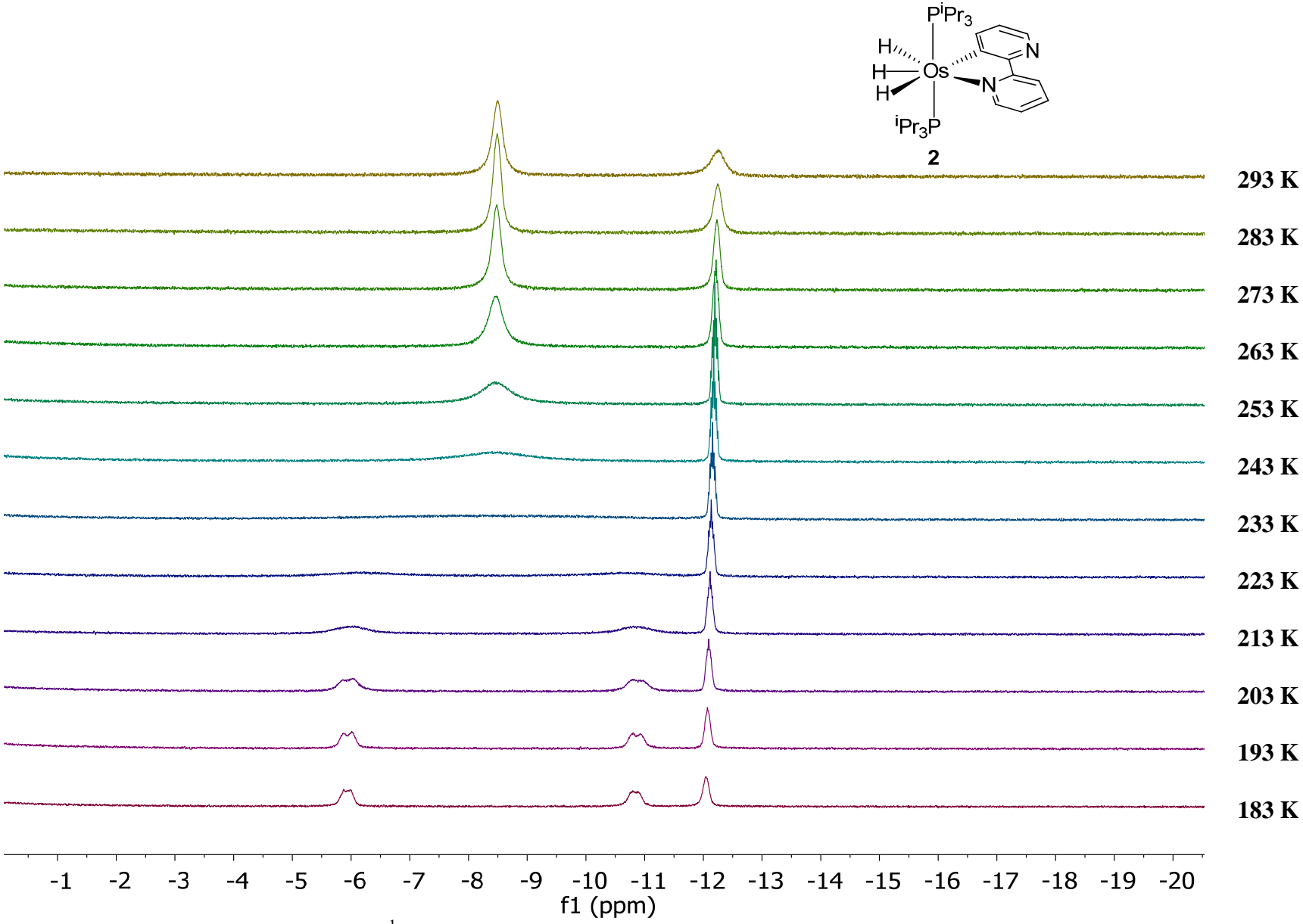

Figure S8. High field region of the ^{1}H NMR spectra (300.13 MHz, toluene-d_8) of compound **2** as a function of the temperature.

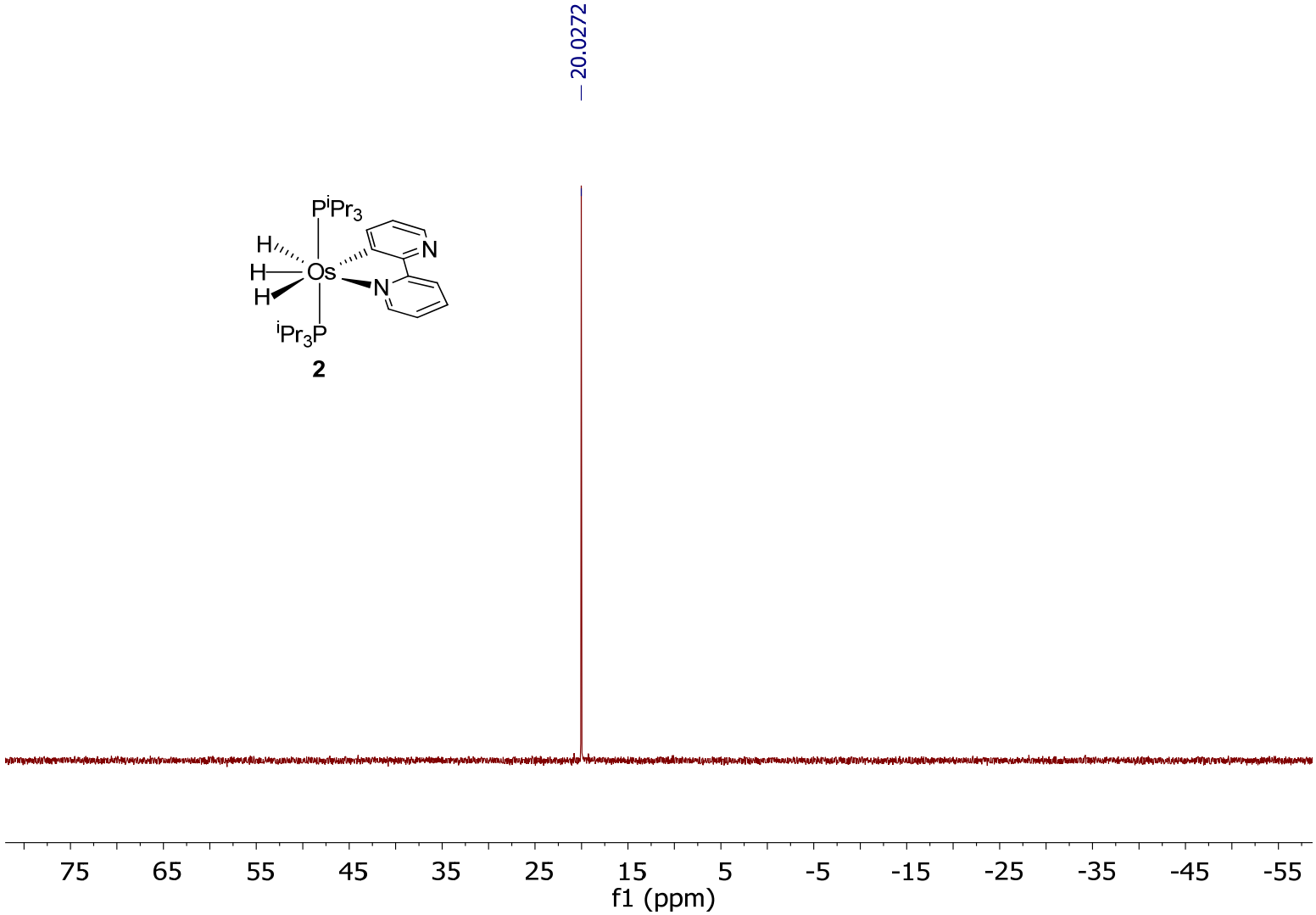

Figure S9. $^{31}P\{^1H\}$ NMR spectrum (121.49 MHz, toluene-d_8, 298 K) of compound **2**.

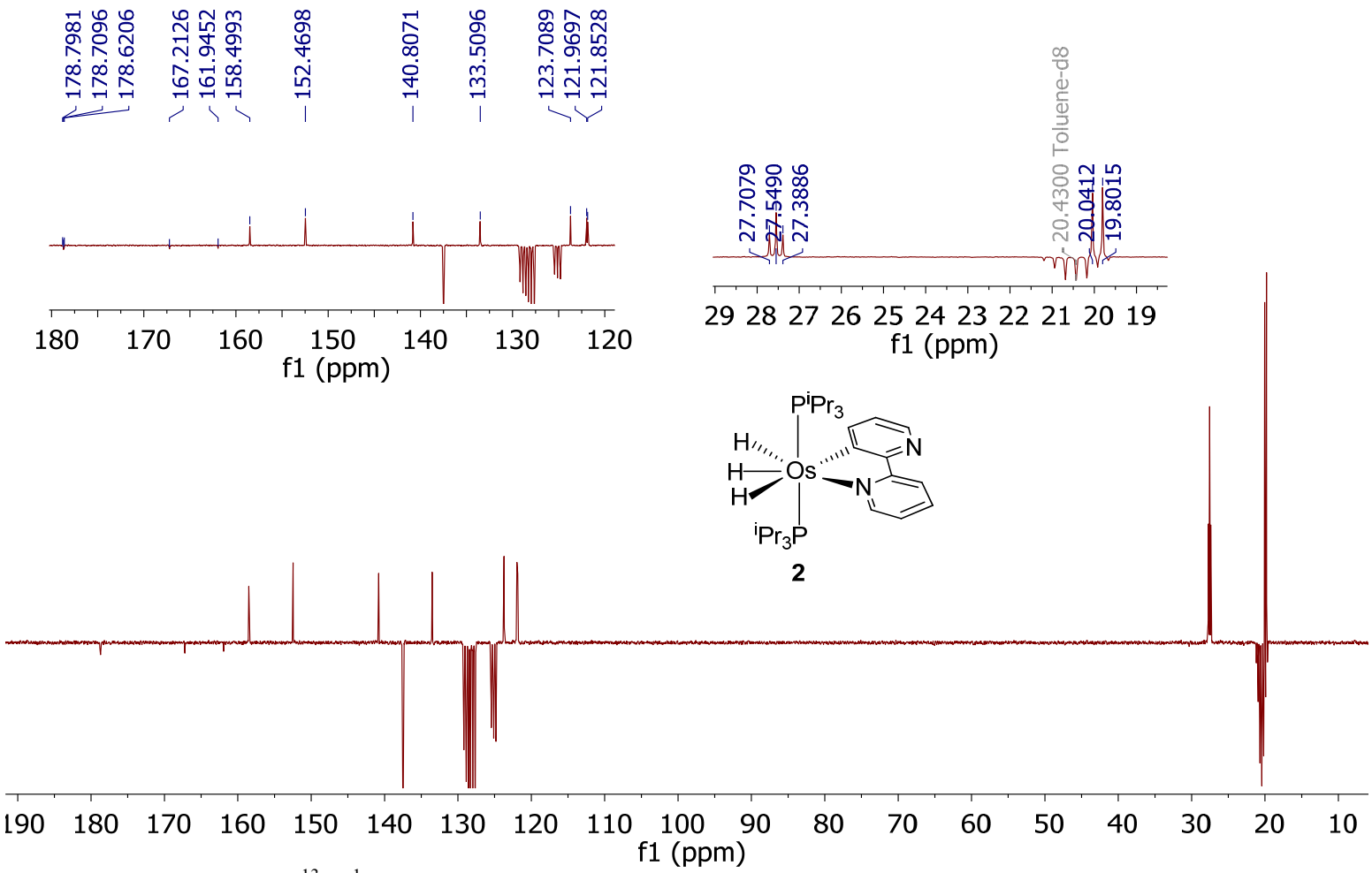

Figure S10. $^{13}C\{^{1}H\}$-apt NMR spectrum (75.48 MHz, toluene-d_8, 298 K) of compound **2**.

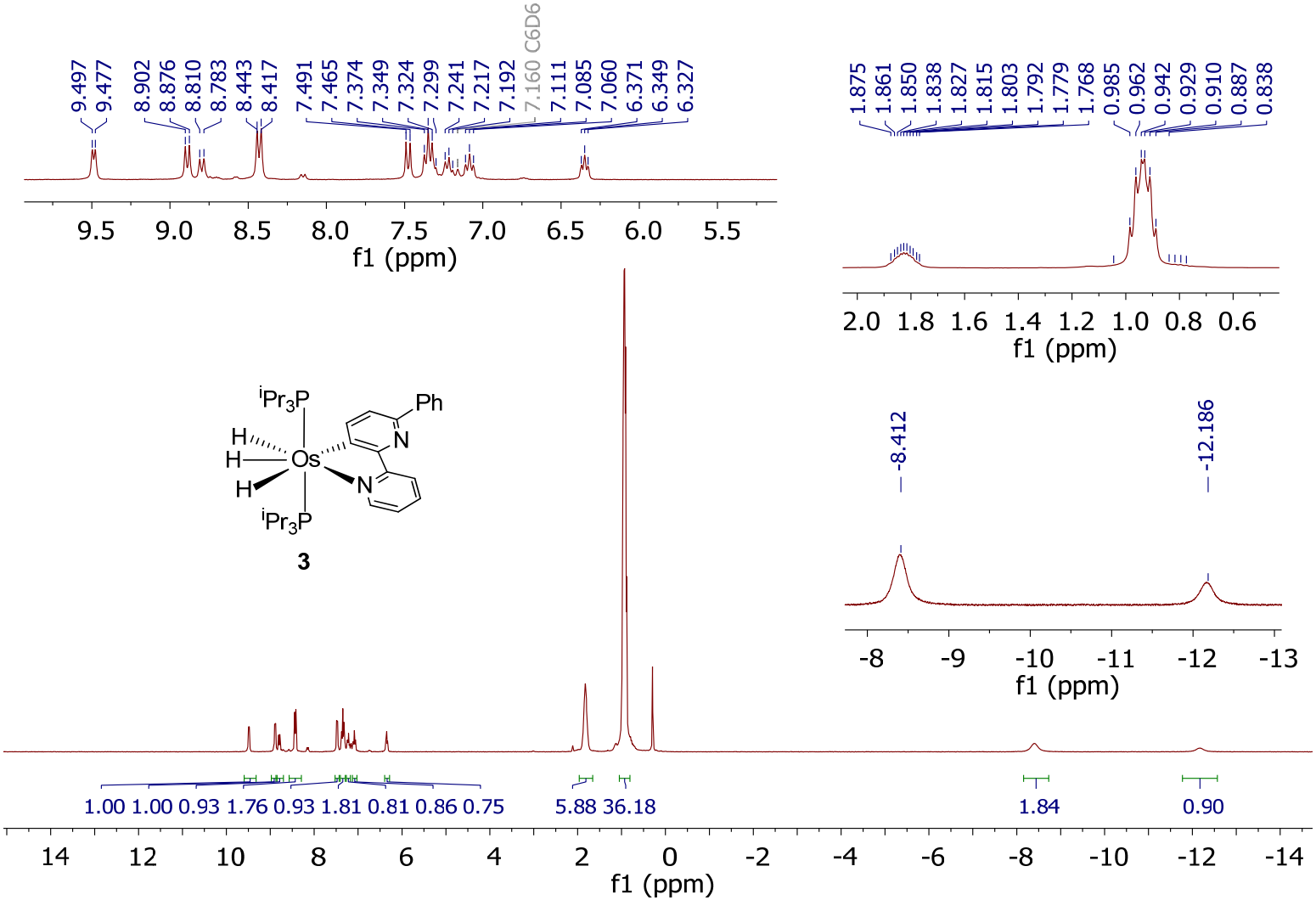

Figure S11. ^{1}H NMR spectrum (300.13 MHz, C_6D_6, 298 K) of compound **3**.

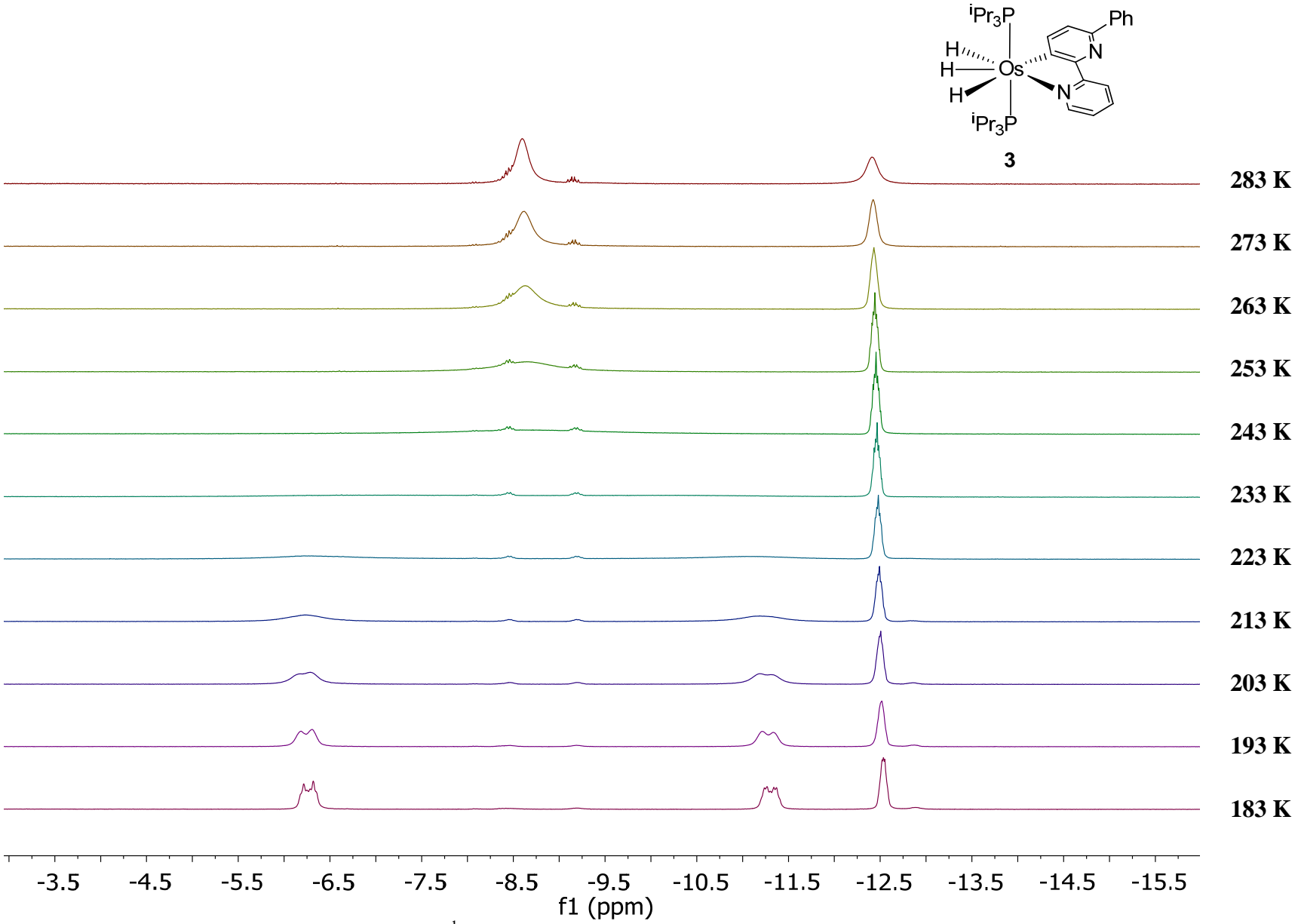

Figure S12. High field region of the ^{1}H NMR spectra (400 MHz, toluene-d_8) of compound **3** as a function of the temperature.

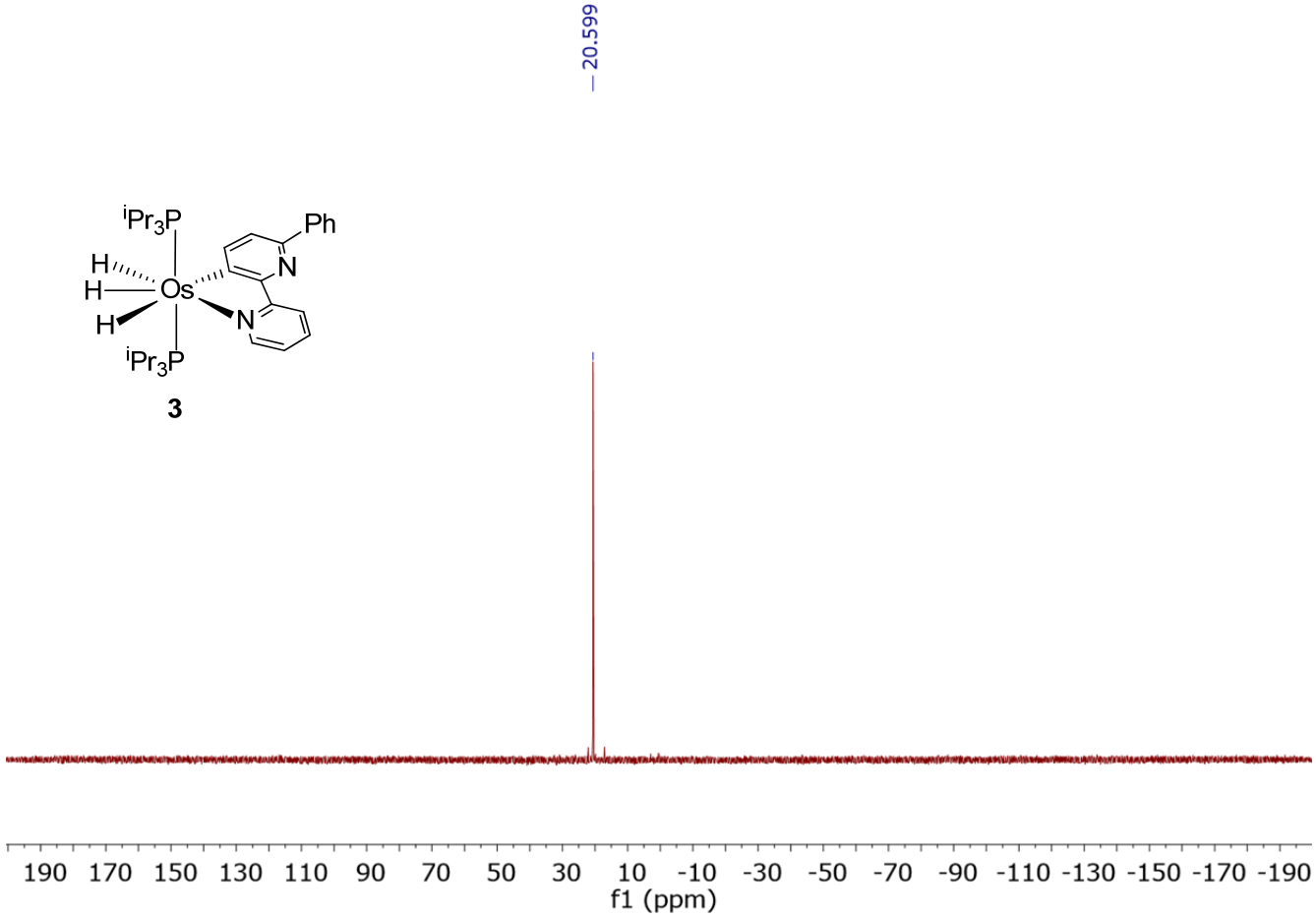

Figure S13. $^{31}P\{^{1}H\}$ NMR spectrum (121.49 MHz, C_6D_6, 298 K) of compound **3**.

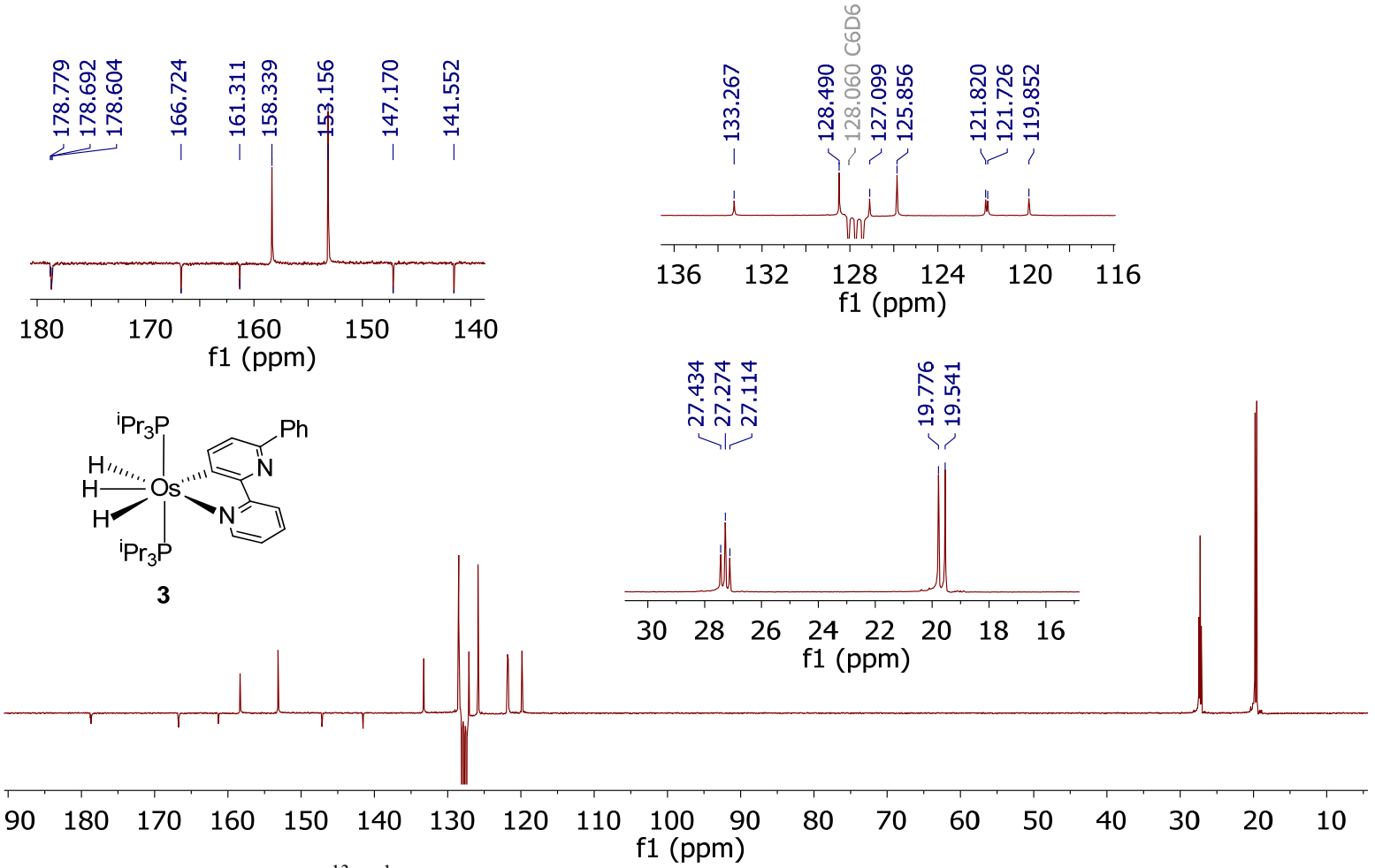

Figure S14. $^{13}C\{^{1}H\}$-apt NMR spectrum (75.48 MHz, C_6D_6, 298 K) of compound **3**.

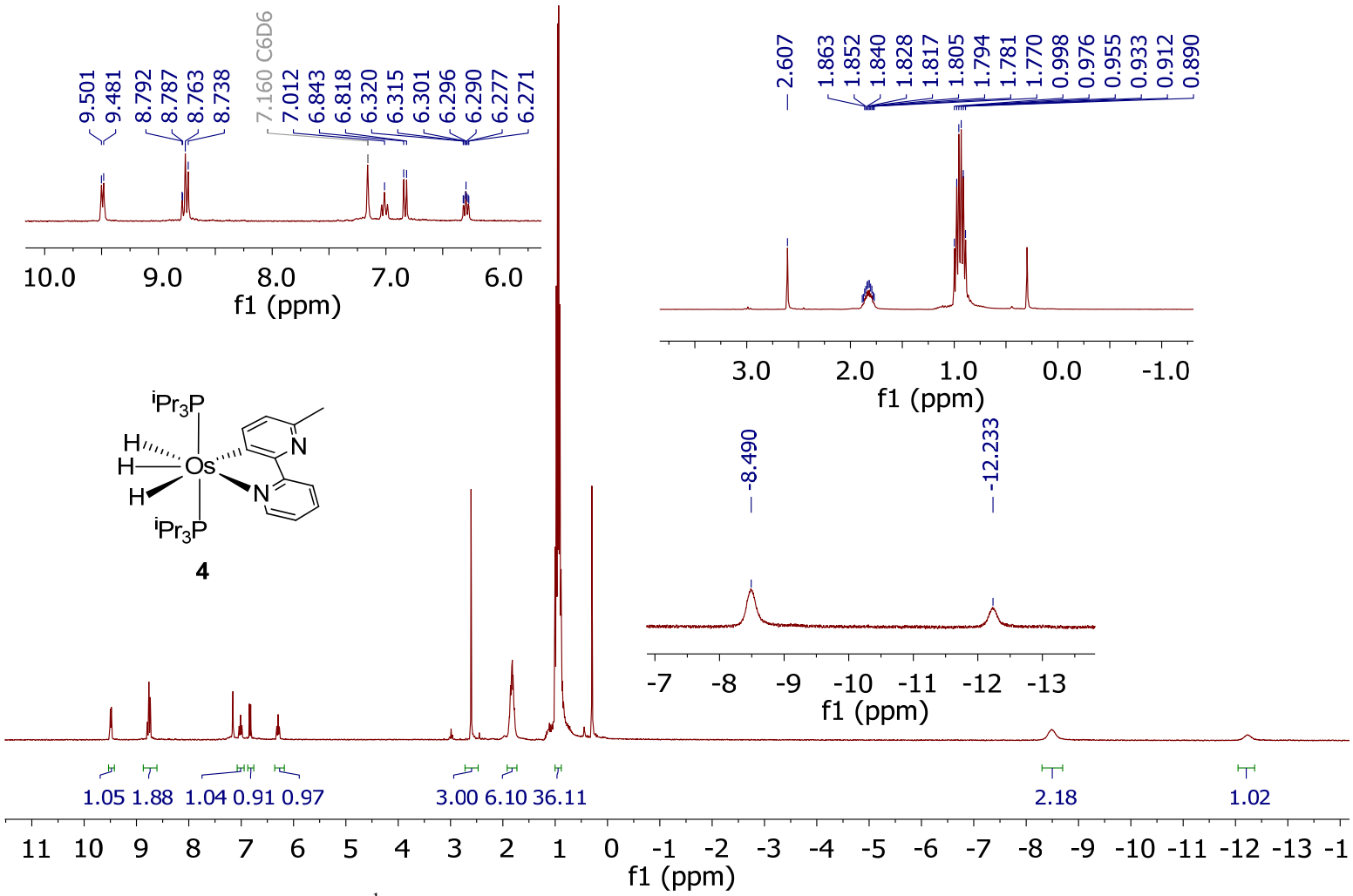

Figure S15. ^{1}H NMR spectrum (300.13 MHz, C_6D_6, 298 K) of compound **4**.

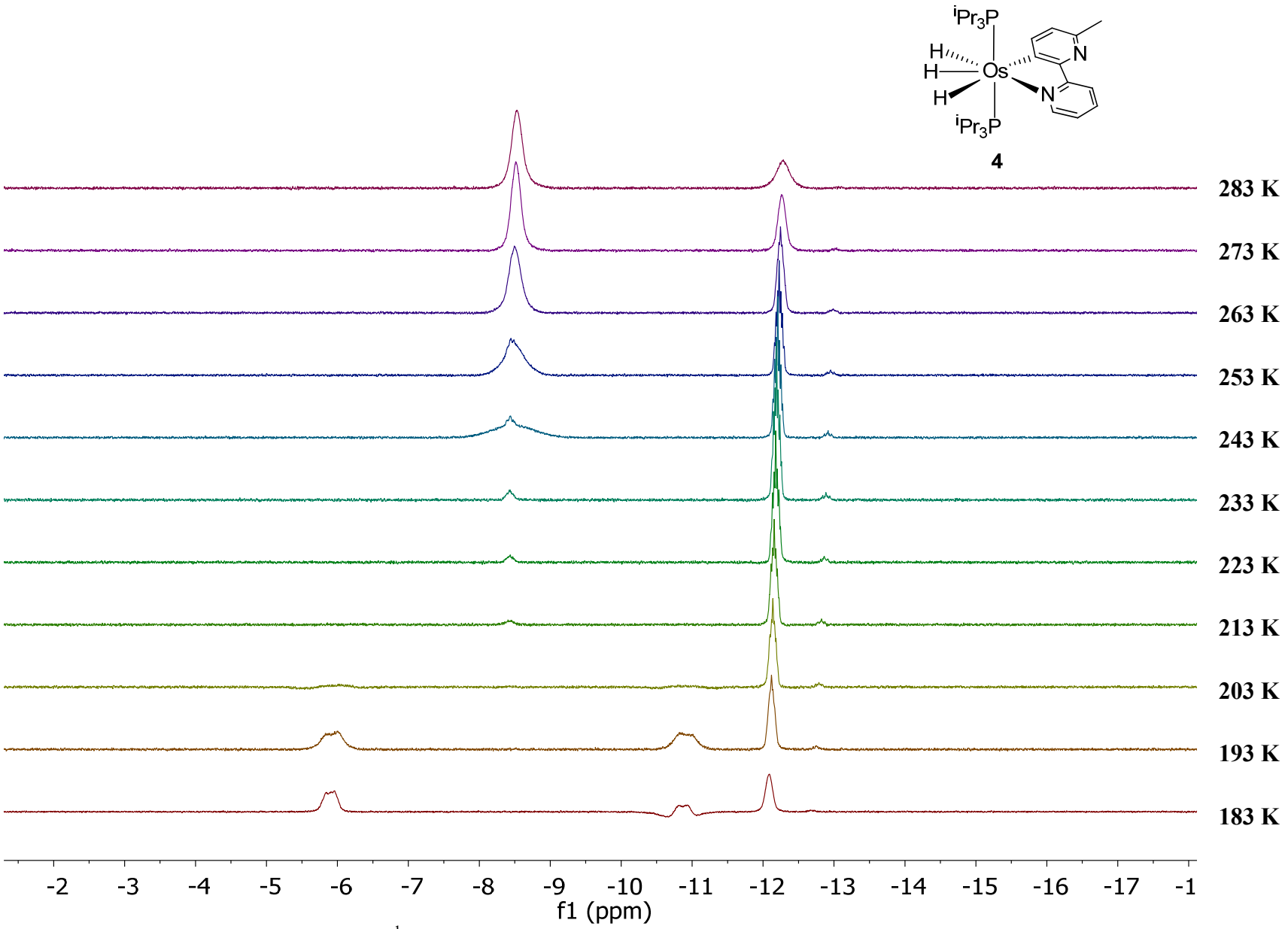

Figure S16. High field region of the ^{1}H NMR spectra (300.13 MHz, toluene-d_8) of compound **4** as a function of the temperature.

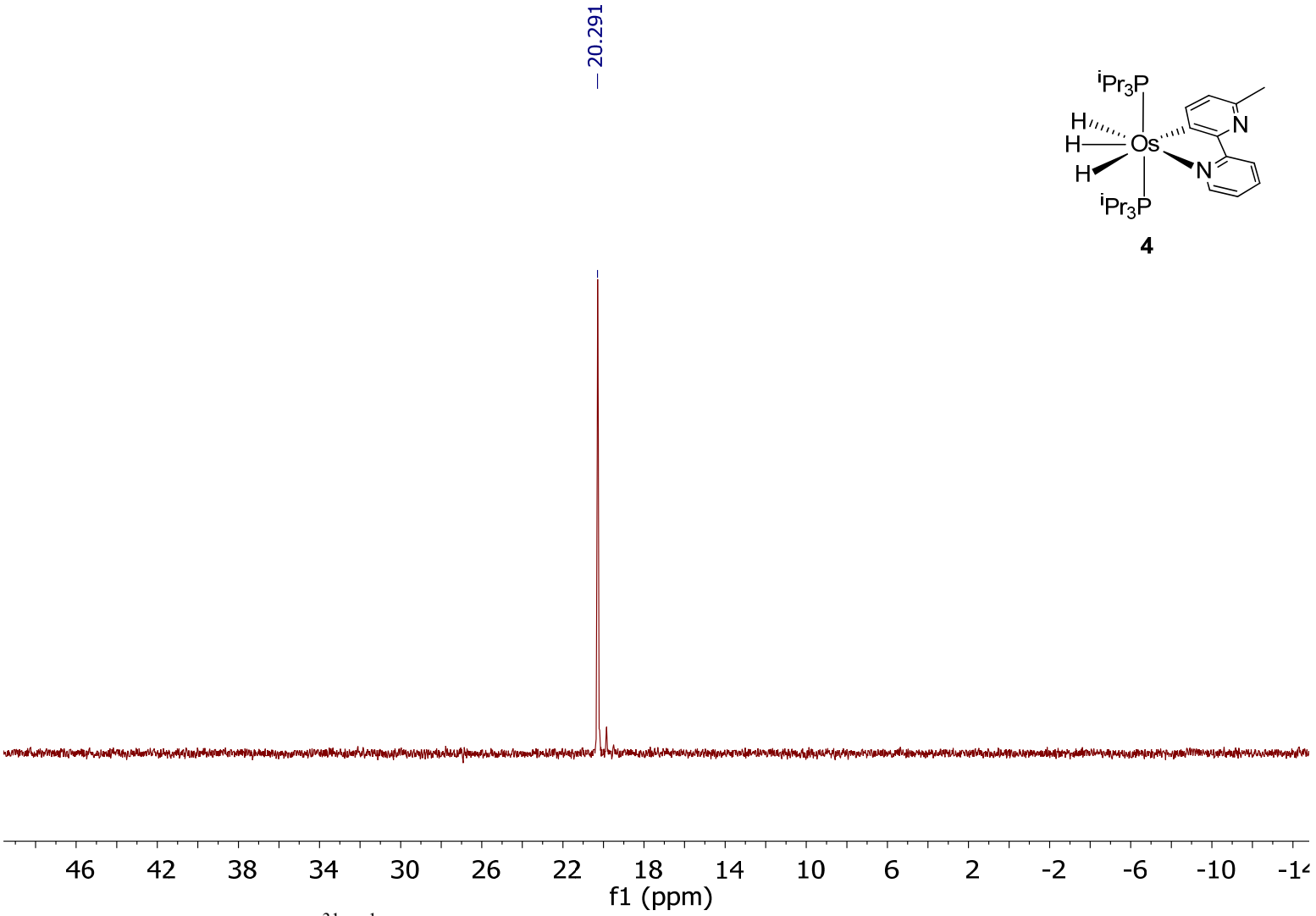

Figure S17. $^{31}P\{^{1}H\}$ NMR spectrum (121.49 MHz, toluene-d_8, 298 K) of compound **4.**

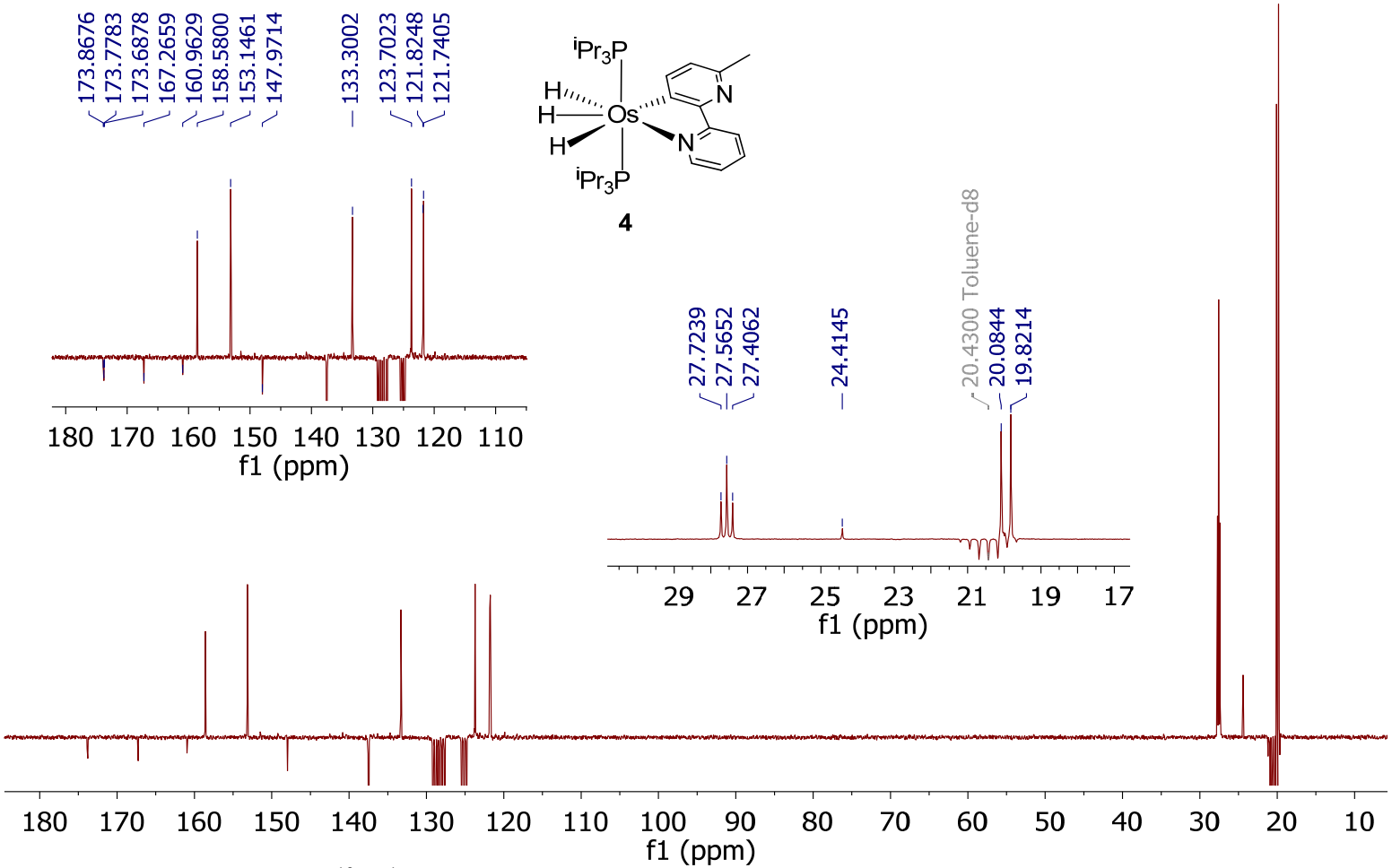

Figure S18. $^{13}C\{^{1}H\}$-apt NMR spectrum(75.48 MHz, toluene-d_8, 298 K) of compound **4**.

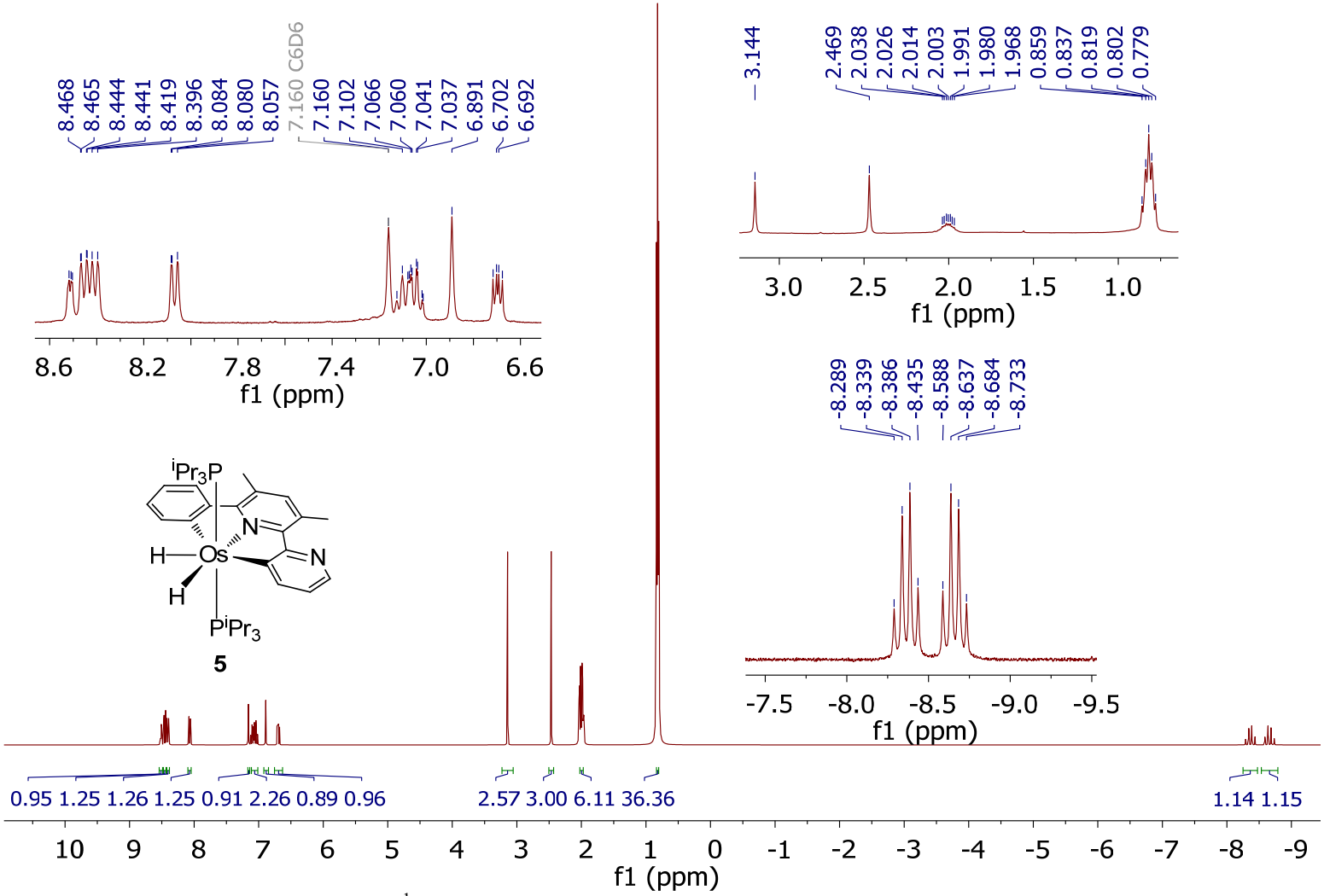

Figure S19. ^{1}H NMR spectrum (300.13 MHz, C_6D_6, 298 K) of compound **5**.

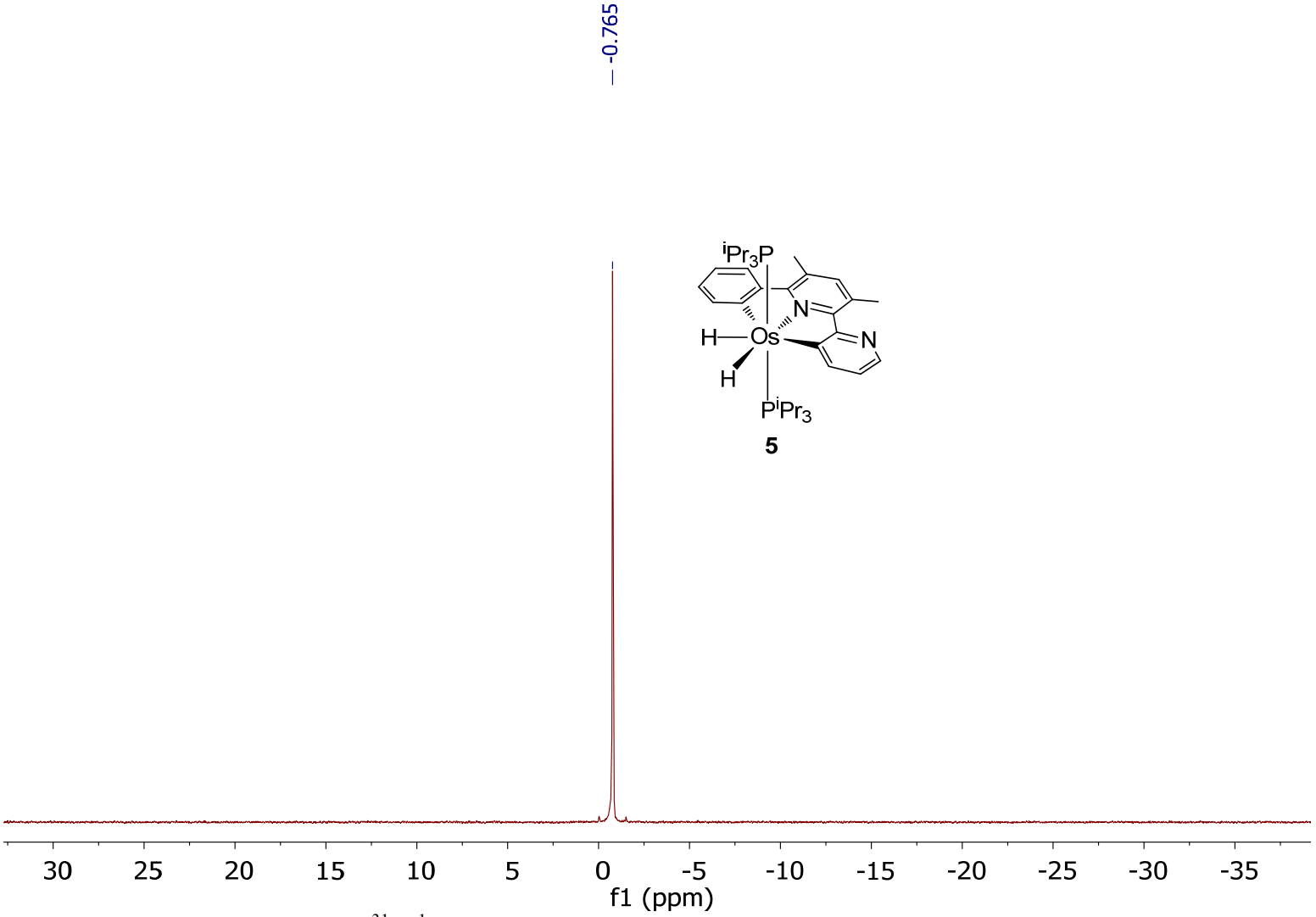

Figure S20. $^{31}P\{^{1}H\}$ NMR spectrum (121.49 MHz, C_6D_6, 298 K) of compound **5**.

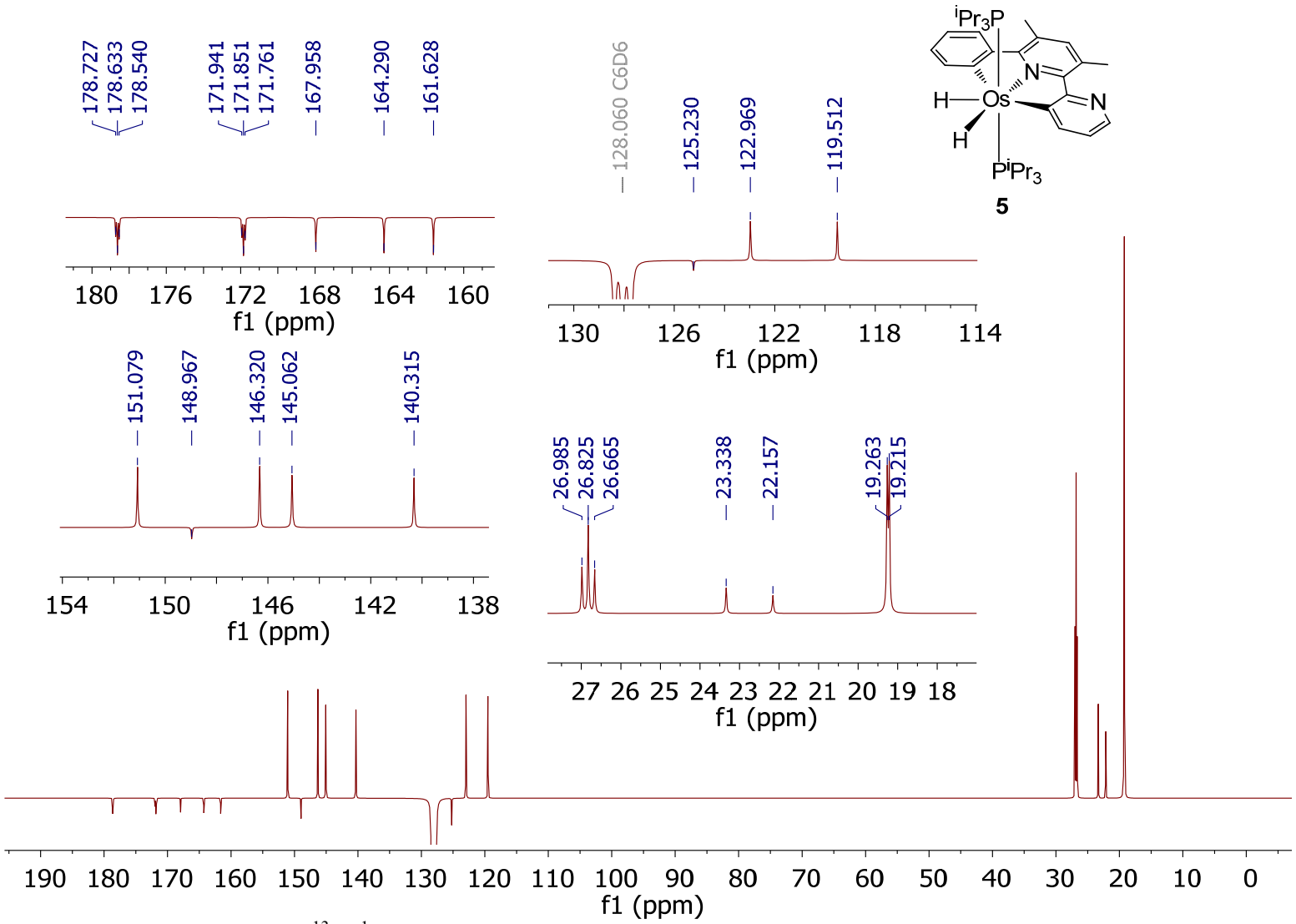

Figure S21. $^{13}C\{^{1}H\}$-apt NMR spectrum (75.48 MHz, C_6D_6, 298 K) of compound **5**.

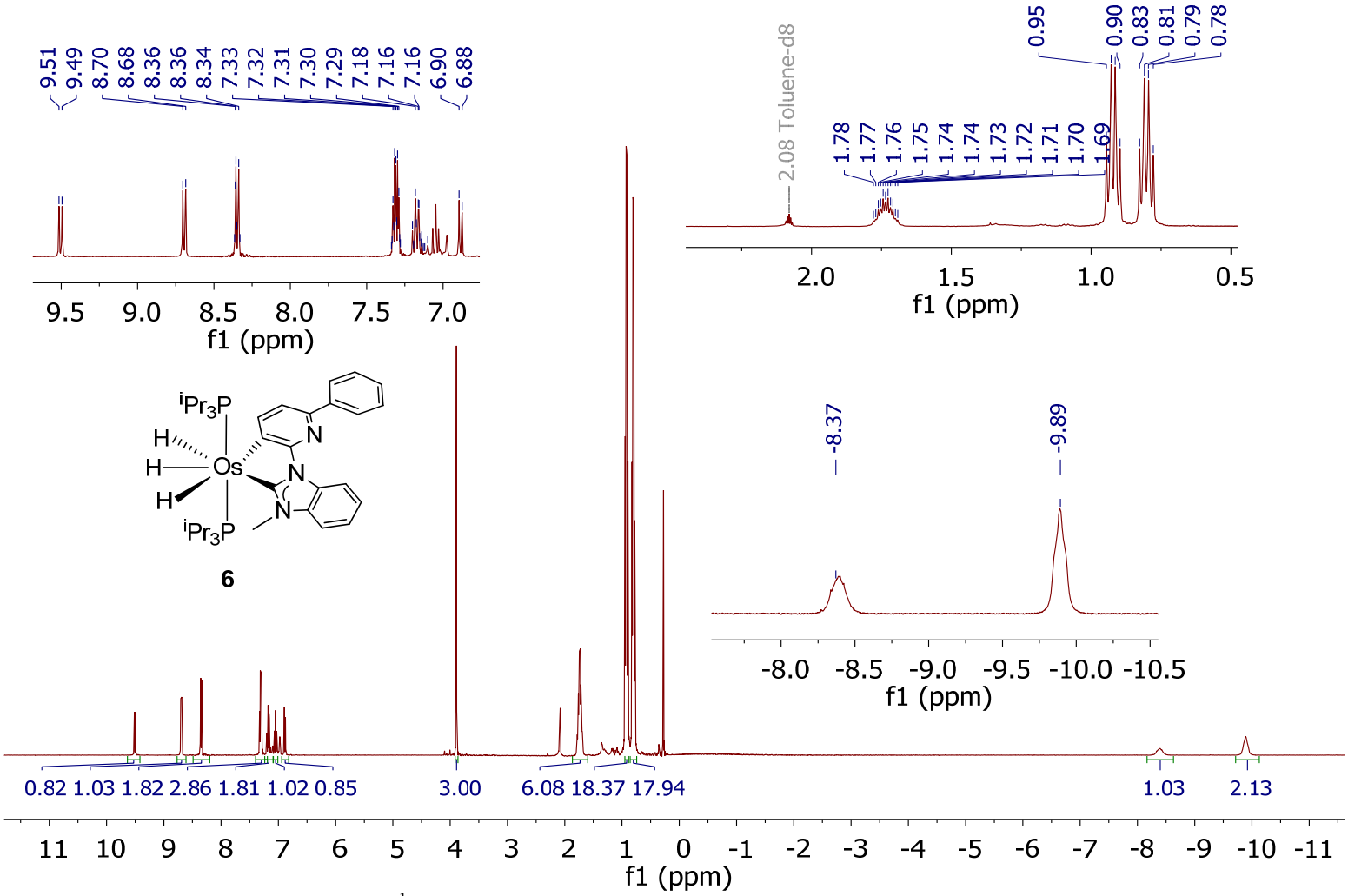

Figure S22. ^{1}H NMR spectrum (400 MHz, toluene-d_8, 298 K) of compound **6**.

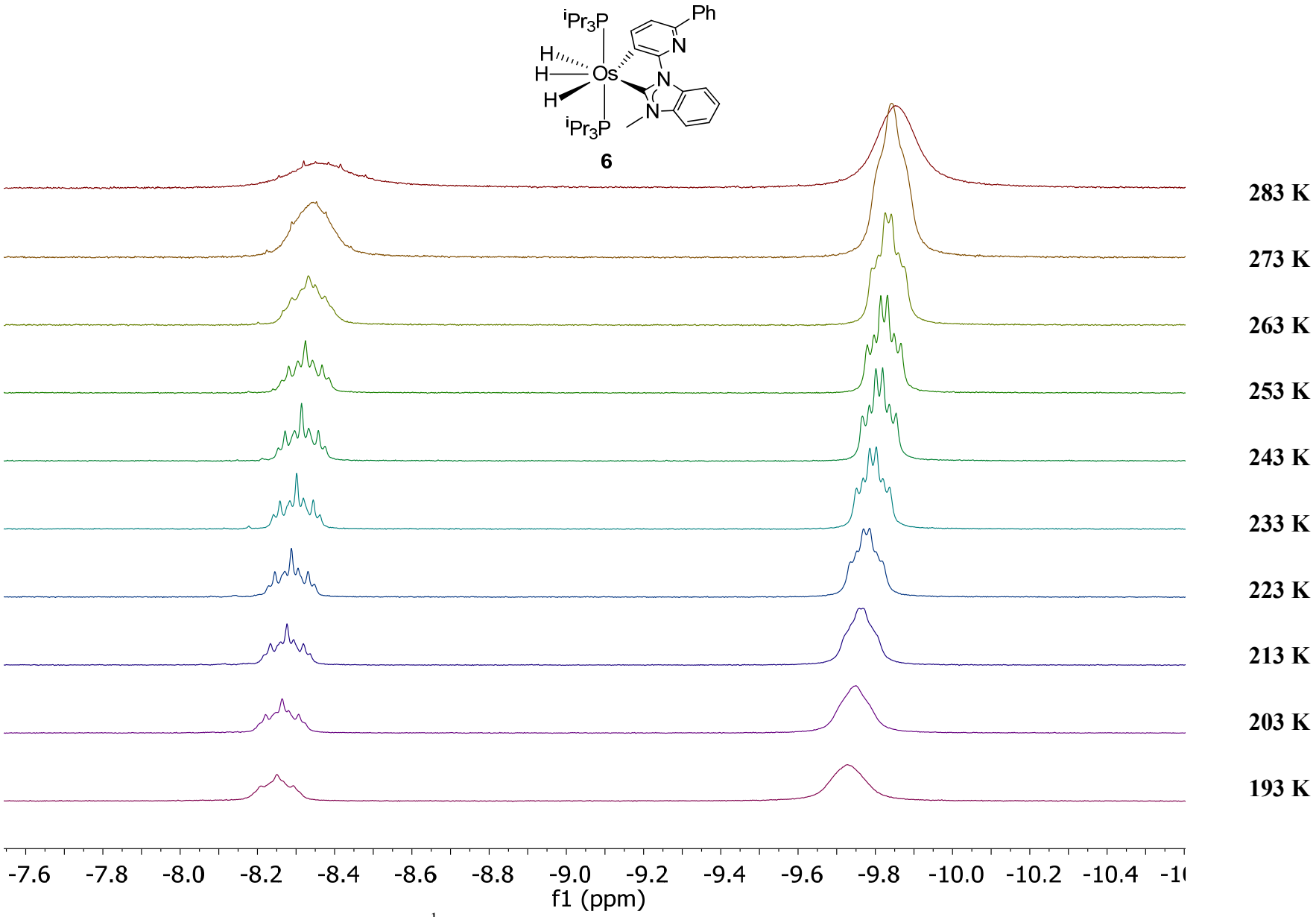

Figure S23. High field region of the ^{1}H NMR spectra (400 MHz, toluene-d_8) of compound **6** as a function of the temperature.

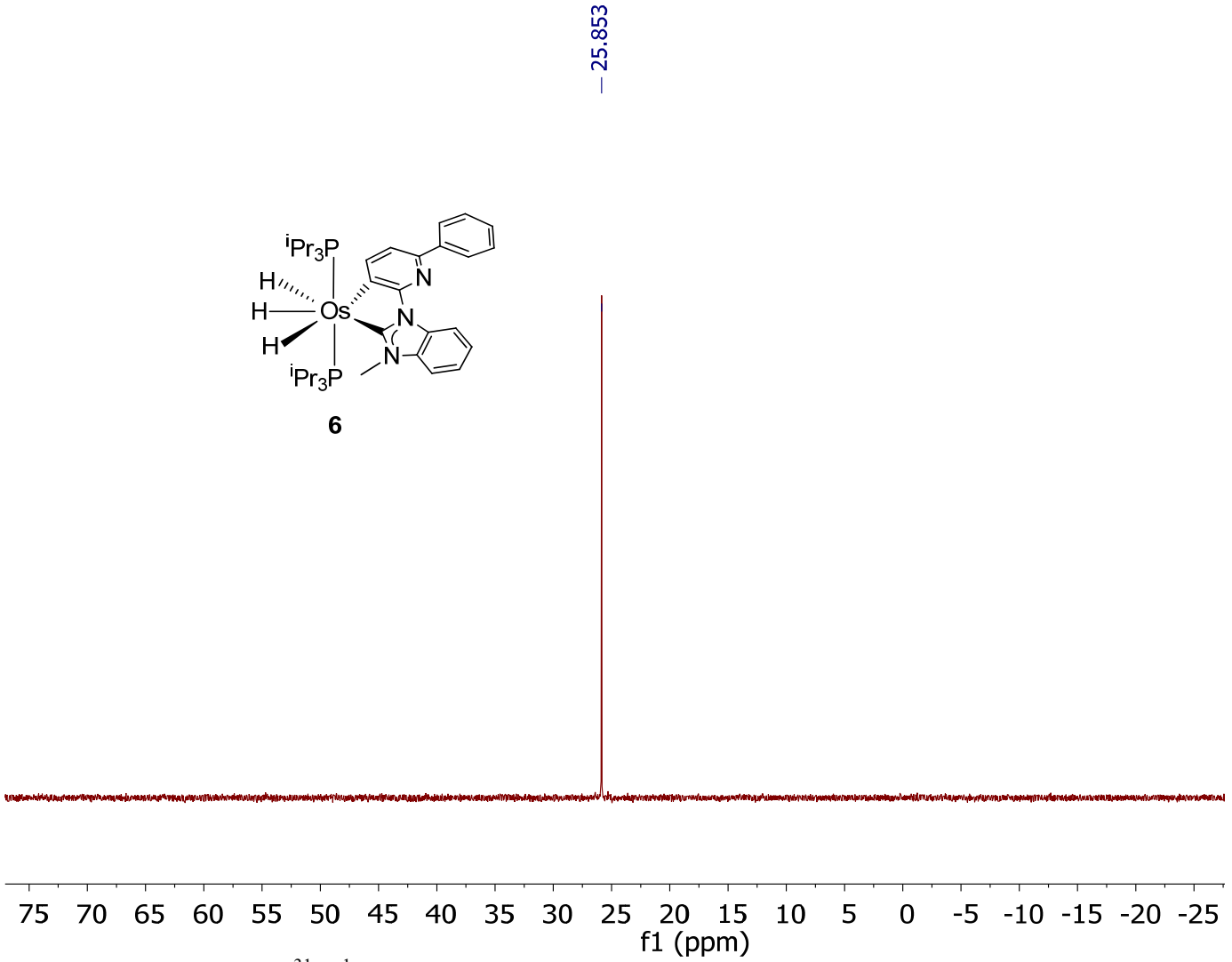

Figure S24. $^{31}P\{^{1}H\}$ NMR spectrum (121.49 MHz, C_6D_6, 298 K) of compound **6.**

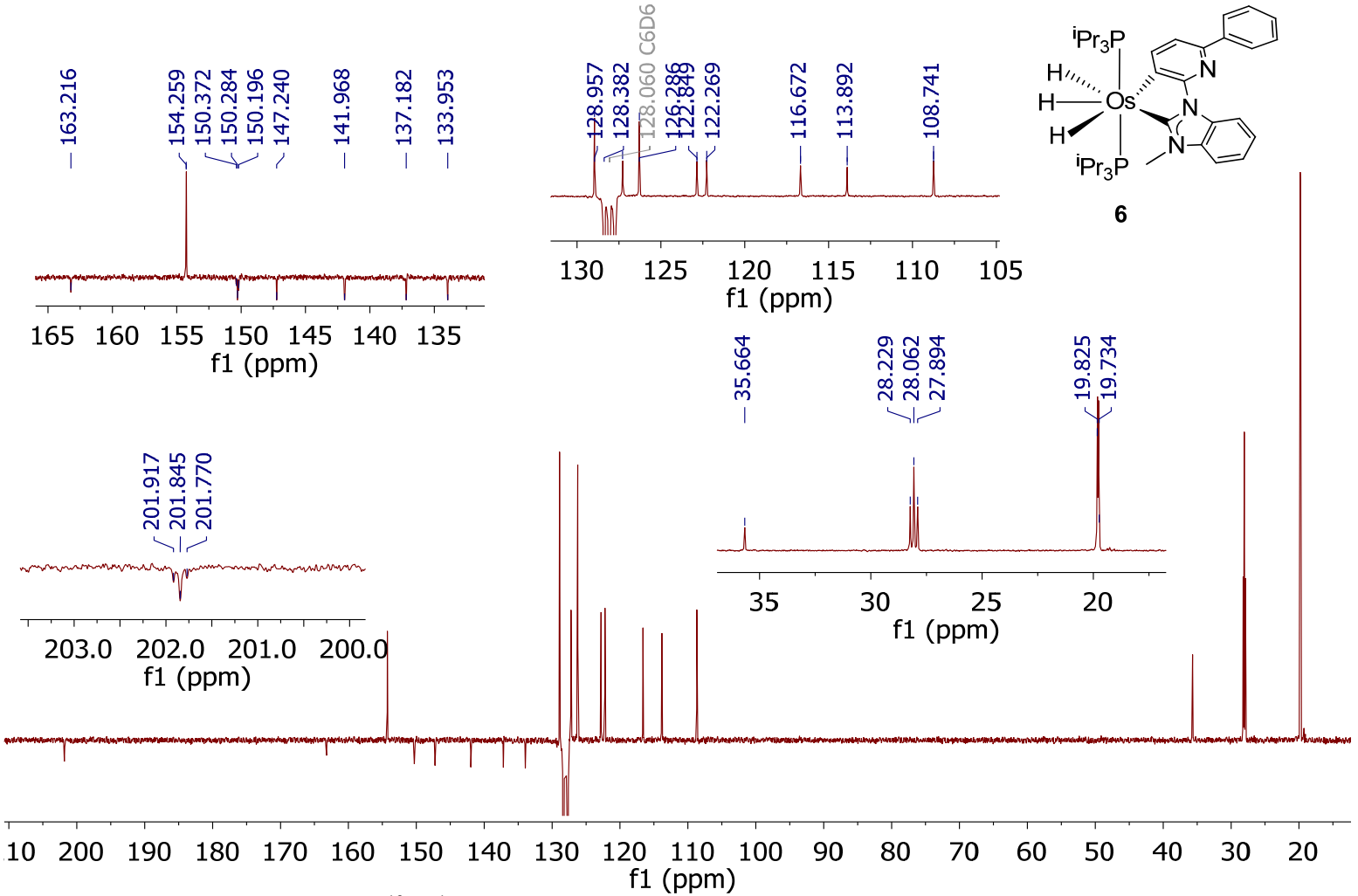

Figure S25. $^{13}C\{^{1}H\}$-apt NMR spectrum (75. 48 MHz, C_6D_6, 298 K) of compound **6**.

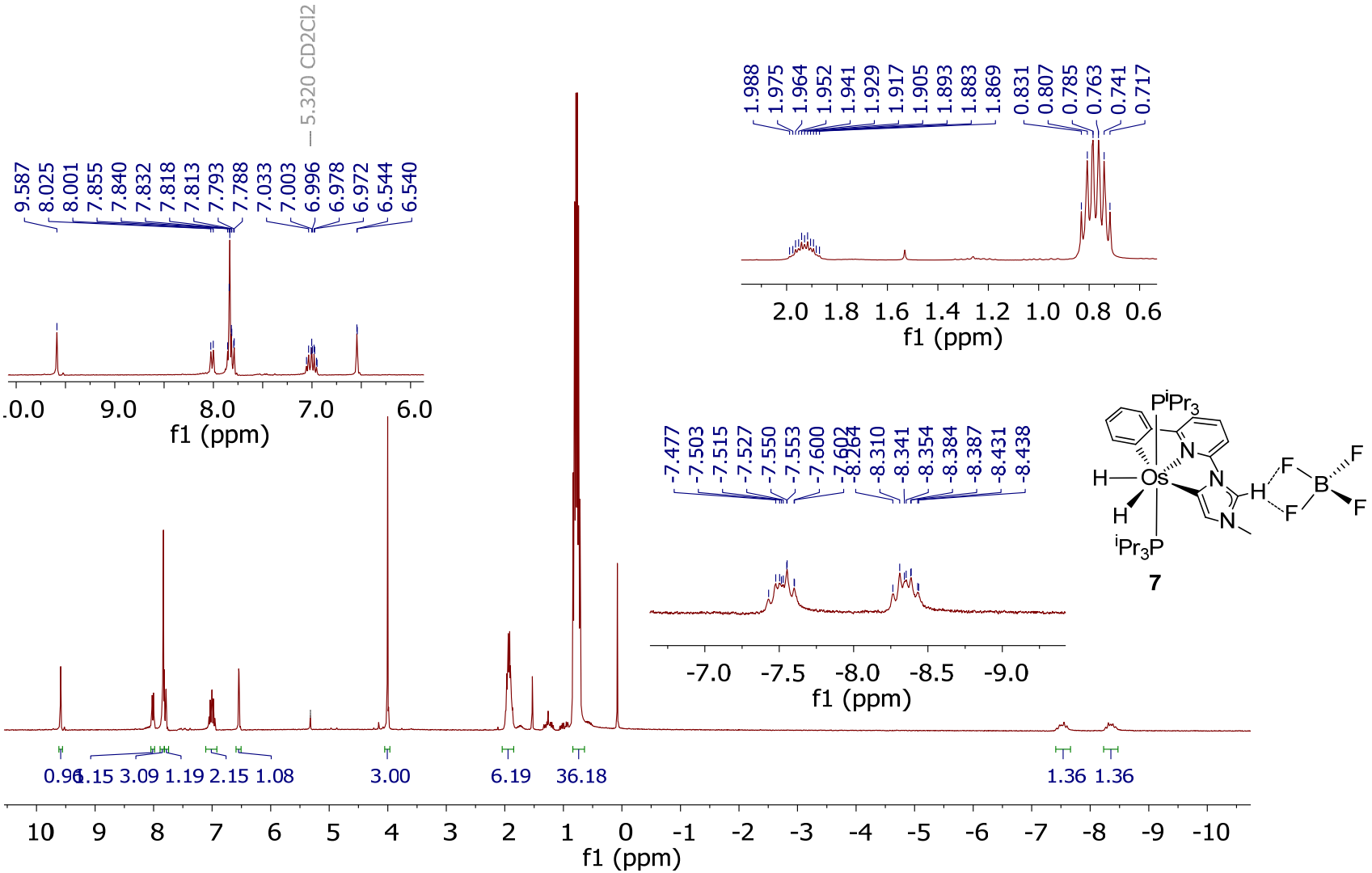

Figure S26. ^{1}H NMR spectrum (300.13 MHz, CD_2Cl_2, 298 K) of compound **7**.

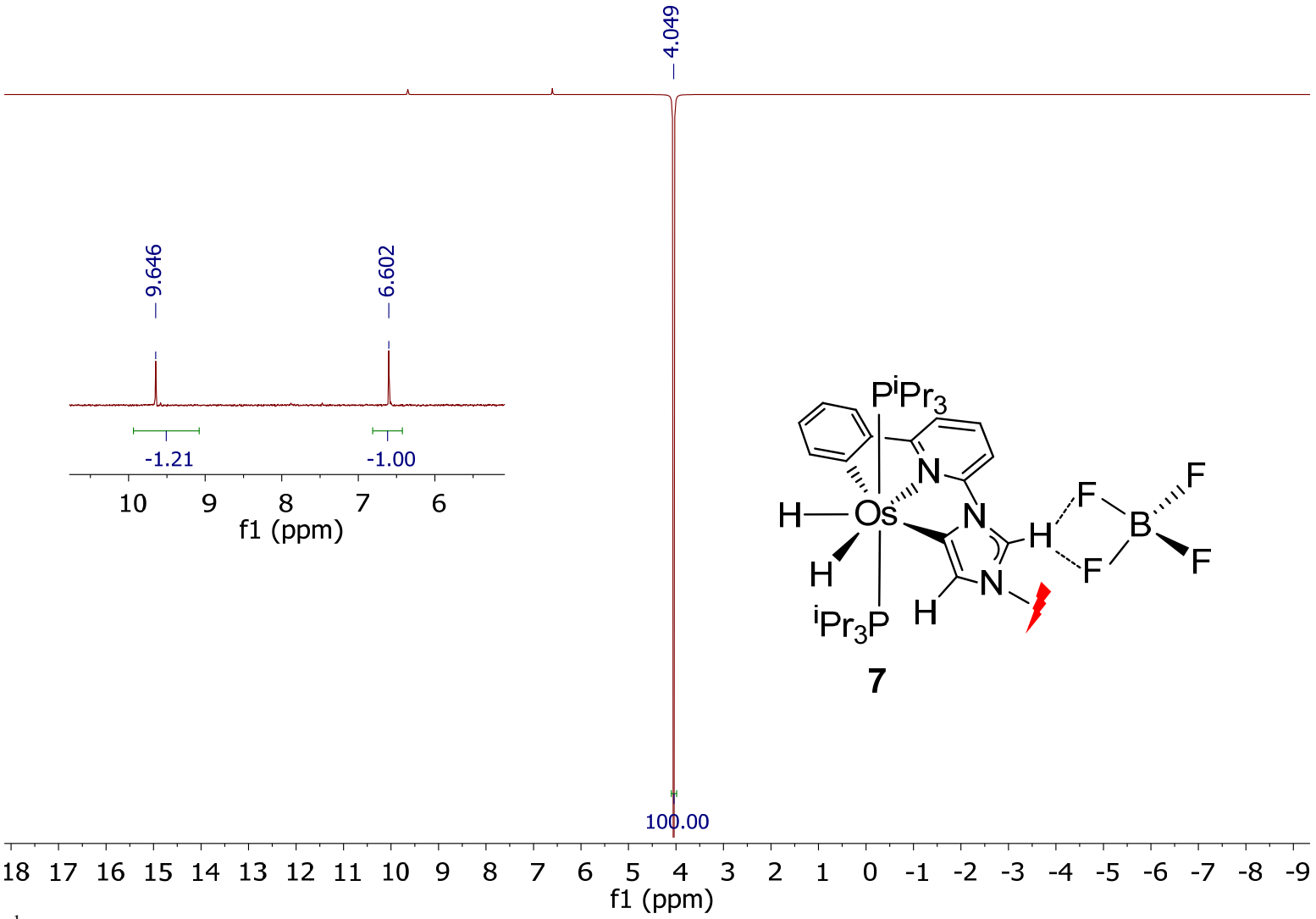

Figure S27. ^{1}H NMR 1D-NOE (400.13 MHz, CD_2Cl_2, 298 K) spectrum of compound **7** obtained by selective excitation of the signal at 4.00 ppm (mixing time d8 = 0.364 s).

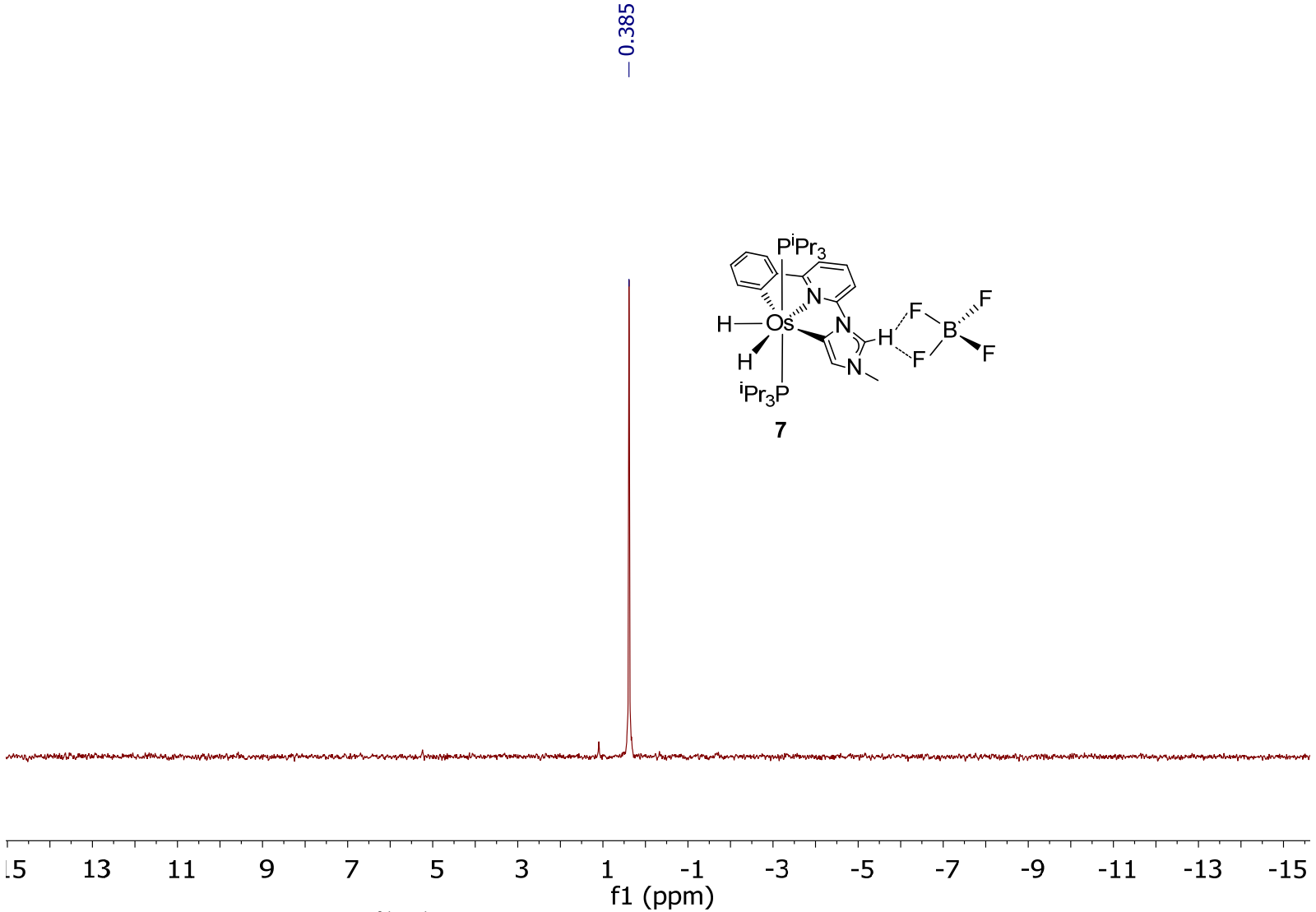

Figure S28. $^{31}P\{^{1}H\}$ NMR spectrum (121.49 MHz, CD_2Cl_2, 298 K) of compound **7**.

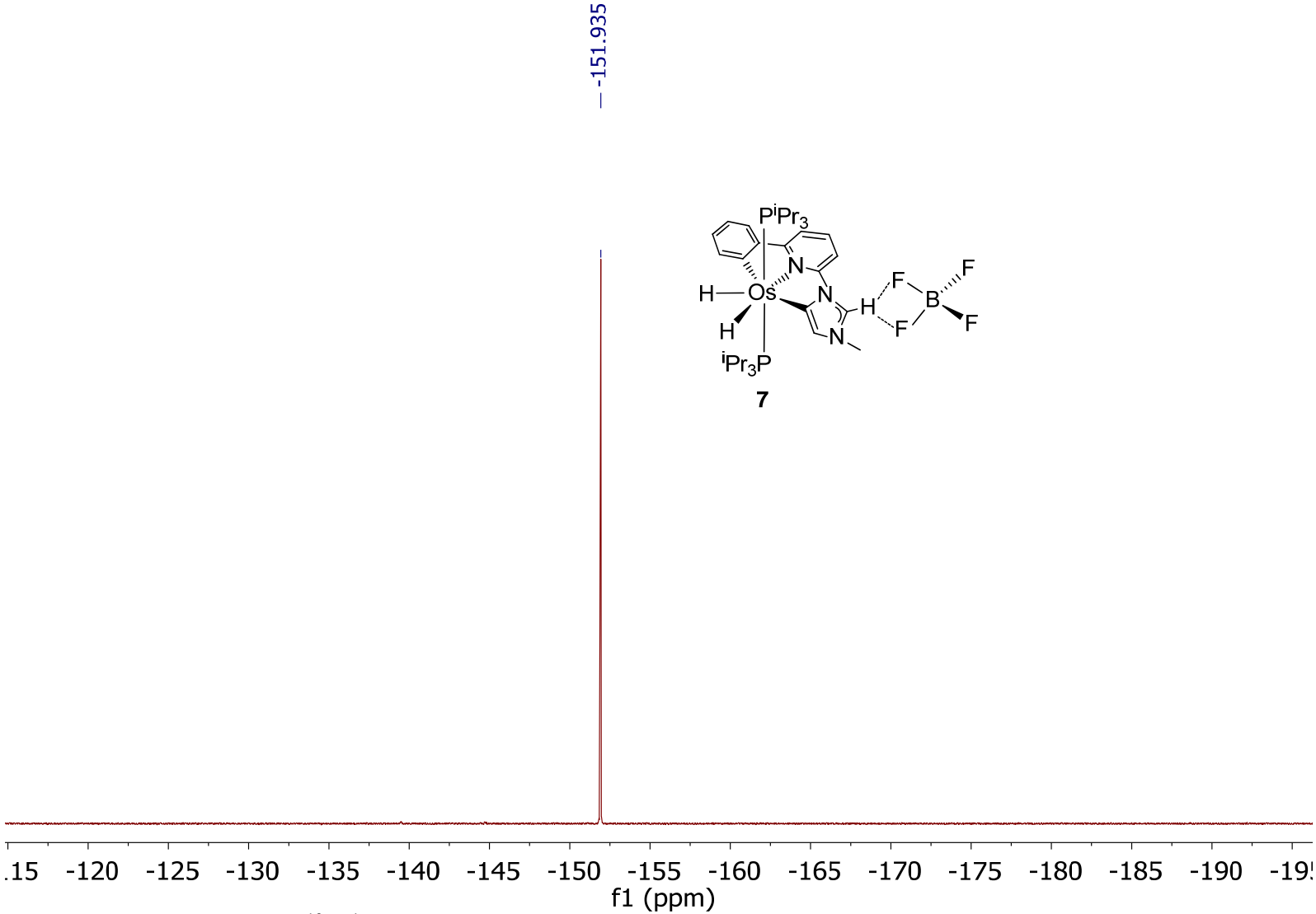

Figure S29. $^{19}F\{^1H\}$ NMR spectrum (376.49 MHz, CD_2Cl_2, 298 K) of compound **7**.

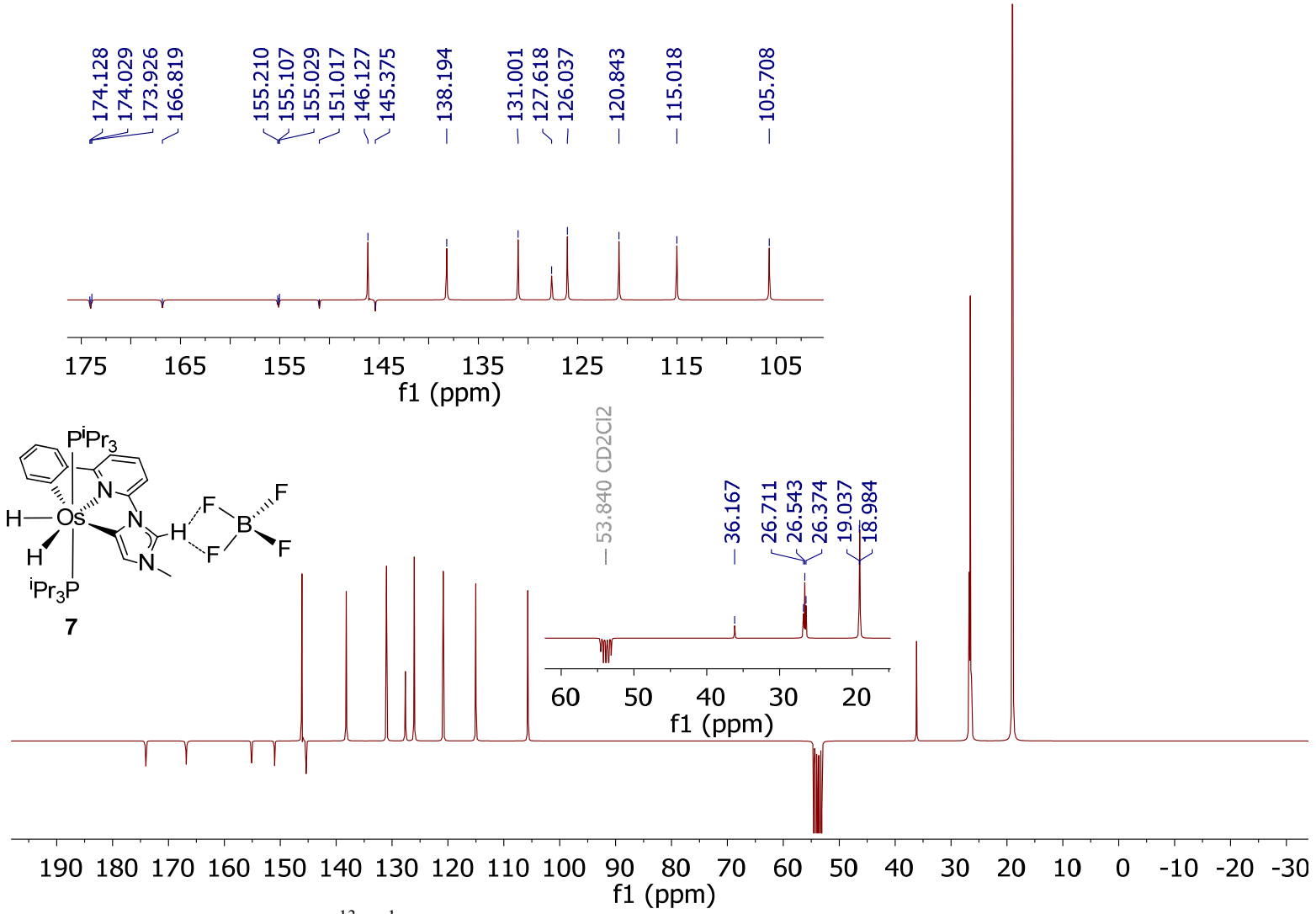

Figure S30. $^{13}C\{^{1}H\}$-apt NMR spectrum (75.48 MHz, CD_2Cl_2, 298 K) of compound **7**.

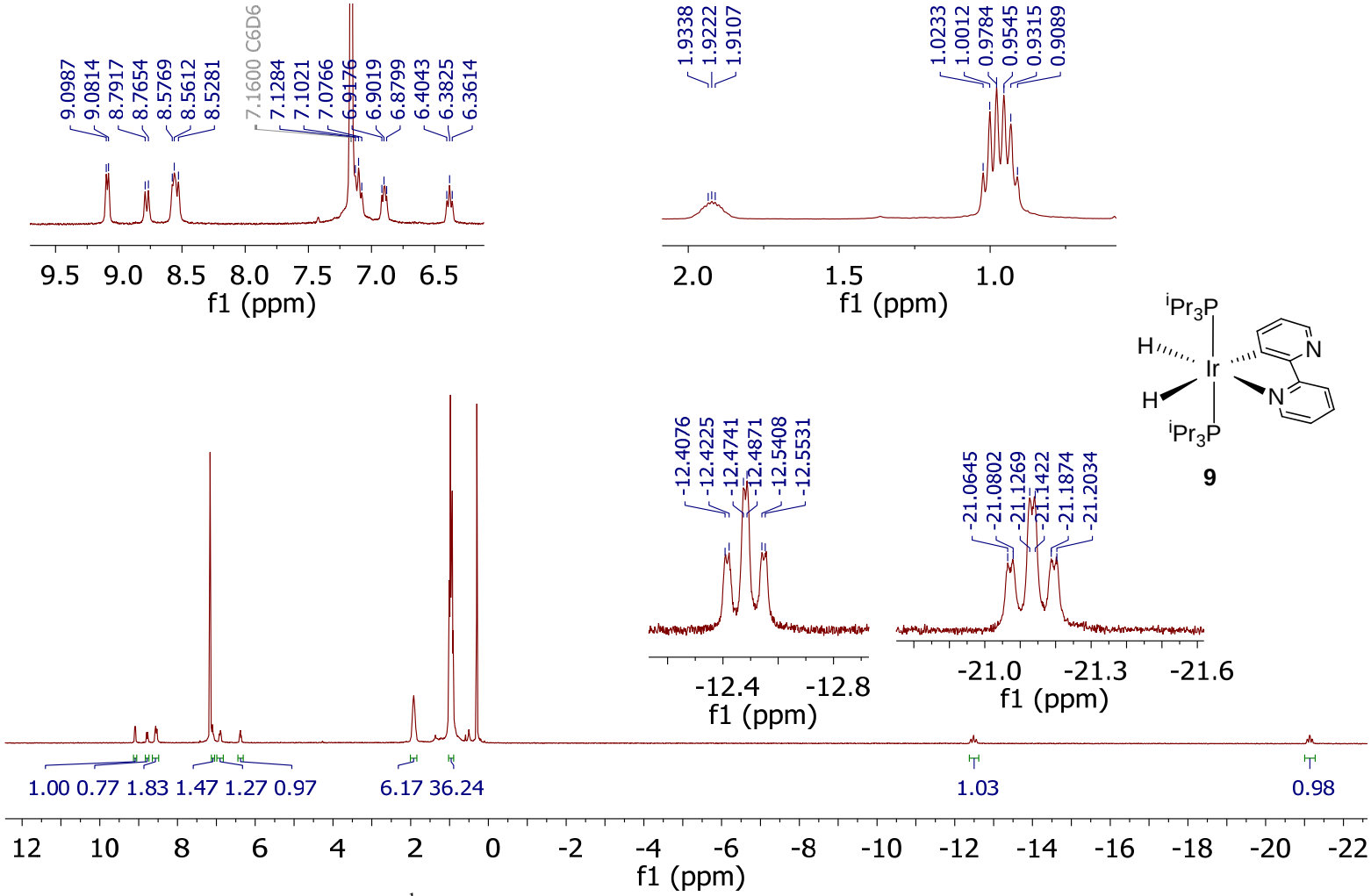

Figure S31. ^{1}H NMR spectrum (300.13 MHz C_6D_6, 298 K) of compound **9**.

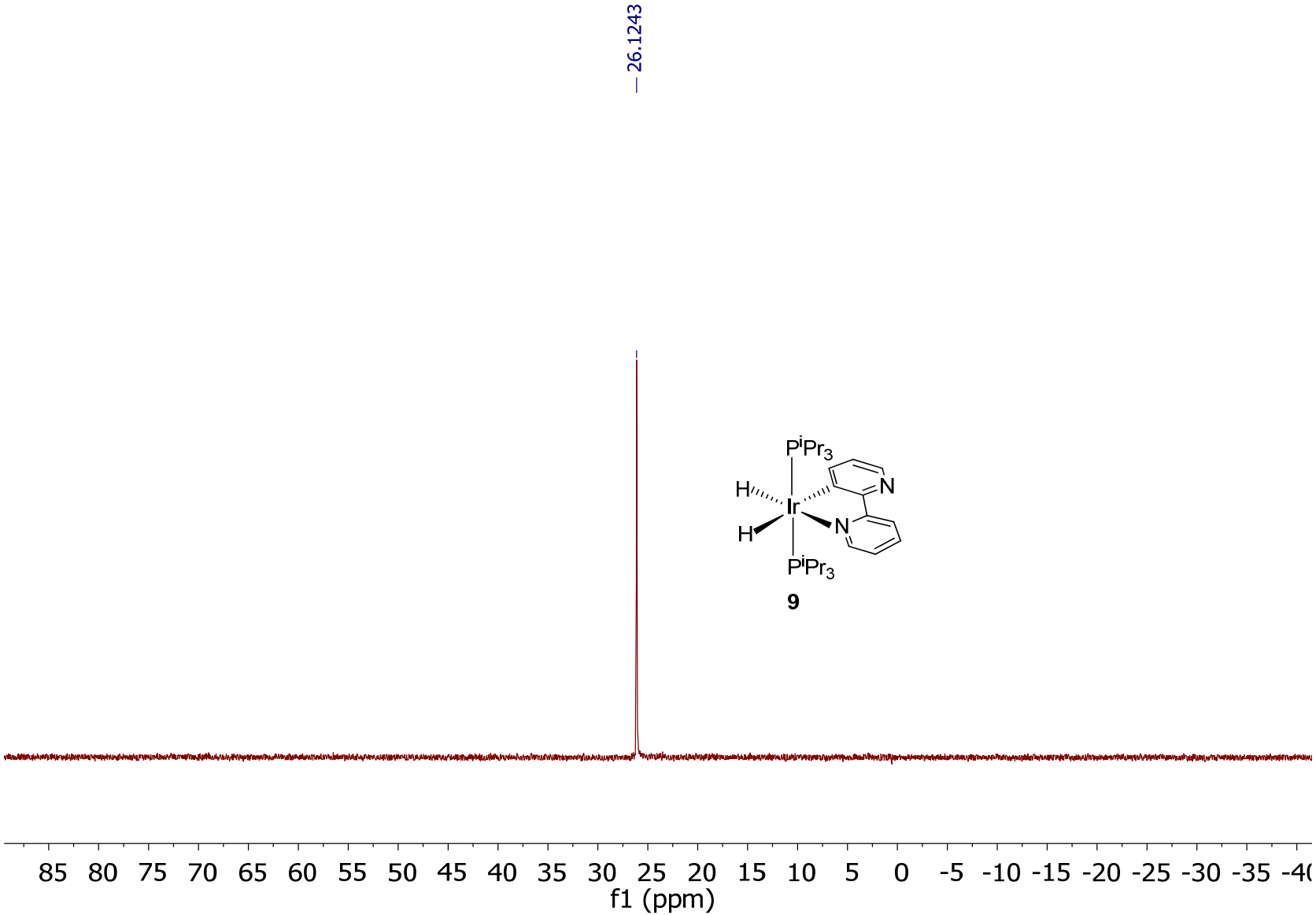

Figure S32. $^{31}P\{^{1}H\}$ NMR spectrum (121.49 MHz C_6D_6, 298 K) of compound **9**.

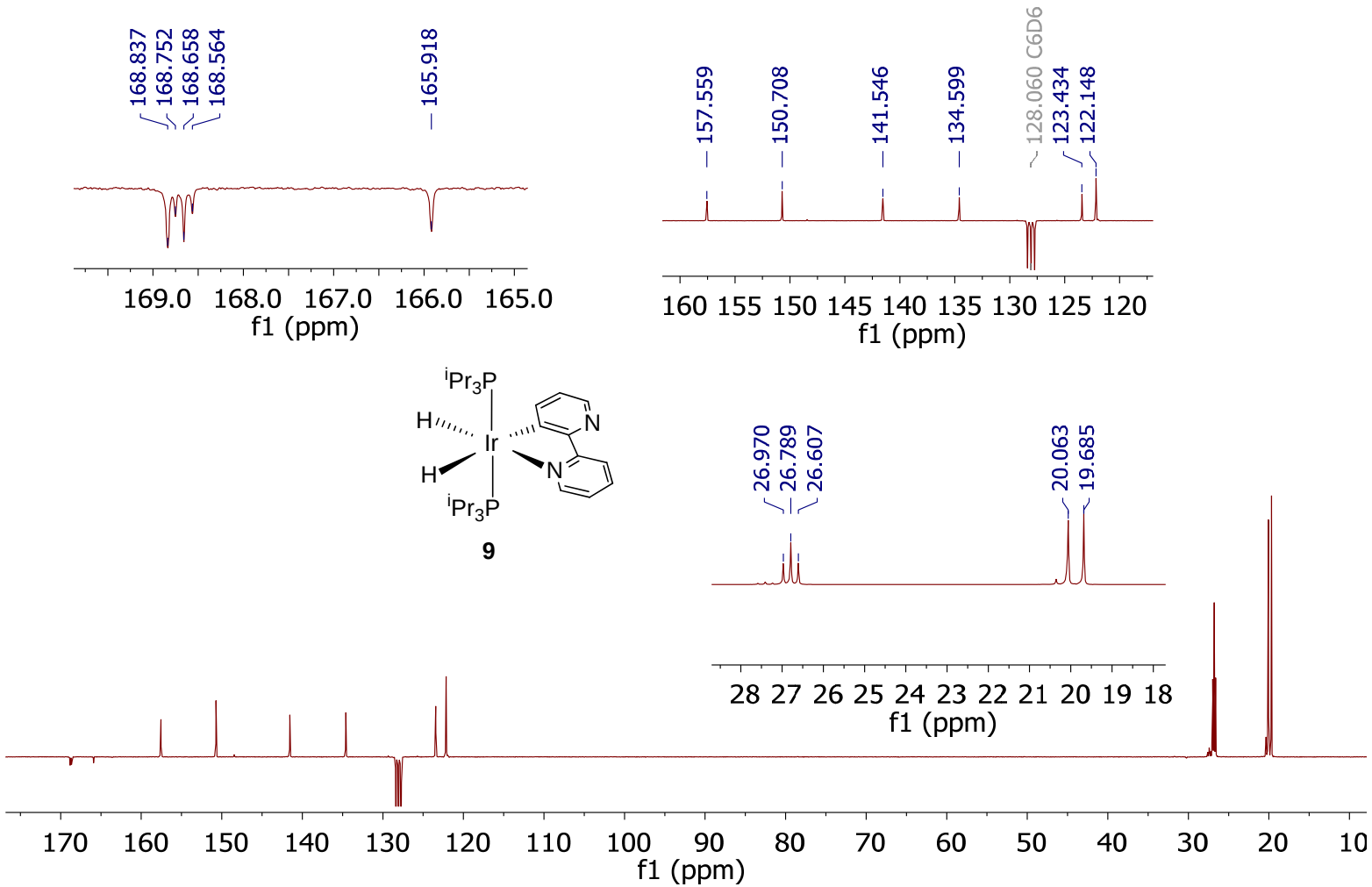

Figure S33. $^{13}C\{^{1}H\}$-apt NMR spectrum (75.48 MHz C_6D_6, 298 K) of compound **9**.

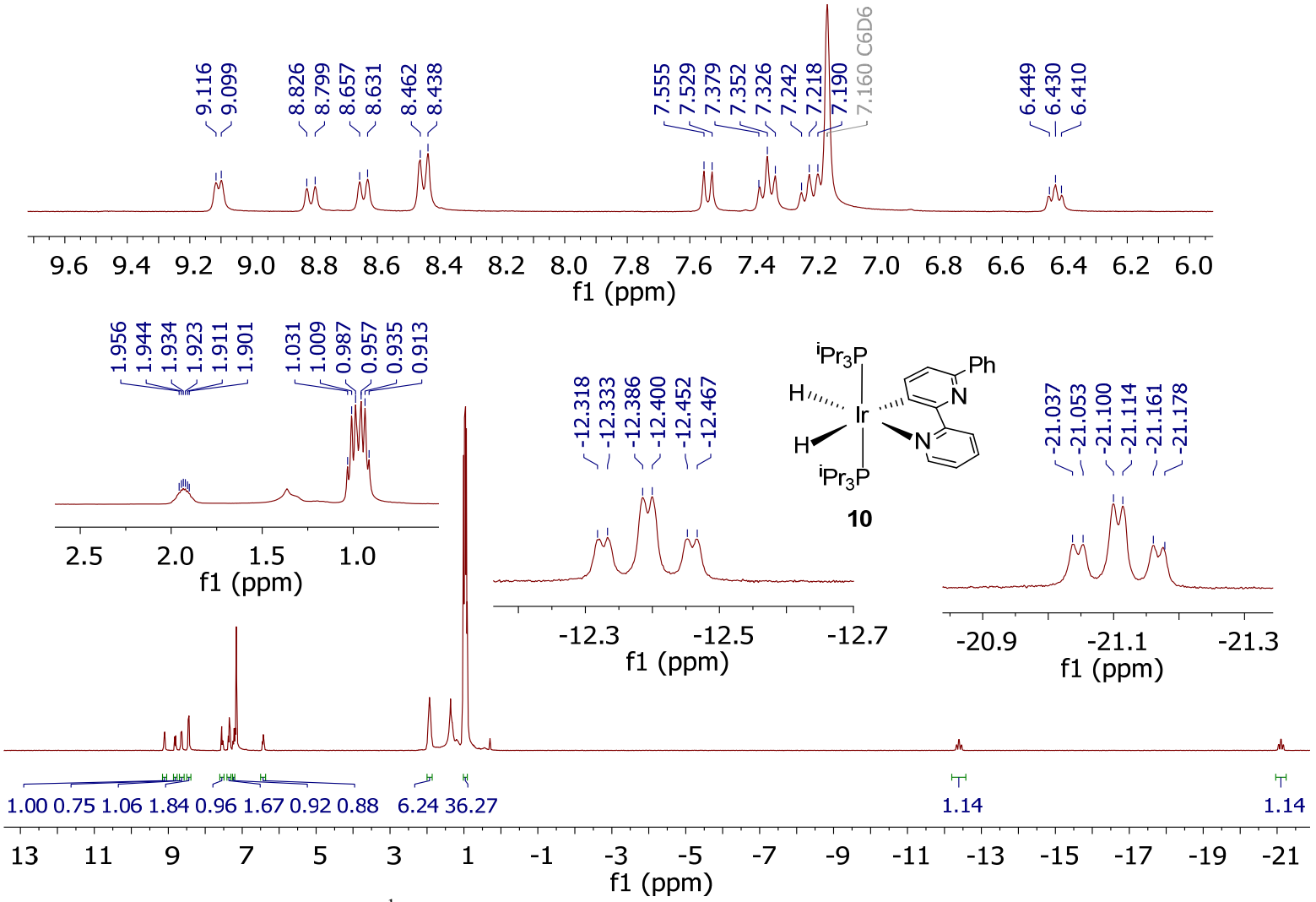

Figure S34. ^{1}H NMR spectrum (300.13 MHz, C_6D_6, 298 K) of compound **10**.

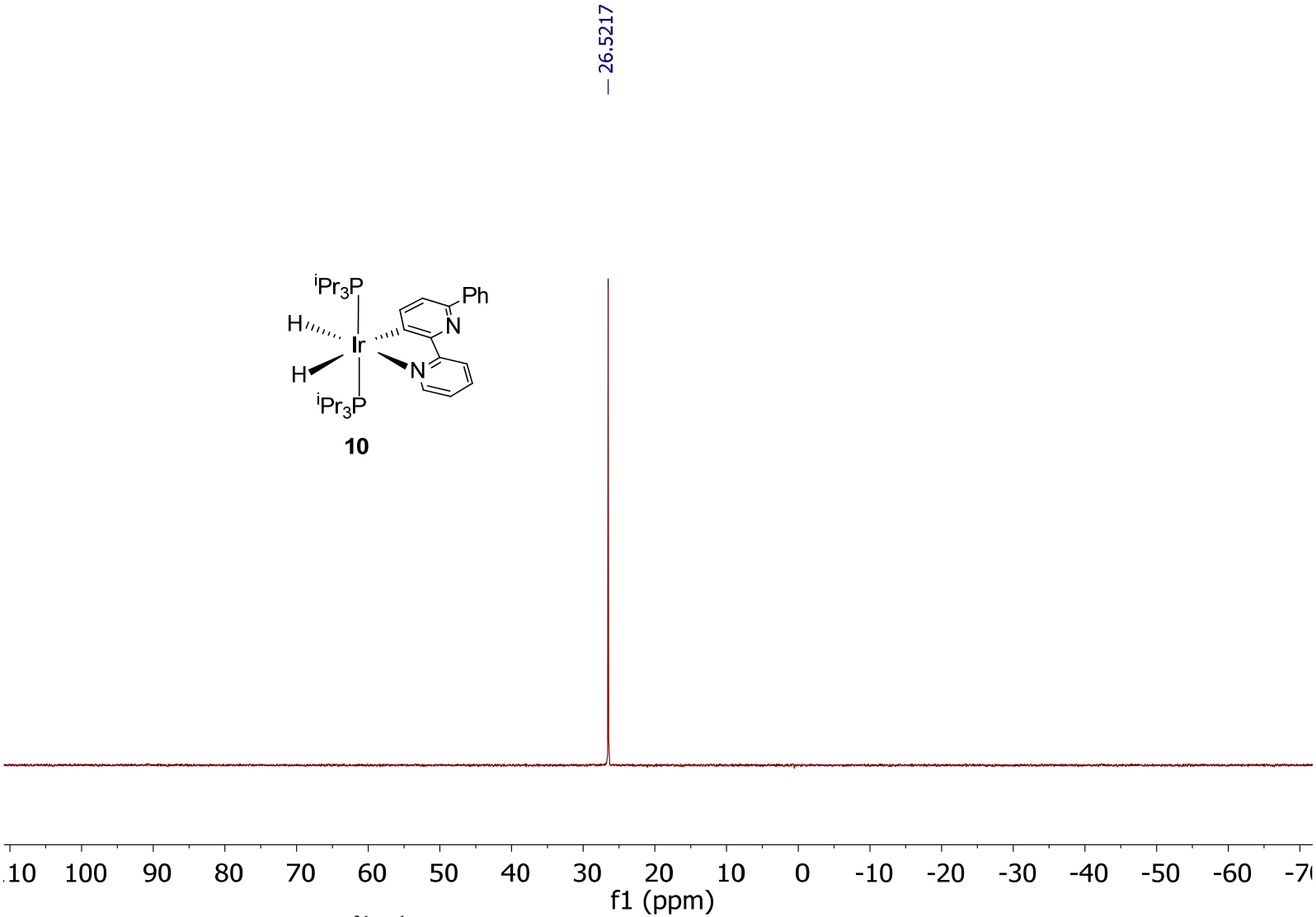

Figure S35. $^{31}P\{^{1}H\}$ NMR spectrum (121.49 MHz, C_6D_6, 298 K) of compound **10**.

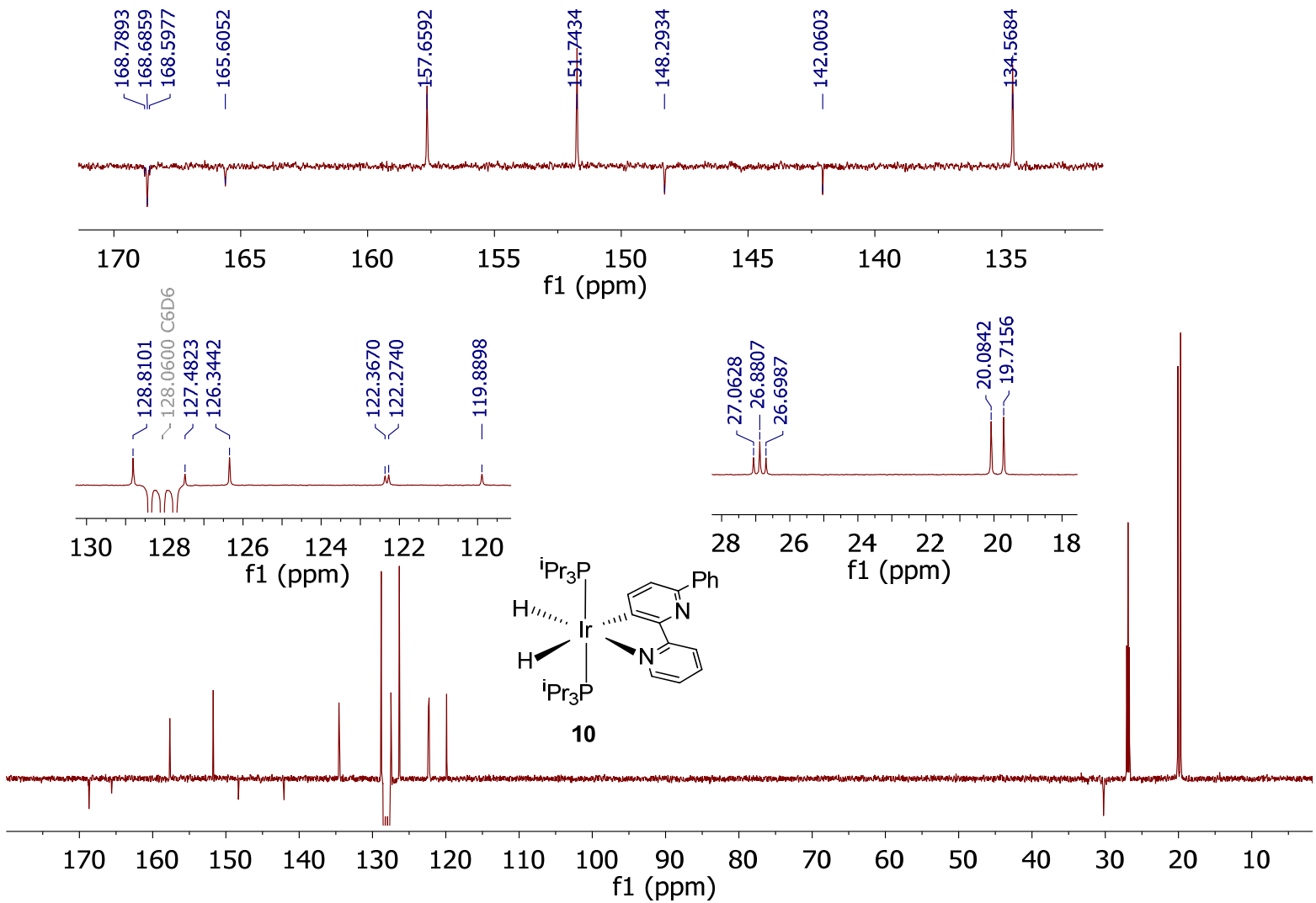

Figure S36. $^{13}C\{^{1}H\}$-apt NMR spectrum (75.48 MHz, C_6D_6, 298 K) of compound **10**.

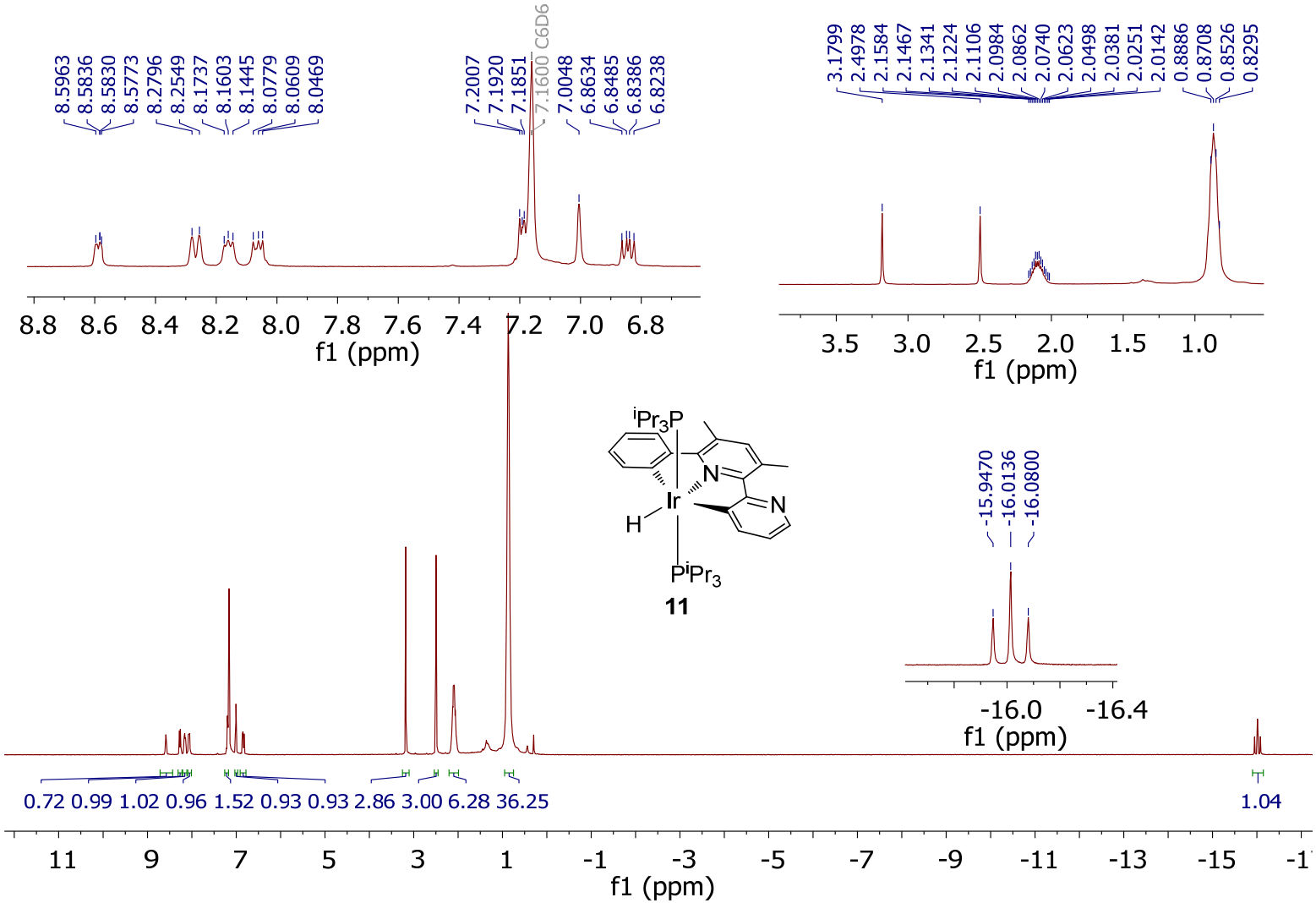

Figure S37. ^{1}H NMR spectrum (300.13 MHz, C_6D_6, 298 K) of compound **11**.

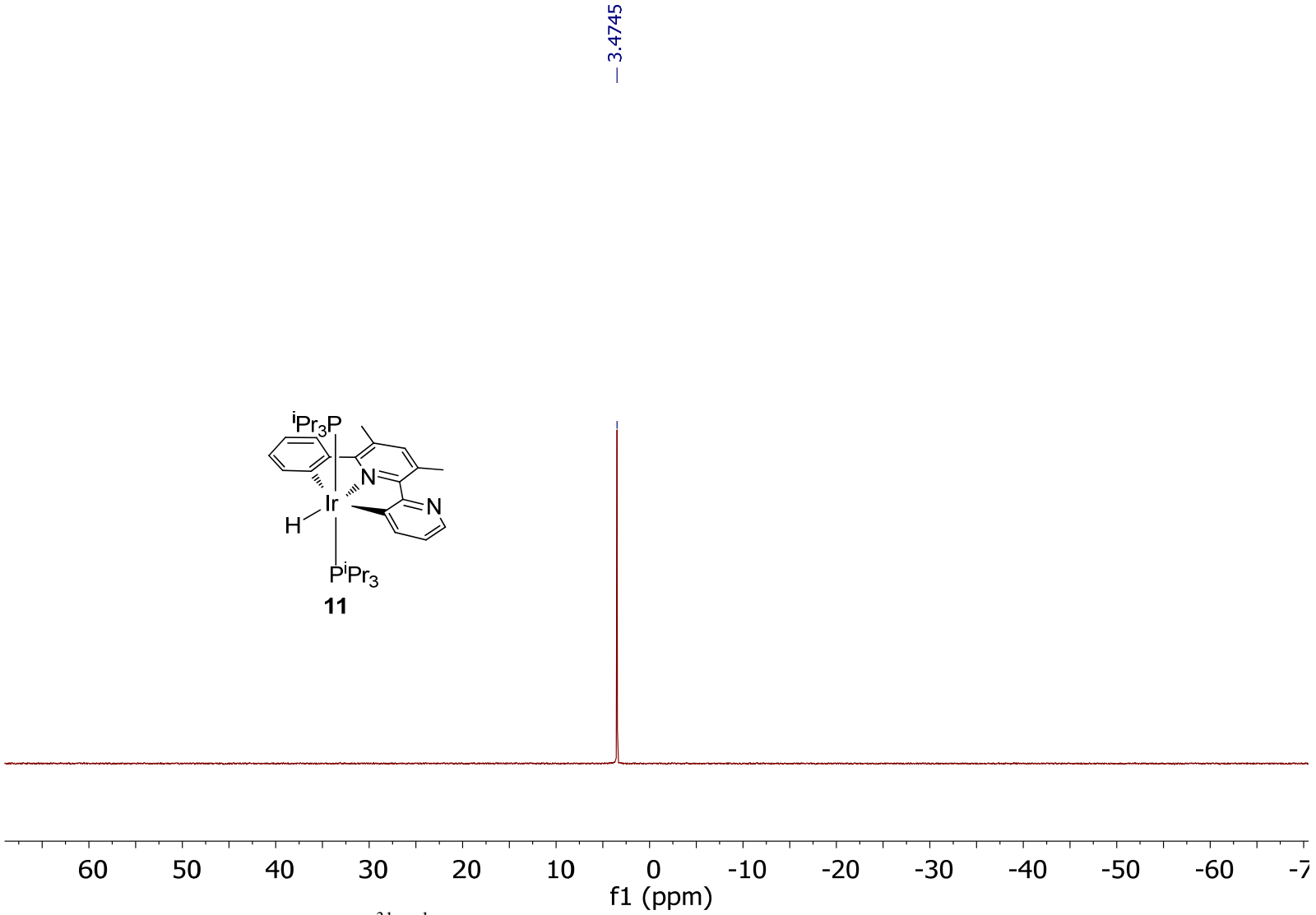

Figure S38. $^{31}P\{^{1}H\}$ NMR spectrum (121.49 MHz, C_6D_6, 298 K) of compound **11**.

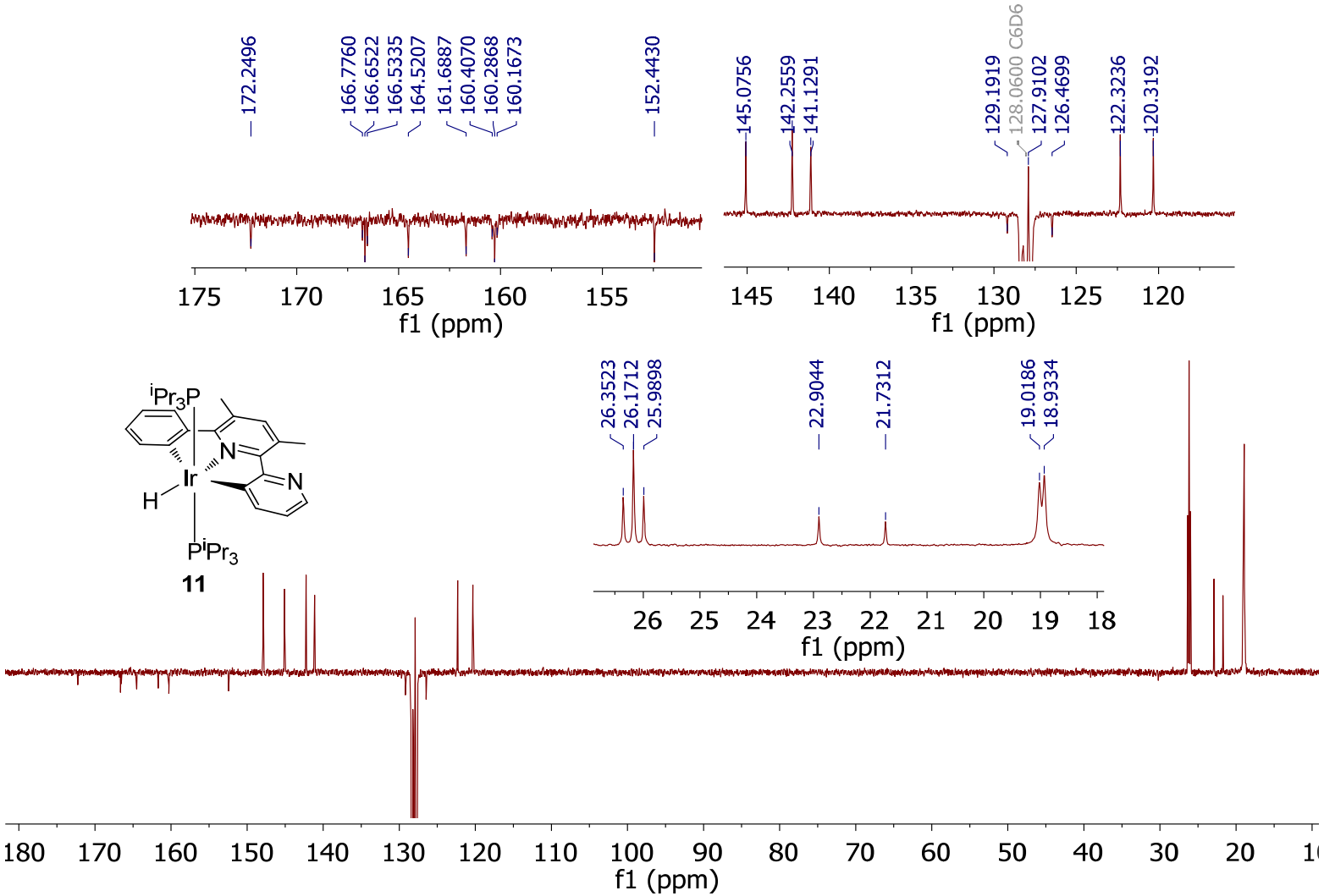

Figure S39. $^{13}C\{^{1}H\}$-apt NMR spectrum (75.48 MHz, C_6D_6, 298 K) of compound **11**.

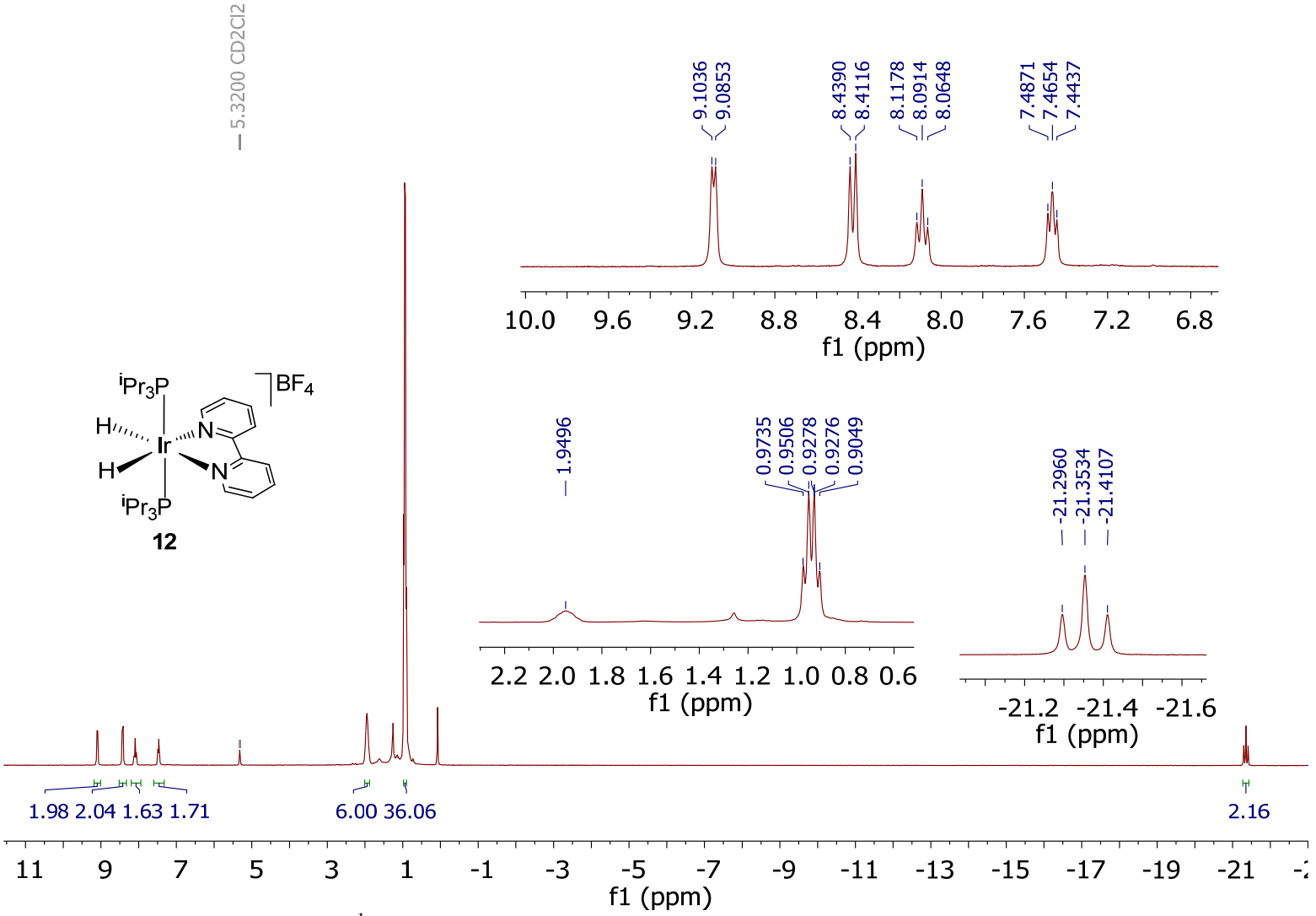

Figure S40. ^{1}H NMR spectrum (300.13 MHz, CD_2Cl_2, 298 K) of compound **12**.

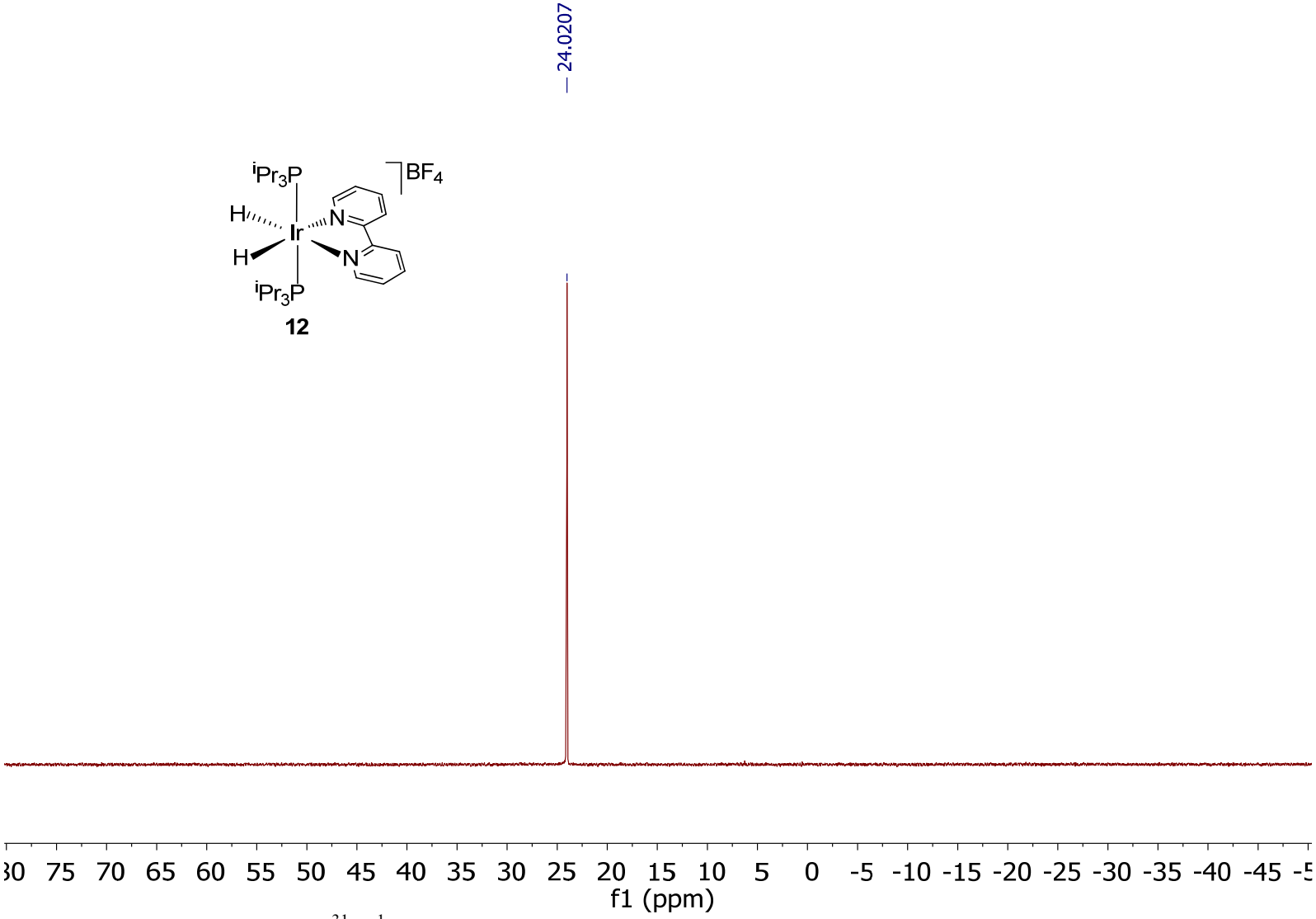

Figure S41. $^{31}P\{^{1}H\}$ NMR spectrum (121.49 MHz, CD_2Cl_2, 298 K) of compound **12**.

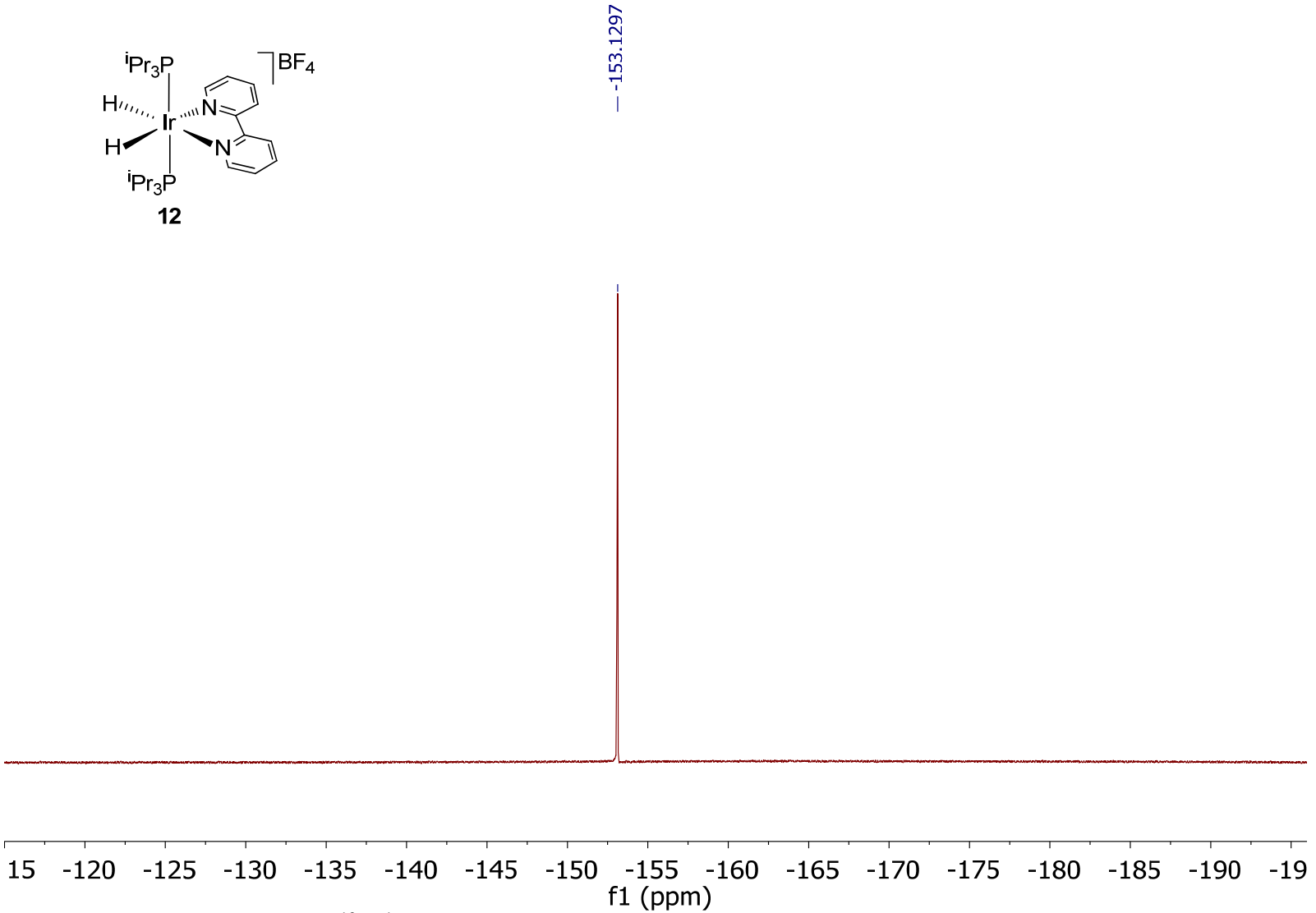

Figure S42. $^{19}F\{^{1}H\}$ NMR spectrum (376.49 MHz, CD_2Cl_2, 298 K) of compound **12**.

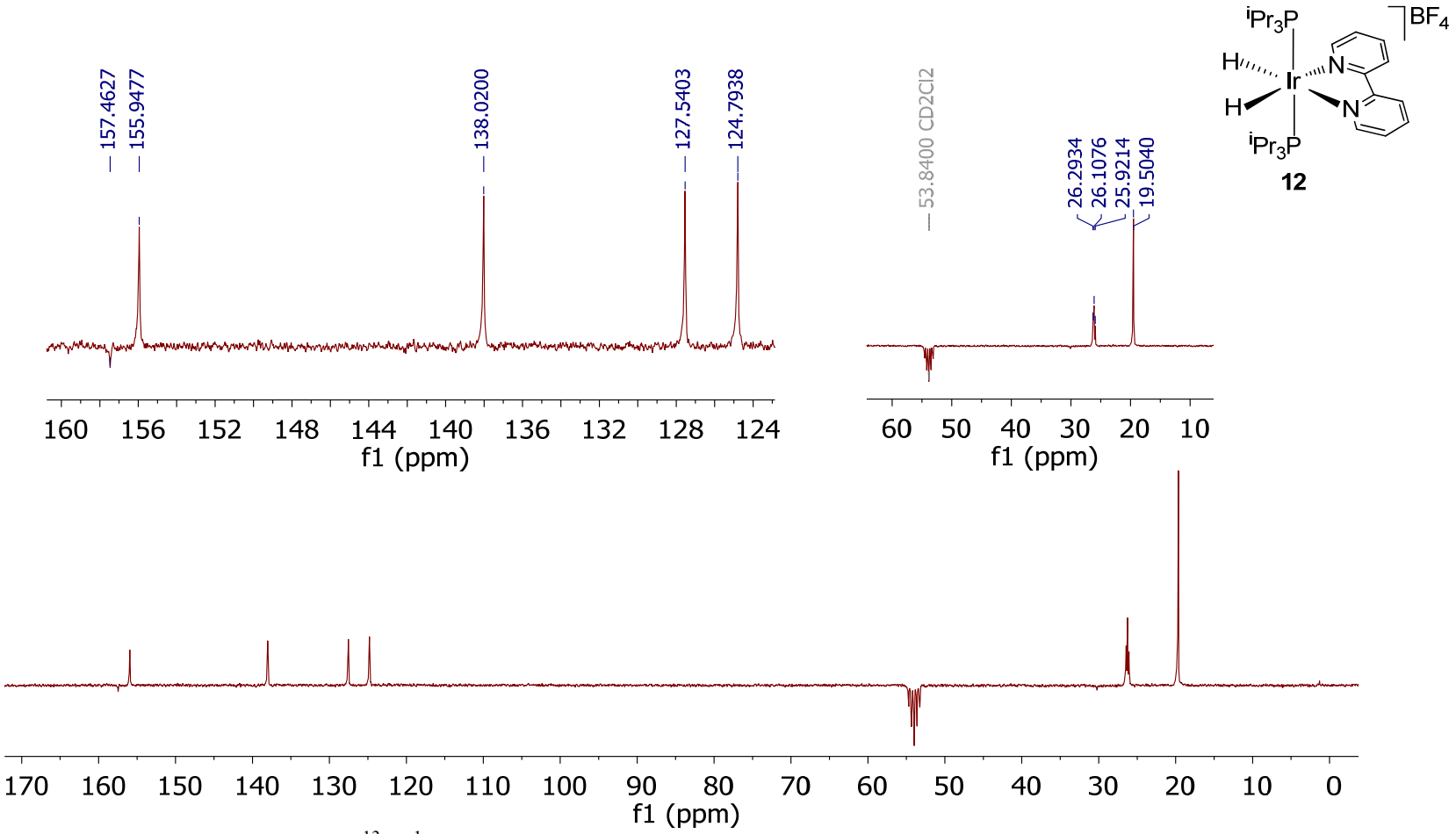

Figure S43. $^{13}C\{^{1}H\}$-apt NMR spectrum (75.48 MHz, CD_2Cl_2, 298 K) of compound **12**.

● **Deuteration Experiments**

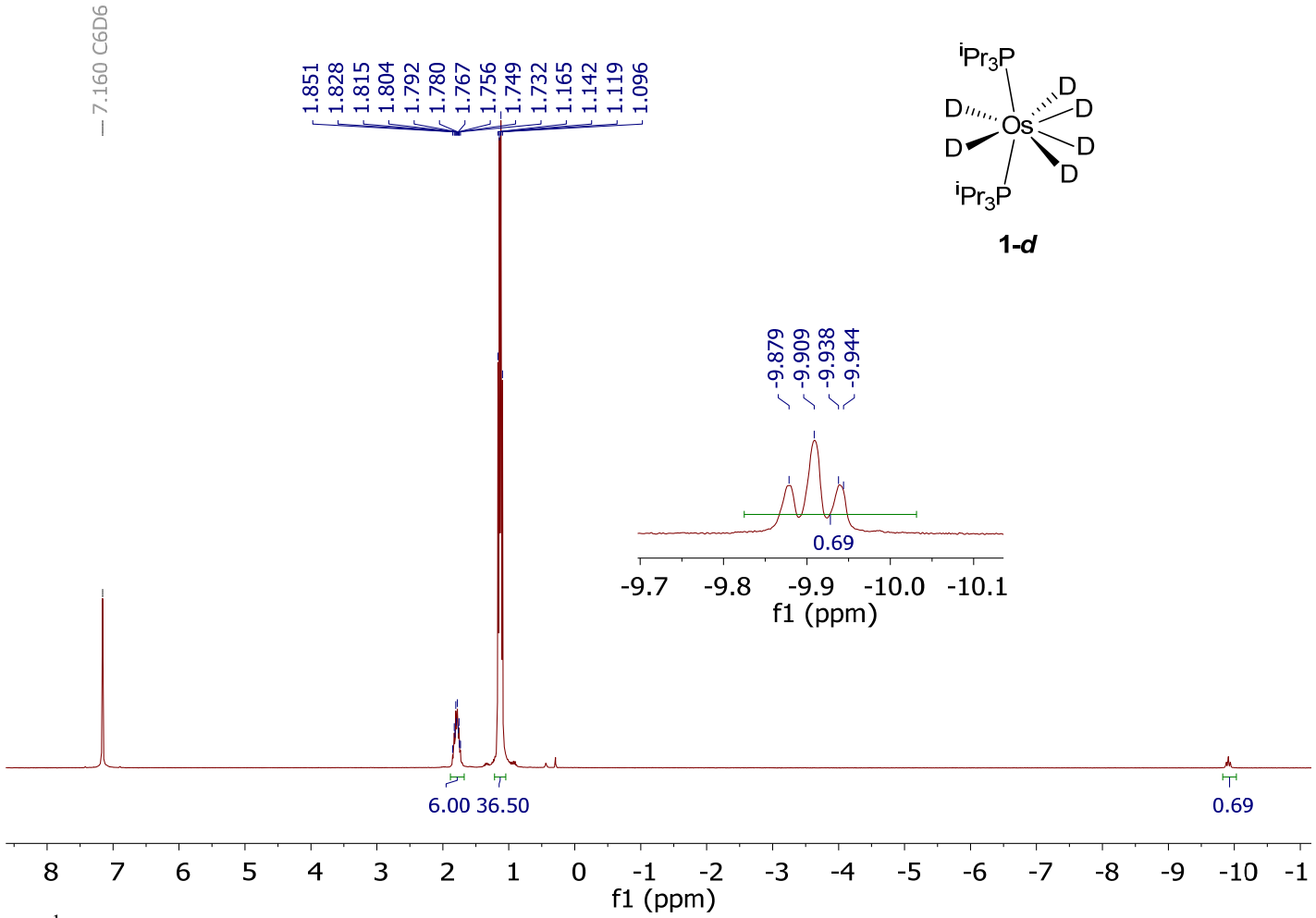

Figure S44. ^{1}H NMR spectrum (300.13 MHz, C_6D_6, 298 K) of compound **1-*d***. A delay (d1) of 5 seconds was used in order to assure the correct integration of the resonances.

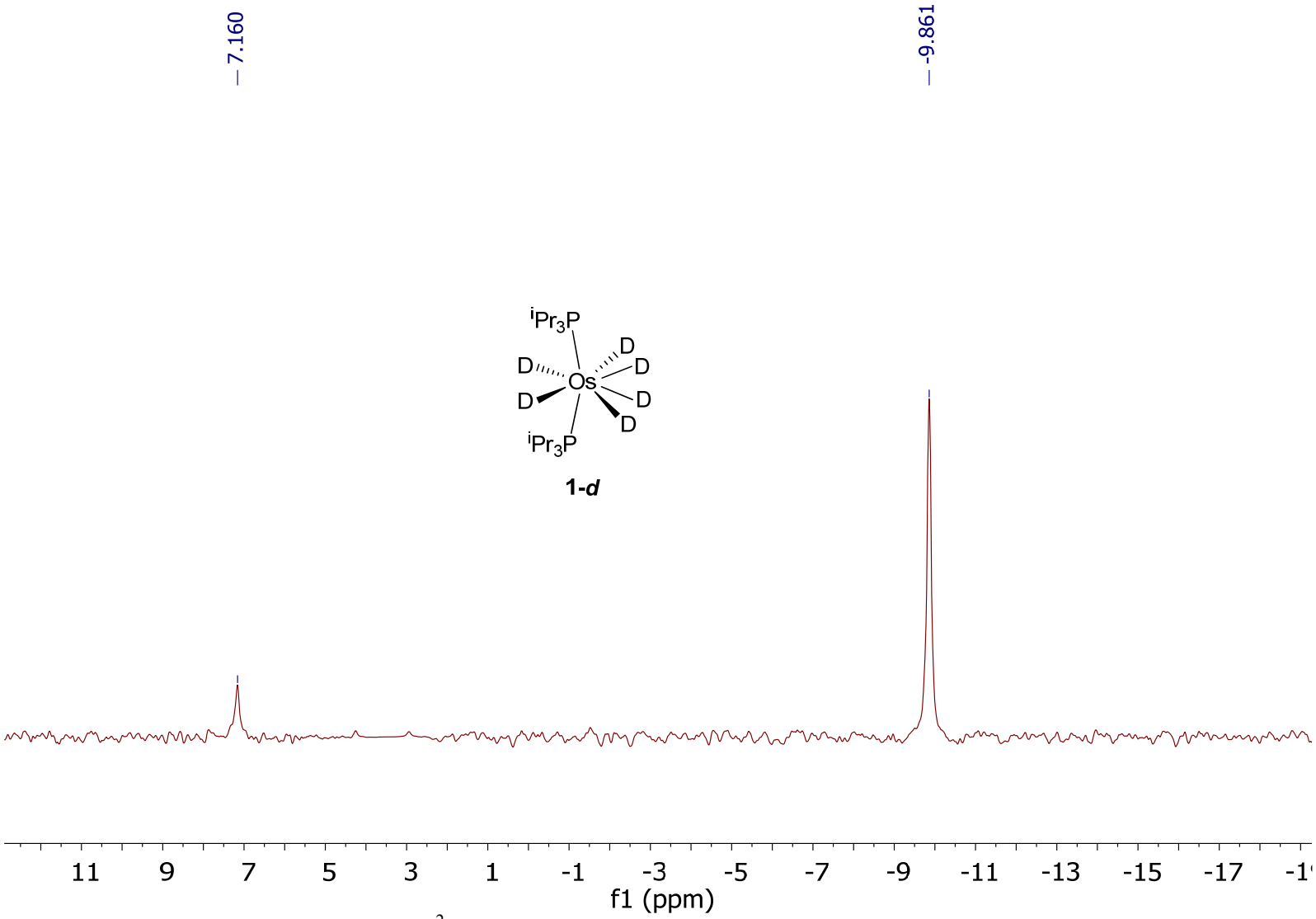

Figure S45. ^{2}H NMR (61.42 MHz, C_6H_6, 298 K) of compound **1-*d***.

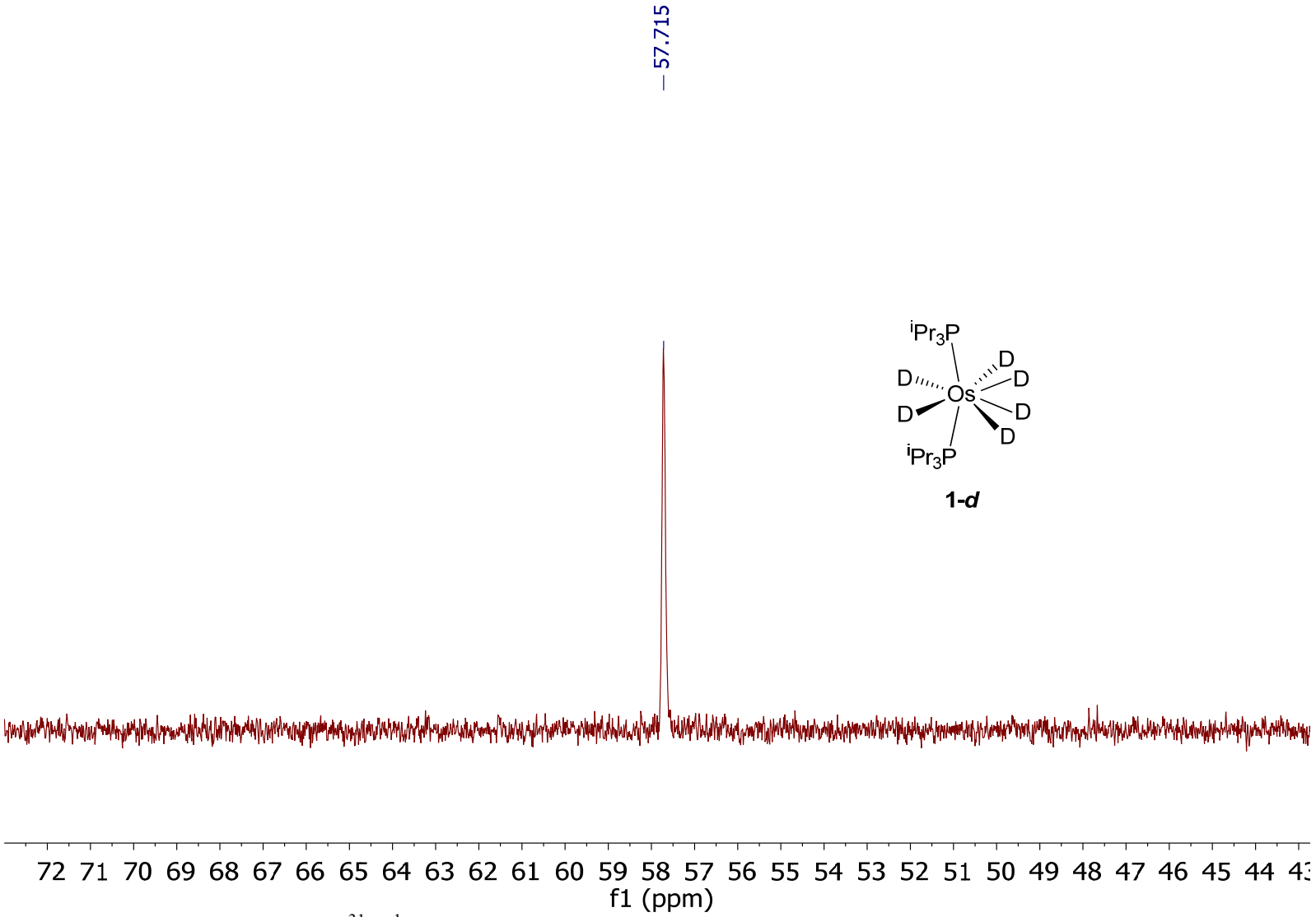

Figure S46. $^{31}P\{^{1}H\}$ NMR spectrum (121.49 MHz, C_6D_6, 298 K) of compound **1-*d*.**

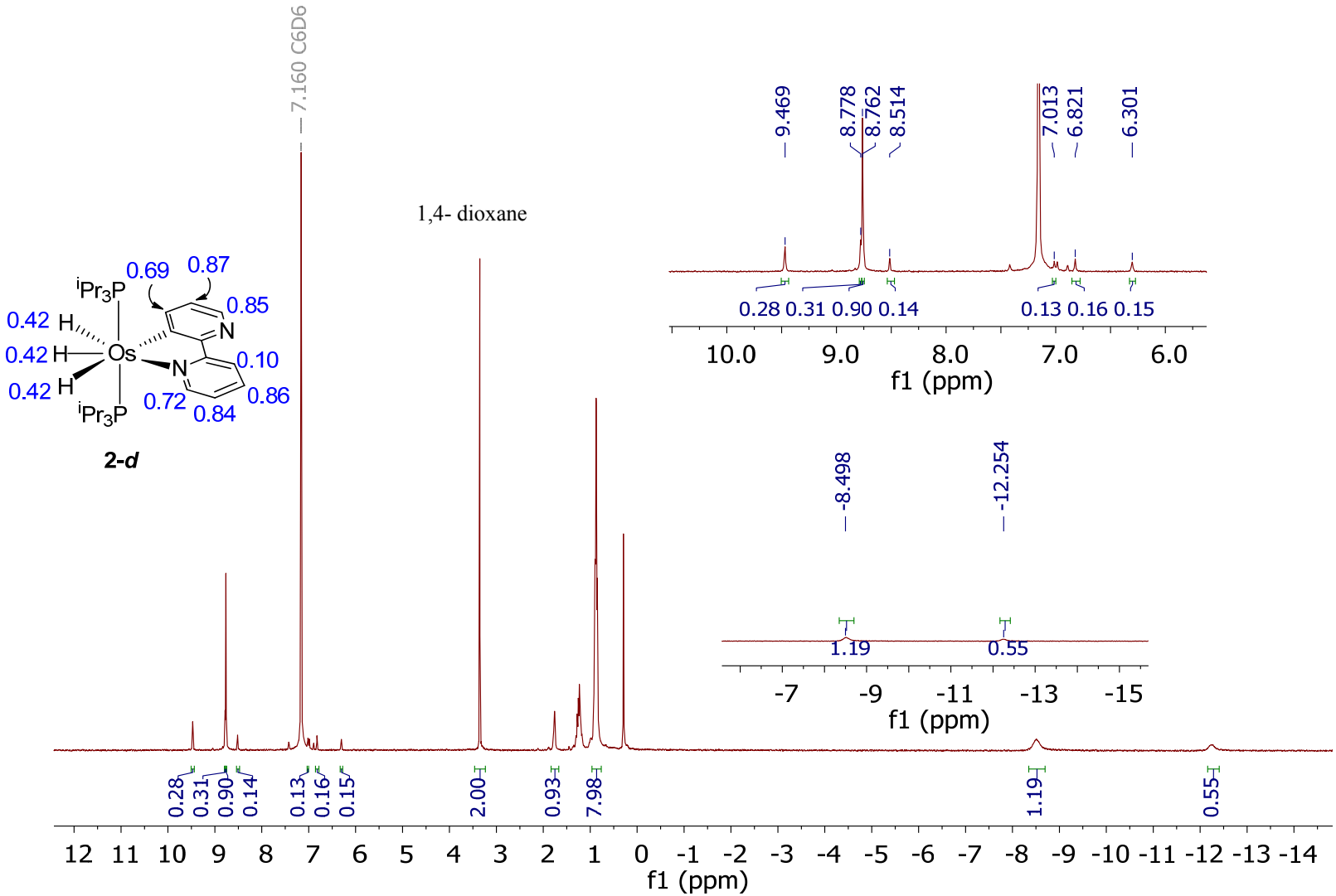

Figure S47. ^{1}H NMR spectrum (300.13 MHz, C_6D_6, 298 K) of compound **2-*d***. A delay (d1) of 5 seconds was used in order to assure the correct integration of the resonances.

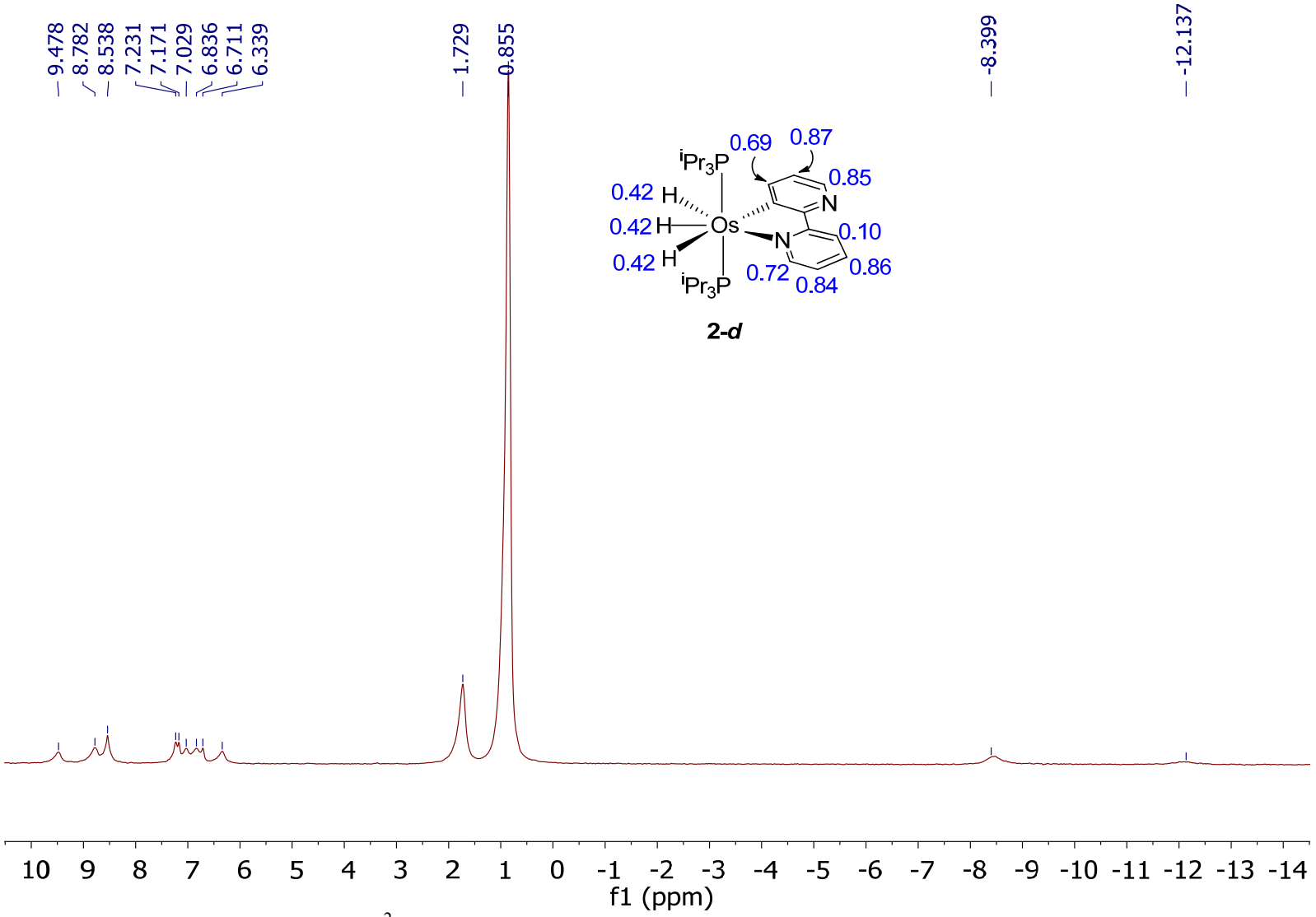

Figure S48. ^{2}H NMR spectrum (61.42 MHz, C_6H_6, 298 K) of compound **2-*d***.

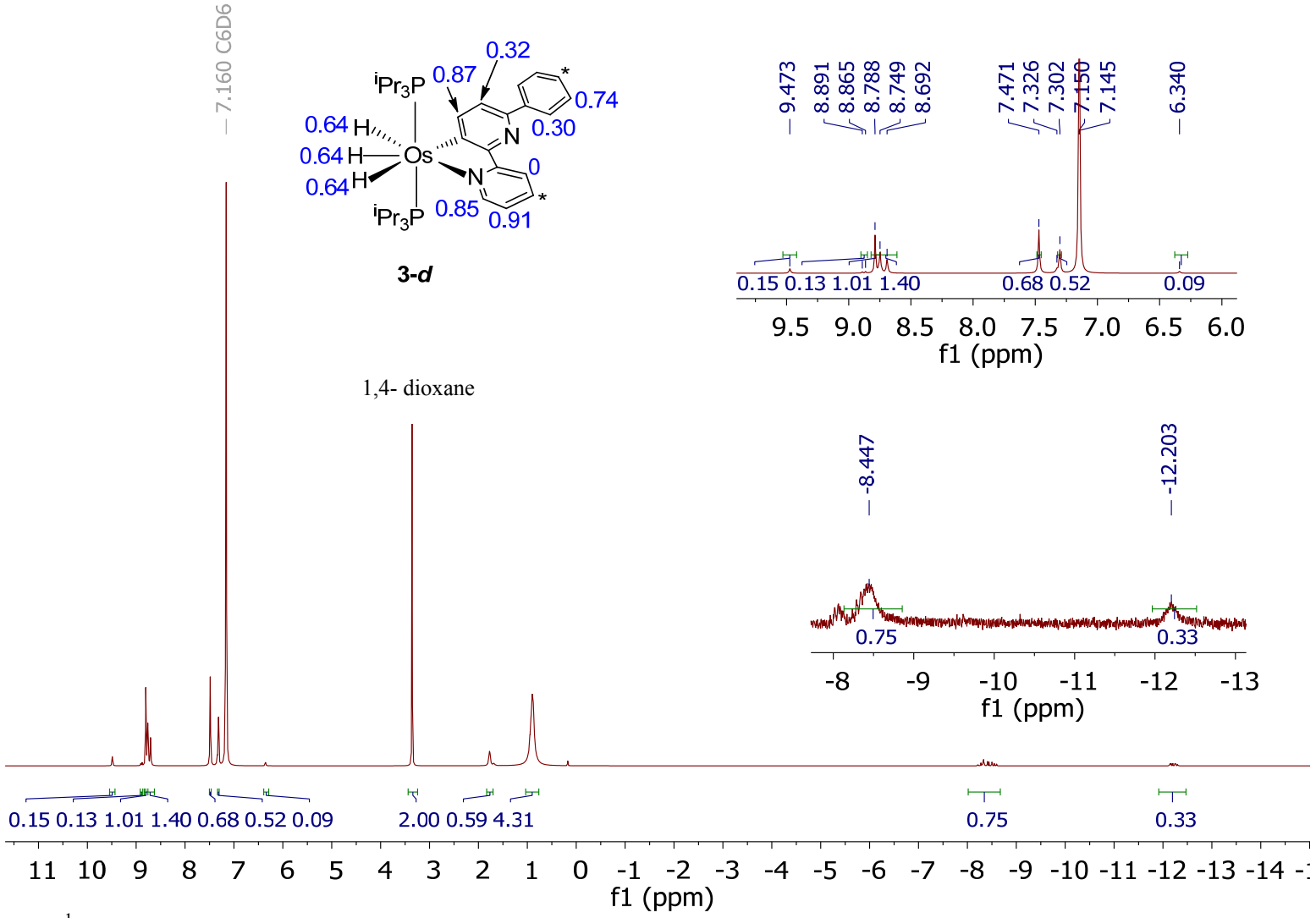

Figure S49. ^{1}H NMR spectrum (300.13 MHz, C_6D_6, 298 K) of compound **3-*d***. A delay (d1) of 5 seconds was used in order to assure the correct integration of the resonances.

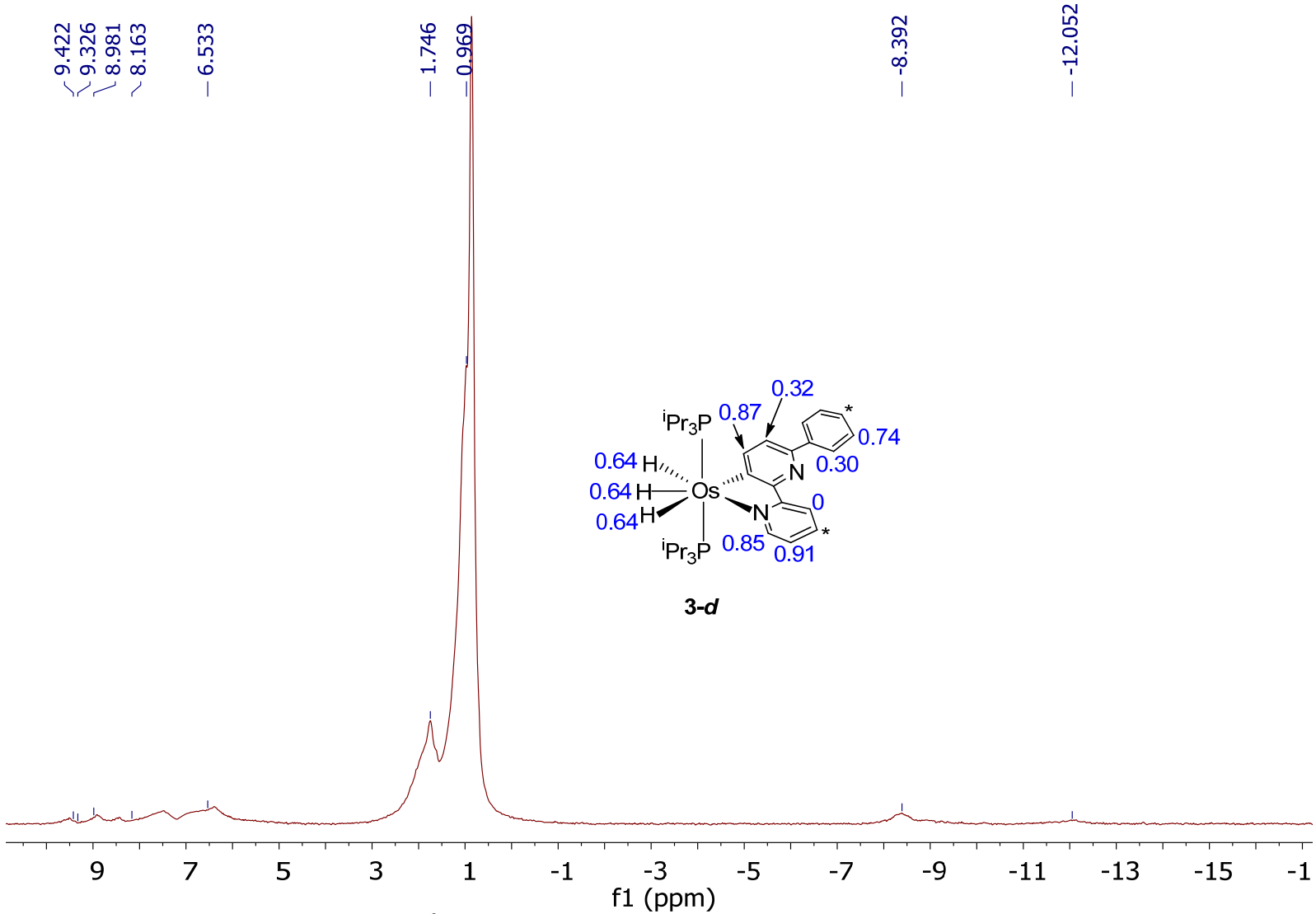

Figure S50. ^{2}H NMR spectrum (61.42 MHz, C_6H_6, 298 K) of compound **3-*d***.

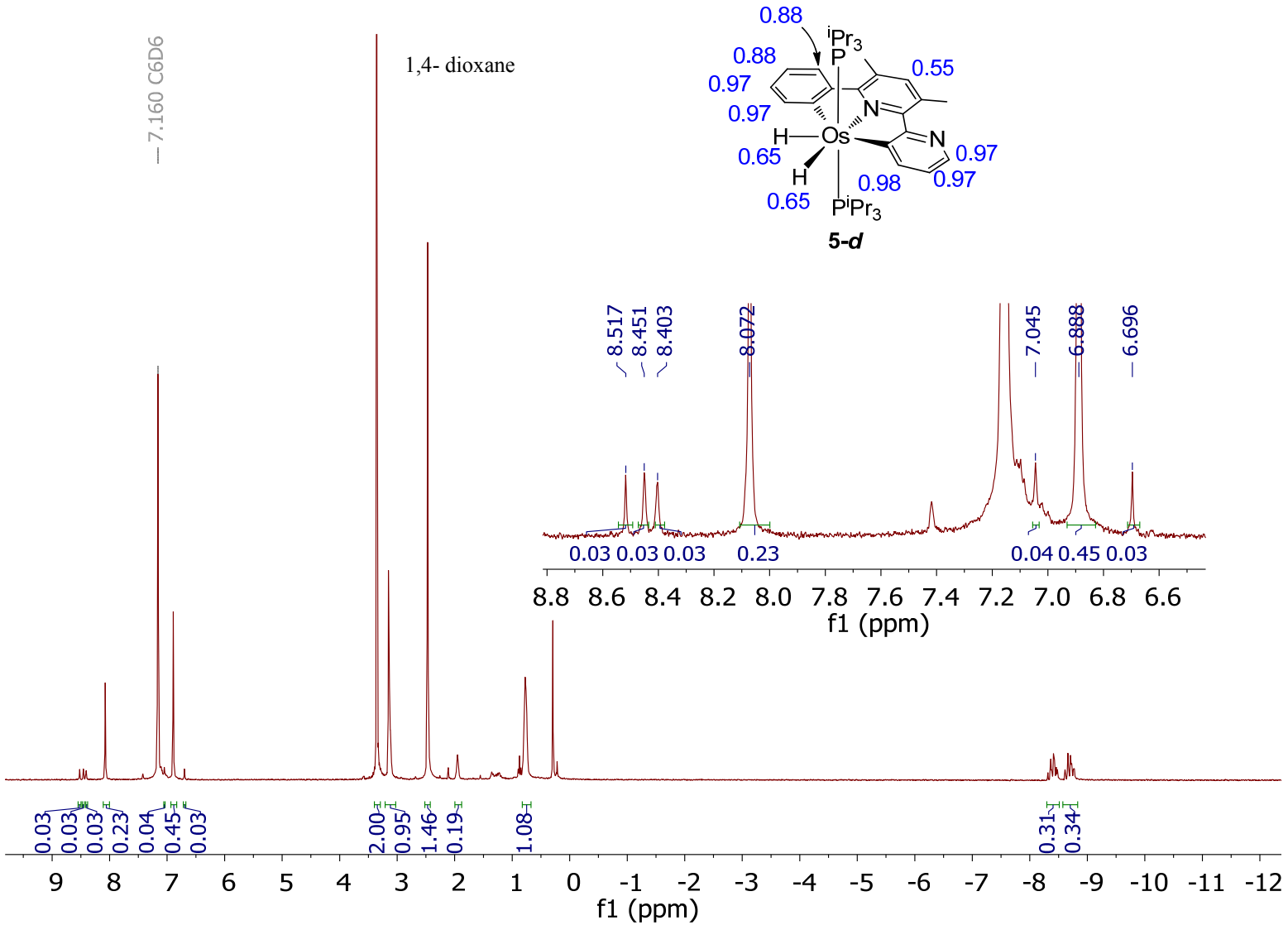

Figure S51. ^{1}H NMR spectrum (300.13 MHz, C_6D_6, 298 K) of compound **5-*d***. A delay (d1) of 5 seconds was used in order to assure the correct integration of the resonances.

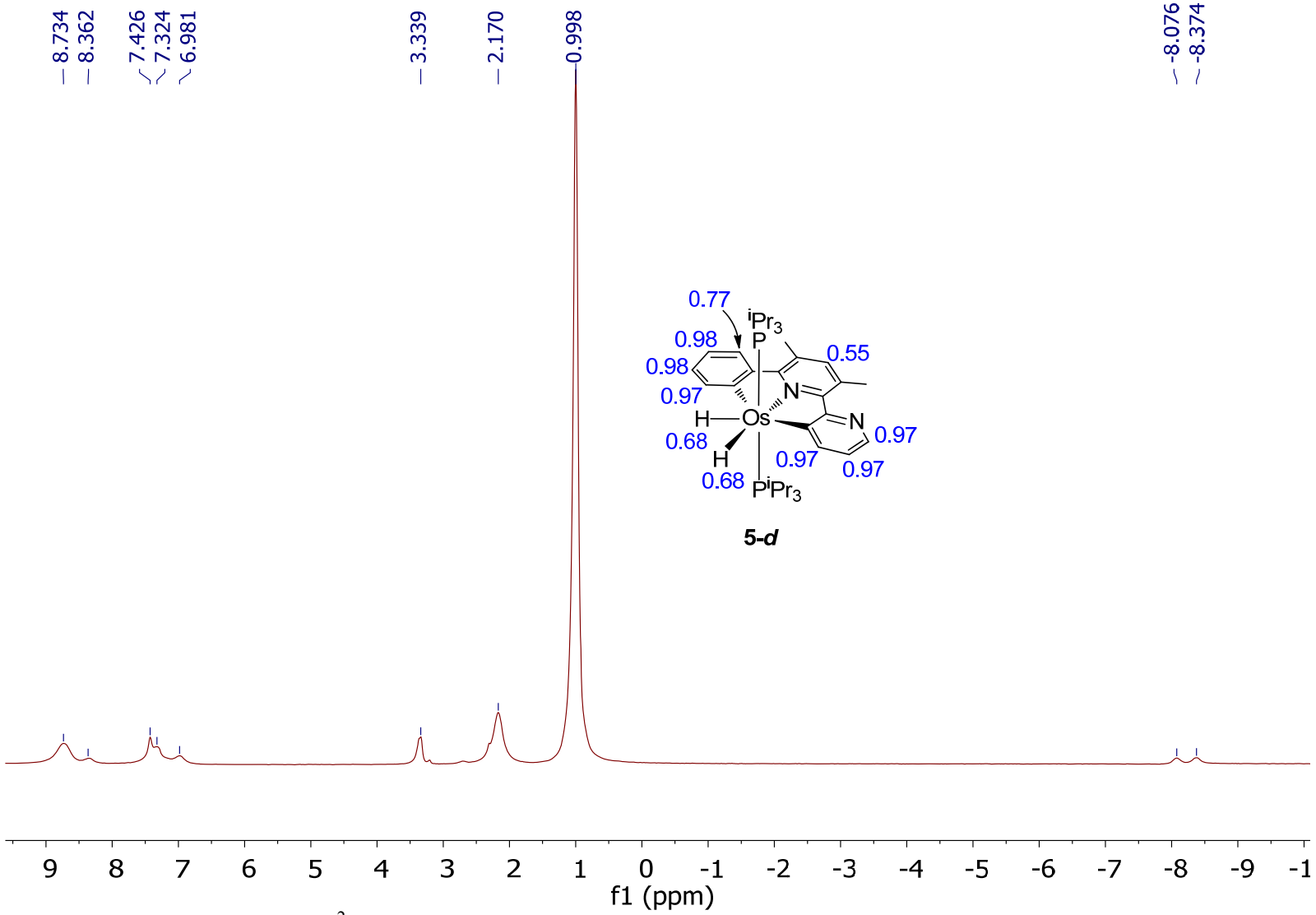

Figure S52. ^{2}H NMR spectrum (61.42 MHz, C_6H_6, 298 K) of compound **5-*d***.

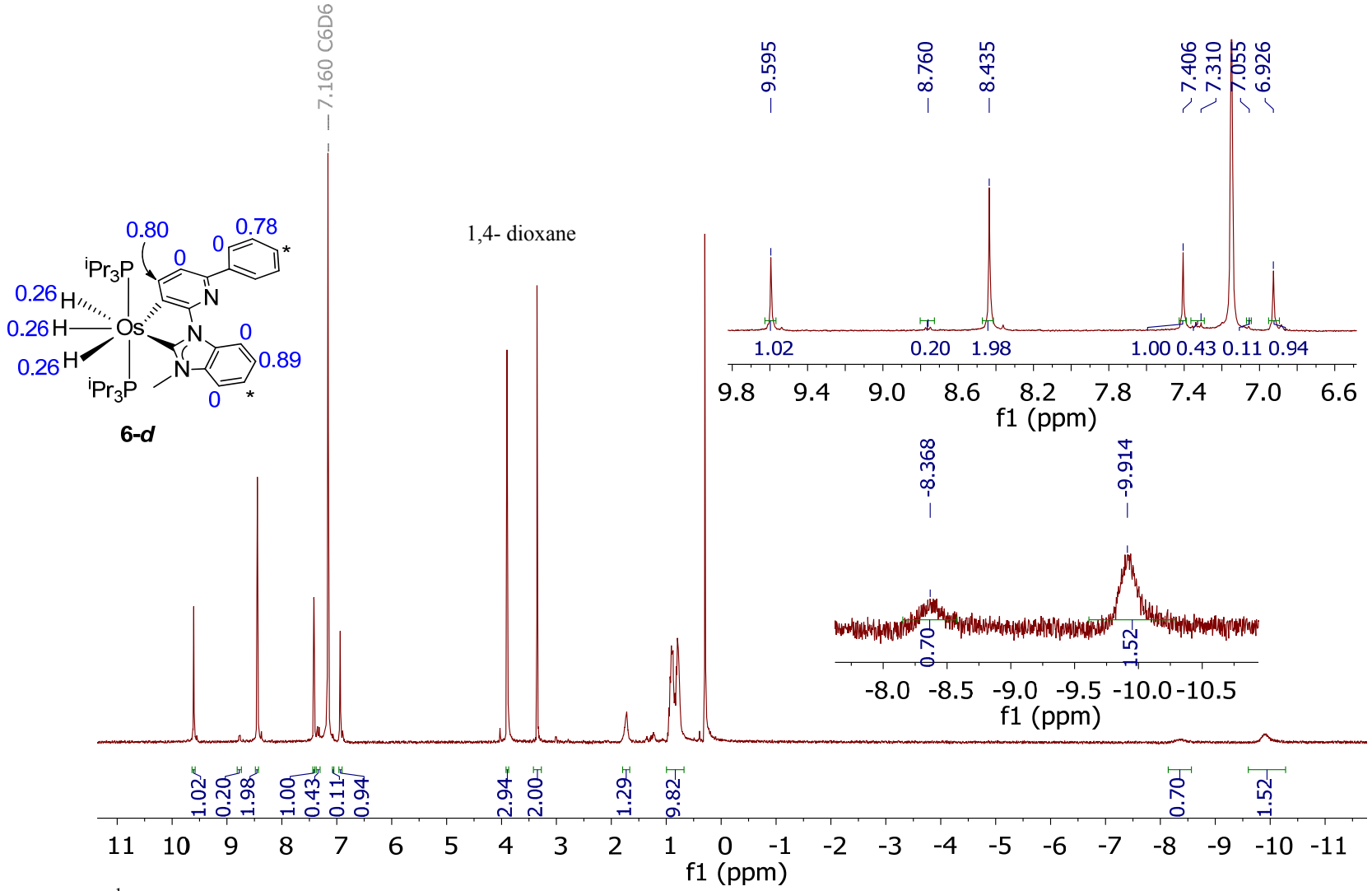

Figure S53. ^{1}H NMR spectrum (300.13 MHz, C_6D_6, 298 K) of compound **6-*d***. A delay (d1) of 5 seconds was used in order to assure the correct integration of the resonances.

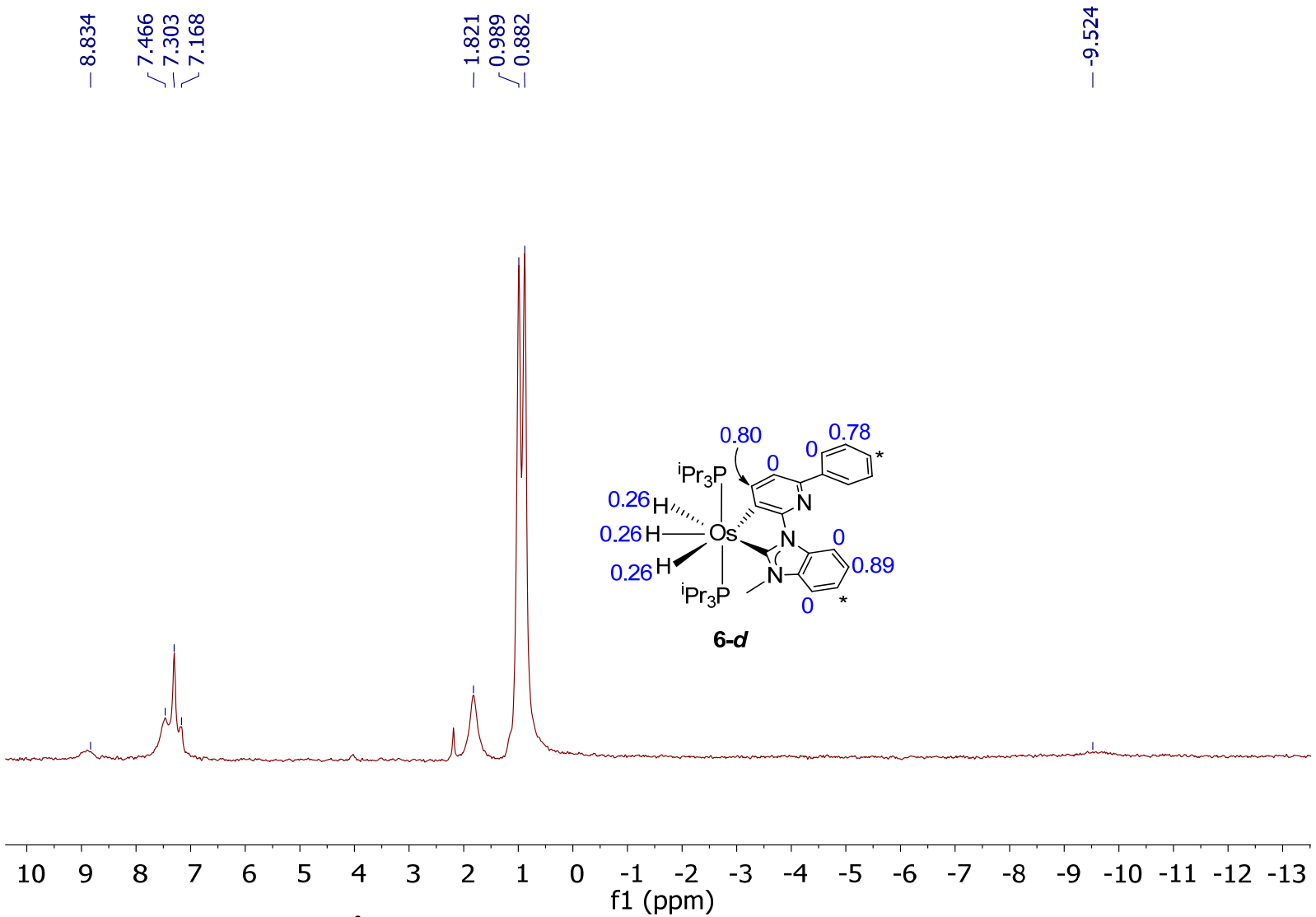

Figure S54. ^{2}H NMR spectrum (61.42 MHz, C_6H_6, 298 K) of compound **6-*d***.

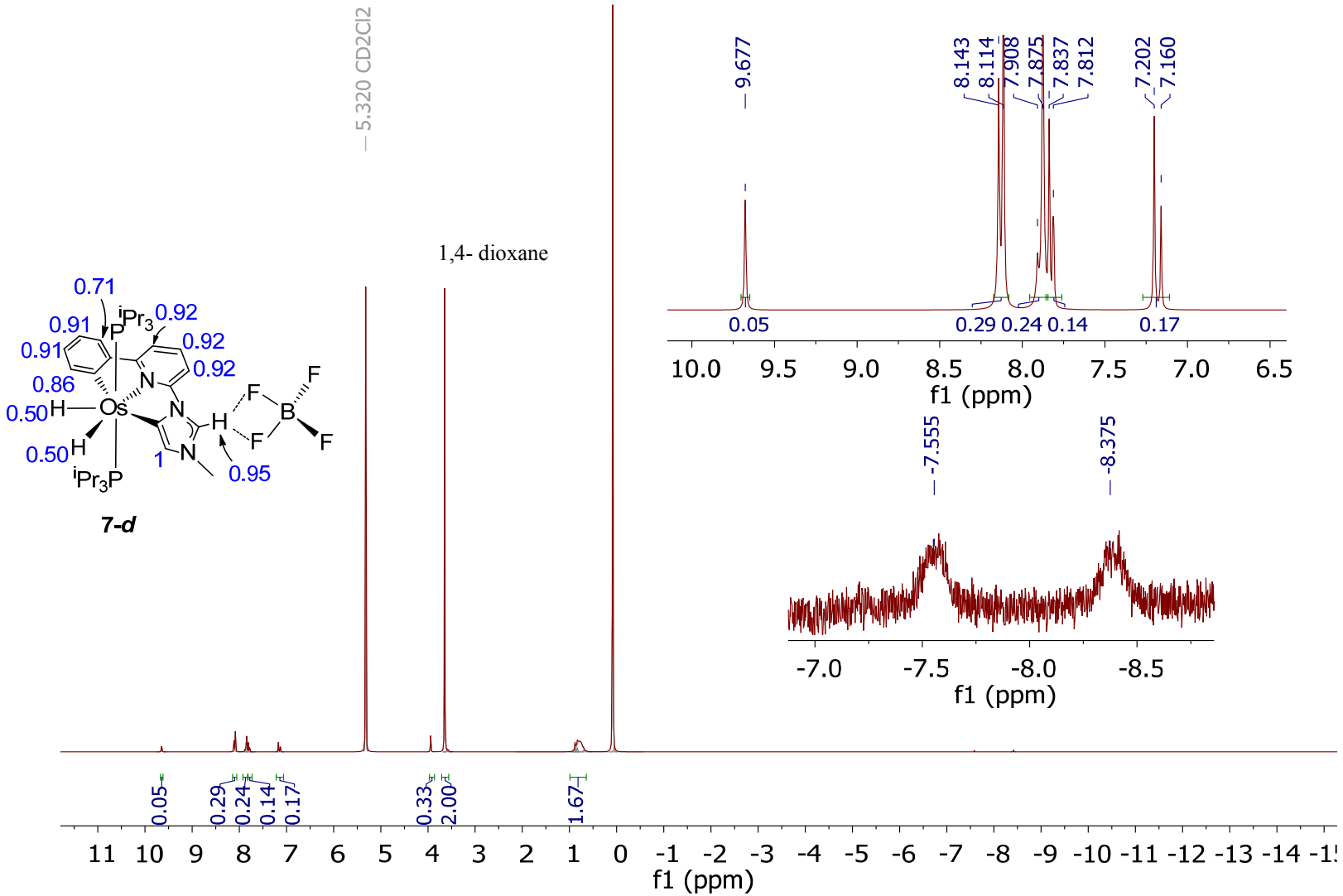

Figure S55. ^{1}H NMR spectrum (300.13 MHz, CD_2Cl_2, 298 K) of compound **7-*d***. A delay (d1) of 5 seconds was used in order to assure the correct integration of the resonances.

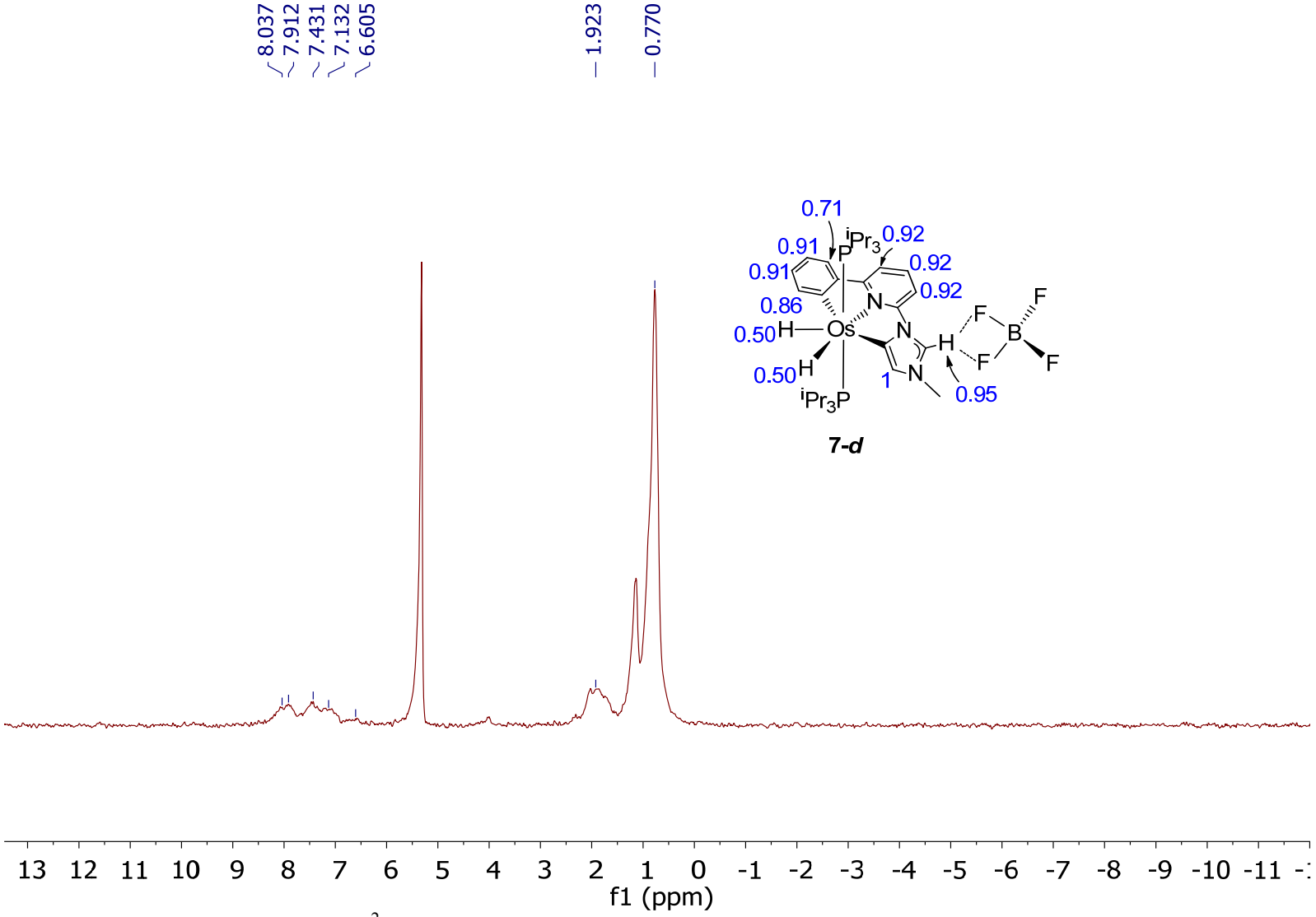

Figure S56. ^{2}H NMR spectrum (61.42 MHz, CH_2Cl_2, 298 K) of compound **7-*d***.

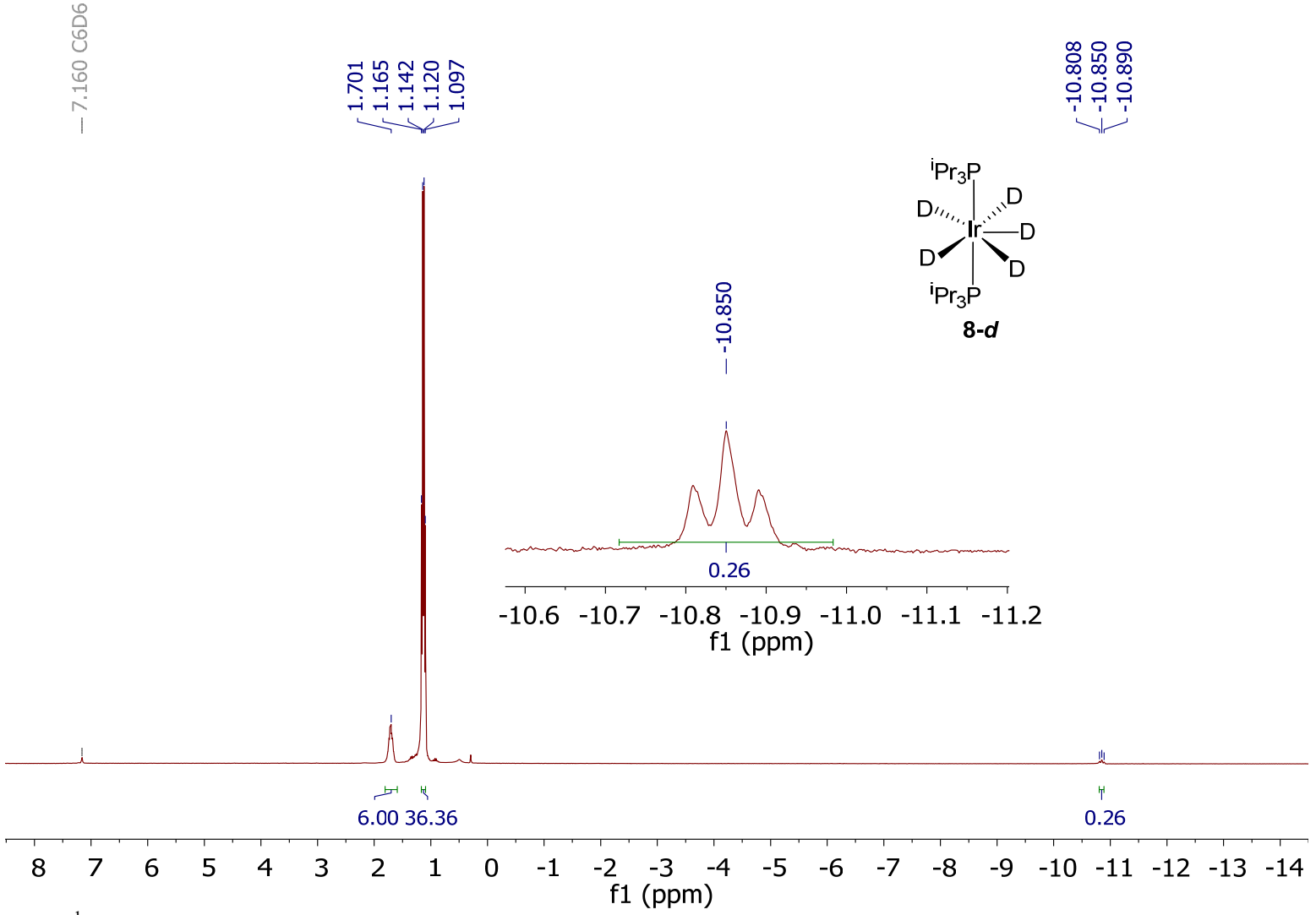

Figure S57. ^{1}H NMR spectrum (300.13 MHz, C_6D_6, 298 K) of compound **8-*d***. A delay (d1) of 5 seconds was used in order to assure the correct integration of the resonances.

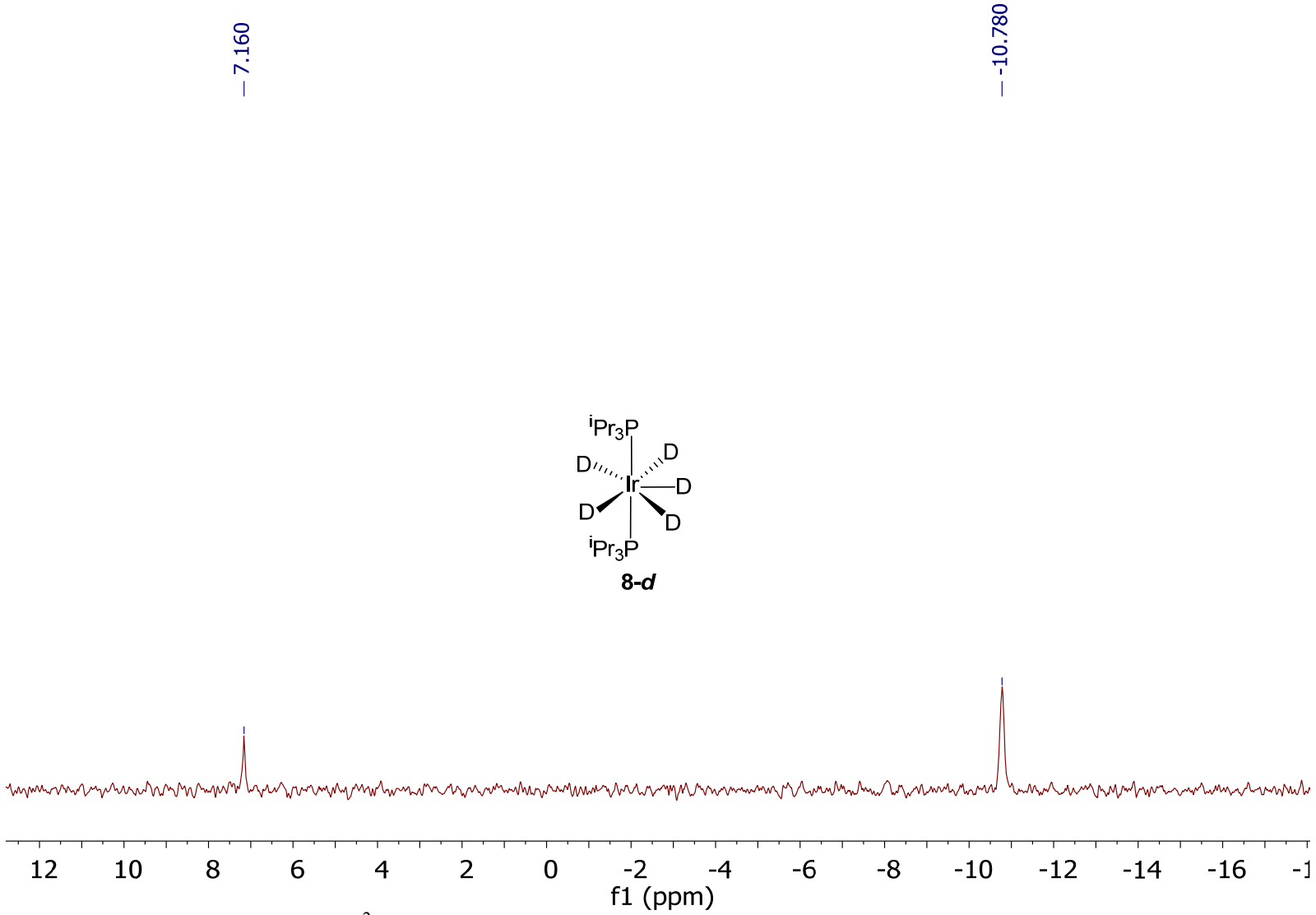

Figure S58. ^{2}H NMR spectrum (61.42 MHz, C_6H_6, 298 K) of compound **8-*d***.

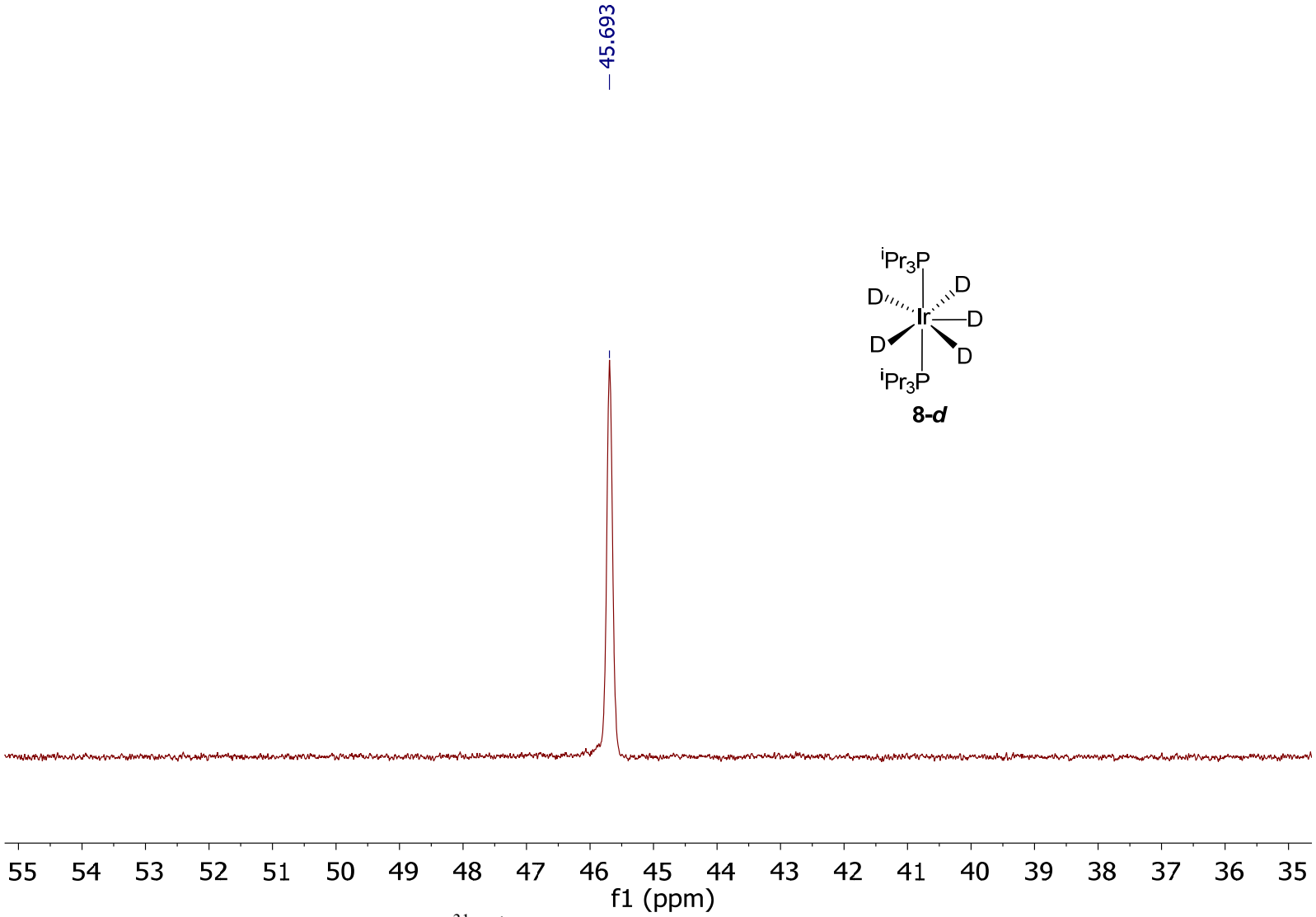

Figure S59. $^{31}P\{^{1}H\}$ NMR spectrum (121.49 Hz, C_6D_6, 298 K) of compound **8-*d***.

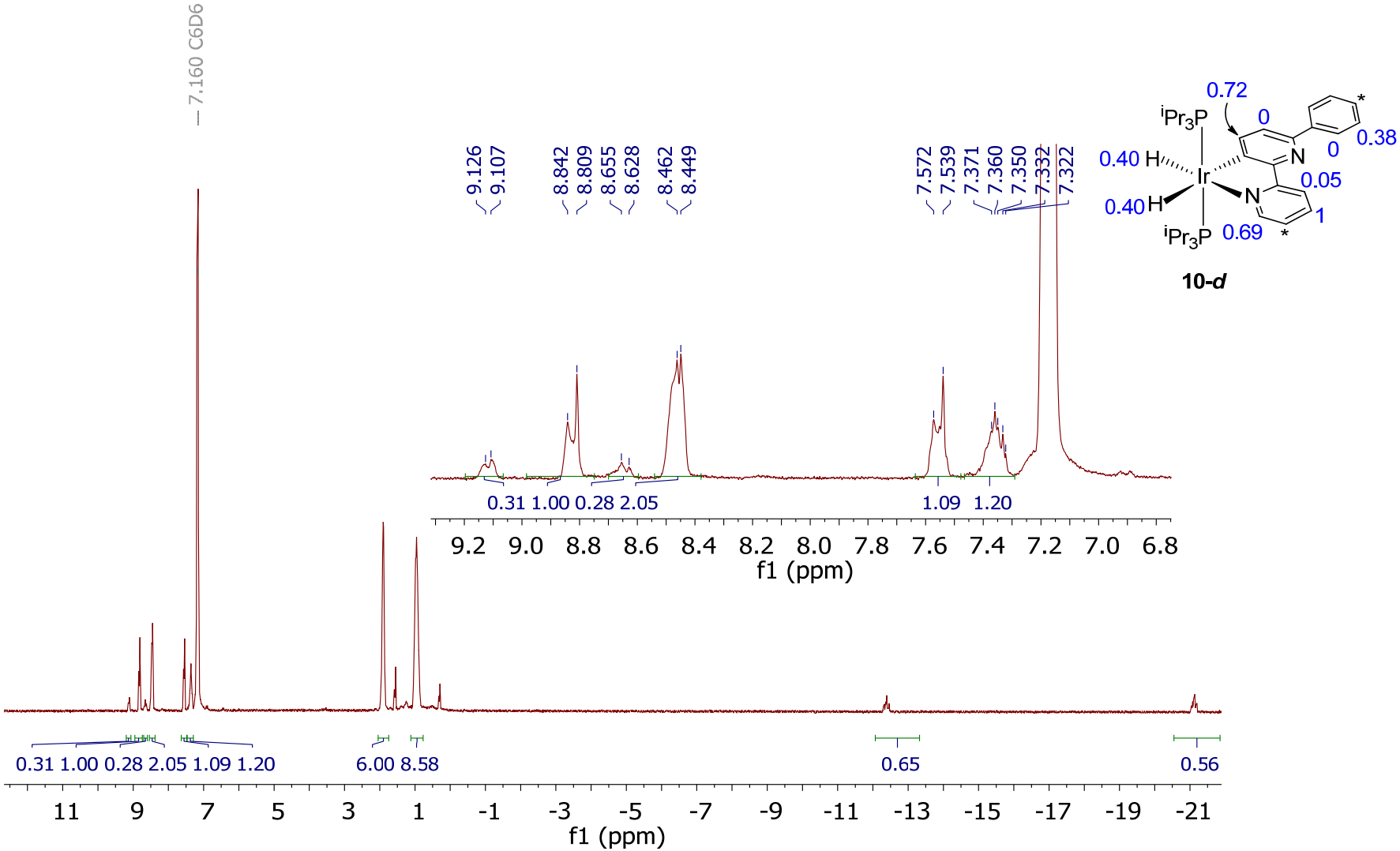

Figure S60. ^{1}H NMR spectrum (300.13 MHz, C_6D_6, 298K) of compound **10-*d***. A delay (d1) of 5 seconds was used in order to assure the correct integration of the resonances.

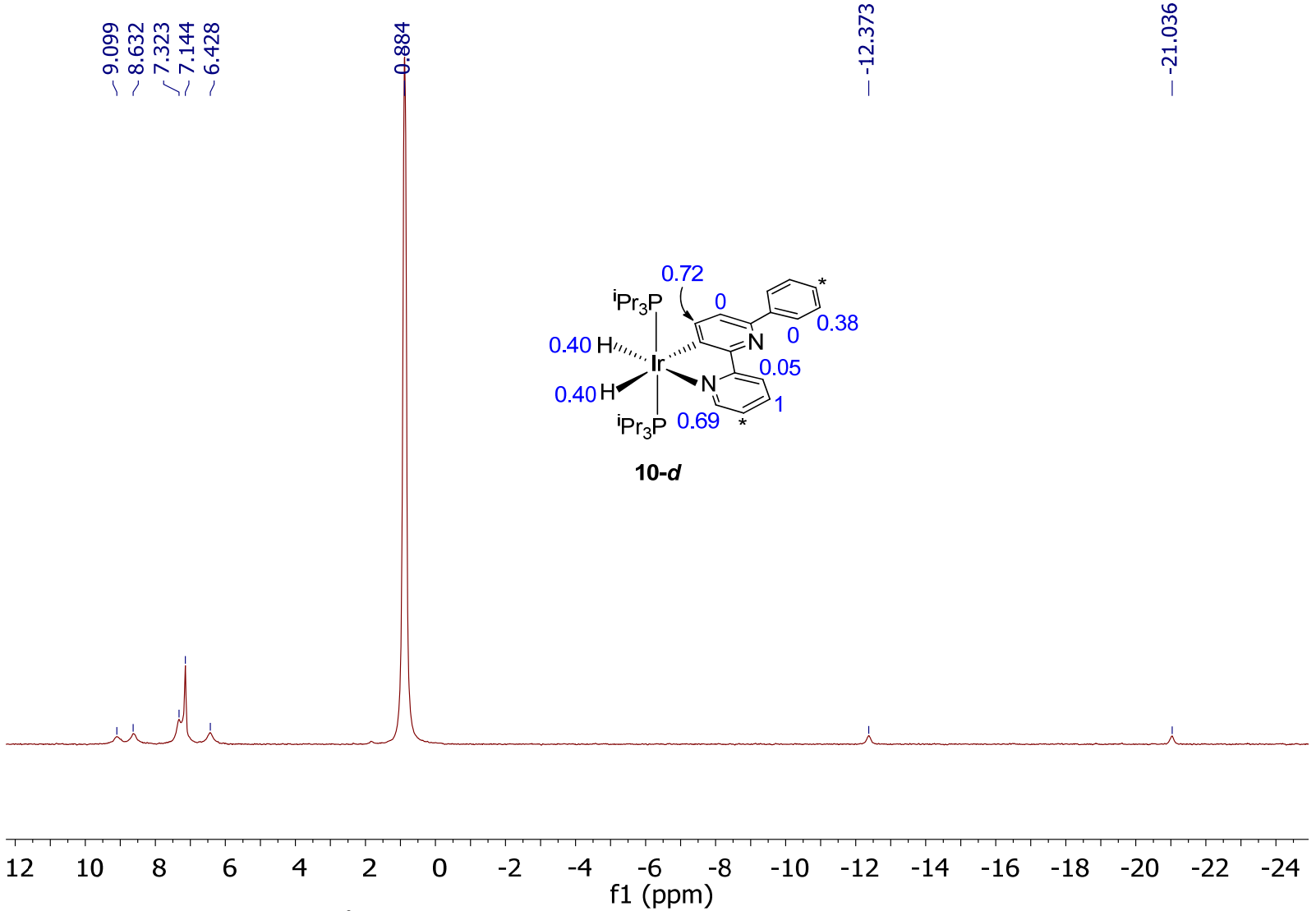

Figure S61. ^{2}H NMR spectrum (61.42 MHz, C_6H_6, 298 K) of compound **10-*d***.

● **References**

(1) Aracama, M.; Esteruelas, M. A.; Lahoz, F. J.; Lopez, J. A.; Meyer, U.; A. Oro, L.; Werner, H. Synthesis, Reactivity, Molecular Structure, and Catalytic Activity of the Novel Dichlorodihydridoosmium(IV) Complexes $OsH_2Cl_2(PR_3)_2$ (PR_3 = P^iPr_3, PMe^tBu_2). *Inorg. Chem.* **1991**, *30*, 288-293.

(2) Werner, H.; Schulz, M.; Esteruelas, M. A.; Oro, L. A. $IrCl_2H(P^iPr_3)_2$ as Catalyst Precursor for the Reduction of Unsaturated Substrates. *J. Organomet. Chem.* **1993**, *445*, 261-265.

(3) Kauffmann, T.; König, J.; Woltermann, A. Nucleophile Alkylierung un Arylierung des 2,2'-Bipyridyils. *Chem. Ber.* **1976**, *109*, 3964-3868.

(4) Serrano, E.; Martin, R. Nickel-Catalyzed Reductive Amidation of Unactivated Alkyl Bromides. *Angew. Chem. Int. Ed.* **2016**, *55*, 11207-11211.

(5) Li, J.; Wang, Z.; Turner, E. Tridentate platinum(II) complexes. US patent 9,203,039 B2, **2015**.

(6) Blessing, R. H. *Acta Crystallogr.* **1995**, *A51*, 33. SADABS: Area-detector absorption correction; Bruker- AXS, Madison, WI, 1996.

(7) SHELXL-2016/6. Sheldrick, G. M. *Acta Cryst.* **2008**, *A64*, 112-122.